UNIVERSIDAD DE GUANAJUATO

Campus Irapuato-Salamanca

División de Ingenierías

“Supermode Interferometer In Coupled Multicore Fiber For Multi-Sensing Applications”

TESIS

QUE PARA OBTENER EL GRADO DE:

MAESTRA EN INGENIERÍA ELÉCTRICA

PRESENTA:

Ing. KARINE NGANGA KAFUTI

DIRECTOR DE TESIS:

Dr. Juan Manuel Sierra Hernández

CODIRECTOR DE TESIS:

Dr. Marco Antonio Contreras Terán

SALAMANCA, GTO. Abril, 2026.

Dedication

To my beloved children, Shawn, Andrea, Leandre, and Carla, your love and support inspire me every day. May this work remind you that with passion and perseverance, anything is possible. To my dear mom, Viviane Kibuluku, your unwavering support and faith in me have been the foundation of all my achievements. This thesis is yours as it is mine. To my dear father, in loving memory. Your strength, wisdom, and values continue to guide me. Although you are no longer here, your spirit lives on in every step I take. With all my heart.

Personal Acknowledgments

I want to thank all who have somehow crossed my path. You are helping me climb every peak, and with a deep-seated feeling of gratitude for your encouragement, I offer my most heartfelt thanks.

I owe a special thanks to my advisor, Dr. Juan Manuel Sierra Hernandez, for the detailed and ongoing assistance he provided me with in this research. I would never have reached where I am today without your advice.

Also, I am deeply grateful to Dr. Marco Antonio Contreras Teran, whom I've worked with as co-supervisor throughout most aspects of the thesis, for his management advice and helpful criticism at all stages in its development. Your guidance has contributed greatly to the esprit de courage of this project, from the beginning onward: it has been an honor working together. Through my association with you, I have learned quite a bit academically.

Thanks go out from the bottom of my heart to those who have cared for me during this journey: my family, my friends, especially Melissa Rosas Ramirez, and my colleagues, for the motivation that is so essential at this moment. Thank you very much for accompanying me.

Institutional Acknowledgments

My deepest gratitude went to the Universidad de Guanajuato, especially the División de Ingeniería Campus Irapuato-Salamanca (DICIS), Department of Electrical Engineering, for providing the academic environment and resources necessary for this investigation:

- *To the Photonic Laboratory of the Universidad de Guanajuato, thanks for granting access and providing technical assistance. NUA 148896.*

Universidad de Guanajuato

- *And to El Consejo Nacional de Humanidades, Ciencias y Tecnologías (Conahcyt) of México, for your financial support, which made this academic journey possible, CVU 1322583.*

CONAHCYT
CONSEJO NACIONAL DE HUMANIDADES CIENCIAS Y TECNOLOGÍAS

Abstract

We study a compact supermode interferometer for simultaneous multi-parameter sensing implemented in a coupled multicore optical fiber (MCF), and we incorporate the novel interferometric setup into a fiber laser design to measure physical parameters, such as temperature, strain, stability, and torsion, broadening their potential in the field of high-precision sensing applications. This architecture allows for the excitation and interference of guided supermodes, whose spectral interference pattern is extremely sensitive to external perturbation, by fusing a segment of coupled MCF between standard single-mode fibers. While axial strain modifies the effective phase propagation of supermodes, resulting in measurable fringe displacement in the interferometric spectrum, temperature variations change the fiber's refractive index and optical path length, resulting in predictable spectral shifts. Furthermore, through photo-elastic effects, torsional deformation causes changes in core refractive indices, resulting in unique wavelength shifts that can be distinguished from other perturbations.

Each physical quantity can be measured with high sensitivity and accuracy through spectral observation of supermode interference in an optical spectrum analyzer (OSA).

The proposed supermode interferometer represents a promising platform for flexible, passive, and multifunctional detection in structural monitoring, industrial process control, etc., because it is simple to fabricate using standard optical fiber fusion splicing, mechanically robust, and compatible with current telecommunication components. The comprehension and practical application of multicore-fiber-based interferometers for real-world multi-sensing problems are improved by this work.

Resumen

Estudiamos un interferómetro de supermodo compacto para la detección simultánea de múltiples parámetros, implementado en una fibra óptica multinúcleo acoplada (MCF), e incorporamos esta novedosa configuración interferométrica al diseño de un láser de fibra para medir parámetros físicos como temperatura, deformación, estabilidad y torsión, ampliando así su potencial en aplicaciones de detección de alta precisión. Esta arquitectura permite la excitación e interferencia de supermodos guiados, cuyo patrón de interferencia espectral es extremadamente sensible a perturbaciones externas, mediante la fusión de un segmento de MCF acoplado entre fibras monomodo estándar. Mientras que la deformación axial modifica la propagación de fase efectiva de los supermodos, lo que se traduce en un desplazamiento de la franja medible en el espectro interferométrico, las variaciones de temperatura modifican el índice de refracción y la longitud del camino óptico de la fibra, lo que se traduce en desplazamientos espectrales predecibles.

Además, mediante efectos fotoelásticos, la deformación torsional provoca cambios en los índices de refracción del núcleo, lo que se traduce en desplazamientos de la longitud de onda únicos que pueden distinguirse de otras perturbaciones.

Cada magnitud física puede medirse con alta sensibilidad y precisión mediante la observación espectral de la interferencia supermodo en un analizador de espectro óptico (OSA). El interferómetro de supermodo propuesto representa una plataforma prometedora para la detección flexible, pasiva y multifuncional en la monitorización estructural, el control de procesos industriales, etc., gracias a su fácil fabricación mediante el empalme por fusión de fibra óptica estándar, su robustez mecánica y su compatibilidad con los componentes de telecomunicaciones actuales. Este trabajo mejora la comprensión y la aplicación práctica de los interferómetros basados en fibra multinúcleo para problemas reales de multidetección.

Contents

Figures Indices

Tables Indices

Chapter 1: Theoretical Framework

1.1. Introduction

Optical fibers have gradually been adopted in sensing technology for their multiple advantages, including multiplexing capability, remote sensing, high flexibility, low optical signal loss, high sensitivity, and immunity to electromagnetic interference. Research has also explored using them to sense temperature, strain, torsion, mode stability, pressure, shift, refractive index, corrosion, operational and ultrasonic speeds, and a wide range of other parameters [1]. Thus, optical fiber sensors have become essential tools for precision measurement in disciplines ranging from structural health monitoring to biochemical detection [1].

1.2. Optical fibers

An optical fiber is a thin, flexible cylindrical waveguide made of glass or plastic that is designed to transmit light over long distances with low loss. It consists of a core with a higher refractive index surrounded by cladding with a slightly lower refractive index. When light enters the fiber core within a certain range of angles, it is confined and guided along the length of the fiber through internal reflection, allowing light to travel from one location to another [2]. In the optical fibers, basic optical phenomena such as refraction, reflection, and diffraction must also be considered:

- Refraction occurs when light moves between two media having different refractive indices and causes it to bend. This is described by Snell's Law, which connects the angle of incidence and angle of refraction to refractive indices in those two media.

$$[n_1 \sin(\theta_1) = n_2 \sin(\theta_2)] \quad (1.1)$$

Where:

- n_1: refractive index of the first medium
- n_2: refractive index of the second medium
- θ_1: angle of incidence (with respect to the normal)
- θ_2: angle of refraction [3].

• Reflection, especially total internal reflection (TIR), is essential for guiding light through the fiber. This occurs when light moves from a higher-index medium (the fiber core) to a lower-index medium (the cladding) at an angle greater than the critical angle.

$$[\theta_c = n_2 / \sin(n_1)] \quad (1.2)$$

This causes the light to reflect completely within the core, so that it travels great distances without any attenuation. This process confines the light to the fiber, and it is also the basis of wave guiding in both single-mode and multimode fibers. These principles are depicted in diagrams 1.1: (a) total internal reflection, (b) partial reflection, and (c) critical angle [3].

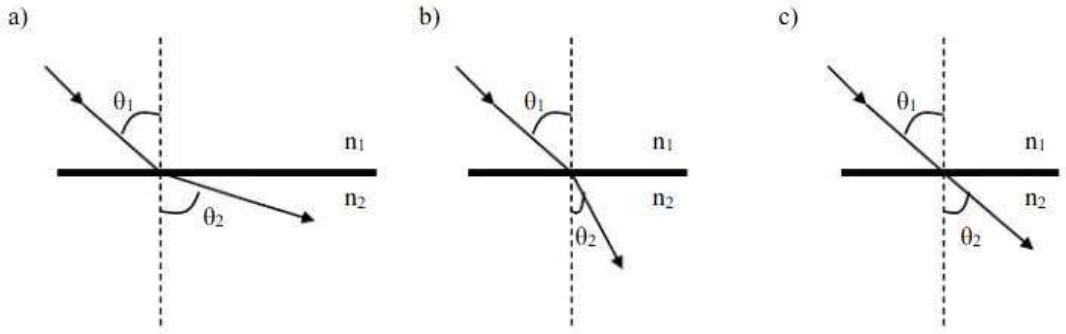

Fig. 1.1. Snell's law and total internal reflection [3].

- Diffraction is the bending or spreading of light waves after they pass an obstacle or opening that is approximately the size of the wavelength of the light.

  In standard optical fibers, diffraction is generally unimportant, but it plays a key role in microstructured or photonic crystal fibers (PCFs), where periodic air holes modify how light travels. Diffraction is also important in FBGs and in the design of interferometric sensors, as it generates interference patterns used in sensing applications.

All three phenomena, refraction, reflection, and diffraction, are critical for comprehension and optimizing the design of optical fiber systems used in communication and sensing enterprises [4].

1.2.1. Standard Single-Mode Fiber

Standard single-mode fibers are widely used in optical communications and sensors. They can support single-mode propagation, with very low losses and minimal dispersion. Its core size is small, around 8-10 μm, with a cladding of 125 μm, and this type guides light by total internal reflection. In the 1260-1650 nm wavelength range, these fibers propagate in the LP_{01} mode. Due to their low loss and high coherence, these fibers are ideal for very fine interferometer work [5]. Figure 1.2 shows a single-mode fiber.

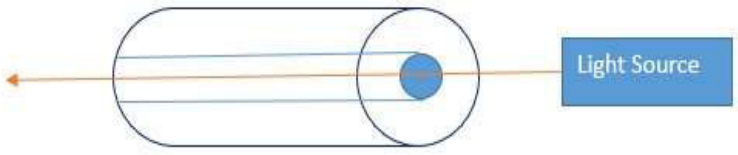

Fig.1.2. Schema of a Single-mode optical fiber

In single-mode optical fibers, refraction is necessary to enable light from a medium to enter to the fiber core. The core has a refractive index that is slightly higher than the cladding, creating the ideal conditions for total internal reflection.

Therefore, two fundamental principles are applied for understanding the loss or guidance of light in an optical fiber:

1. Snell's Law

Snell's law shows how light enters and is confined in the core.

$$[n_{core}\sin(\theta_{core}) = n_{clad}\sin(\theta_{clad})] \quad (1.3)$$

Where:

- n_{core} is the refractive index of the first medium (Core).
- n_{clad} is the refractive index of the first medium (Cladding).
- θ_{core} is an angle of incidence in the core.
- θ_{clad} is an angle of refraction into the cladding.

Total internal reflection occurs only when:

- $n_{core} > n_{clad}$
- Light travels from a denser to a less dense medium
- $\theta_{clad} = 90°$

From (1.3), Or Sin (90°) = 1, (1,3) become:

$n_{core}\sin(\theta_{core}) = n_{clad}$

$$sin(\theta_{core}) = \frac{n_{clad}}{n_{core}} \quad (1.4)$$

Thus,

$$(\theta_{core}) = \frac{n_{clad}}{\sin(n_{core})} \quad (1.5)$$

2. Fresnel Equations

Fresnel's equations describe how light is reflected and transmitted when it strikes the interface between two media with different refractive indices.

Refractance (R) for perpendicular (s) and parallel (p) polarization components:

$$Rs = |n_1 cos\theta_i - n_1 cos\theta_t / n_1 cos\theta_i + n_1 cos\theta_t\ |^2 \quad (1.6)$$

$$Rp = |n_1 cos\theta_i - n_1 cos\theta_t / n_1 cos\theta_i + n_1 cos\theta_t|^2 \quad (1.7)$$

Transmittance (T)

$$T = 1 - R \quad (1.8)$$

Where: θi and θt are angles of incidence and transmission, and n_1, n_2 are the refractive indices of the two media [5,6].

1.2.2. Multimode Fiber

Multimode fibers (MMFs) have larger core diameters: 50 to 62.5 μm. This allows for multiple modes of light propagation, causing modal dispersion. Modal dispersion, however, limits its use in interferometry.

Using MMFs at 850 nm and 1300 nm has yielded good results for short-range communications and sensing. Multimode fibers have the advantages of being easy to couple to light, withstanding high power, and being cost-effective for deployment. Nevertheless, due to a lower coherence and a higher level of noise,

this kind of fiber is not so useful in interferometry [7]. Figure 1.3 shows a multimode optical fiber.

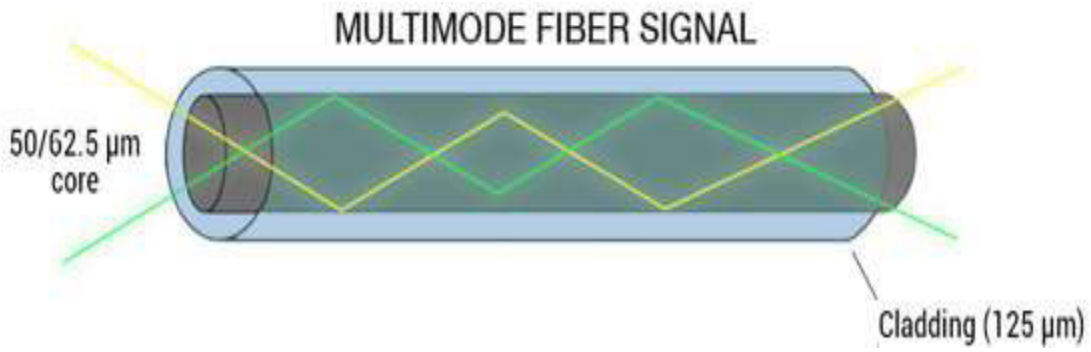

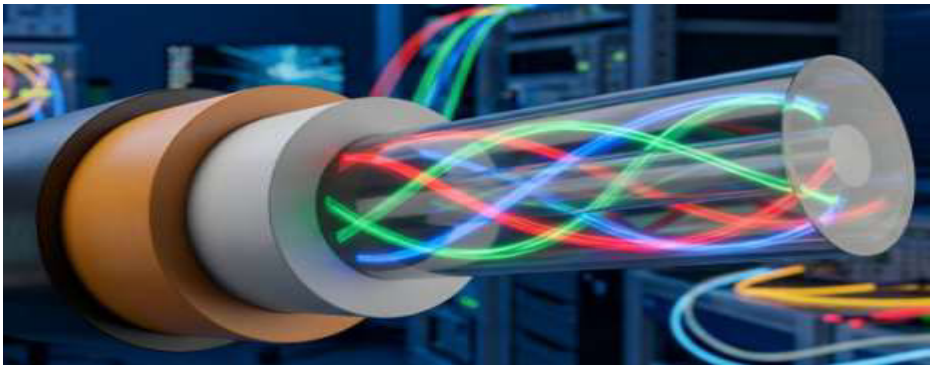

Fig.1.3. Multimode Fiber Signal [8].

1.2.3. Photonic Crystal Fibers

Photonic Crystal Fibers (PCFs) are a special type of optical fiber that contains a pattern of tiny air holes running along their length. Unlike conventional optical fibers, which guide light using a simple core and cladding structure, PCFs control light through their unique microstructured design. This structure allows better control of light propagation, reduces signal distortion, and enables guidance over a wide range of wavelengths. Because of these properties, PCFs are widely used in advanced applications such as supercontinuum light generation, environmental sensing, medical diagnostics, and high-power laser systems.

However, their fabrication and integration with standard optical fibers remain technically challenging [9-11]. Diagram 1.4 shows a microstructure arrangement of photonic crystal fibers.

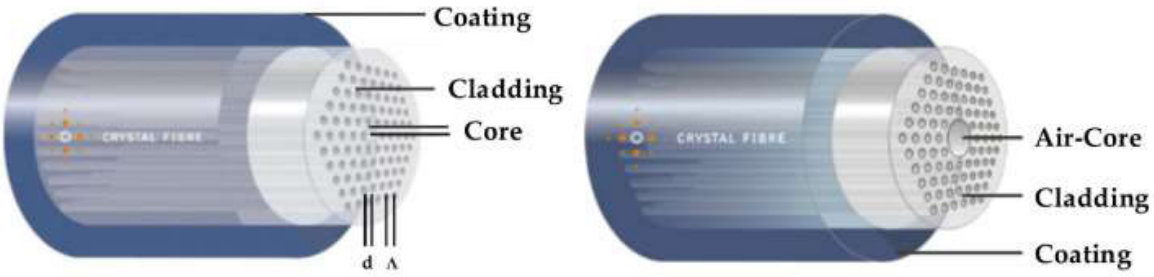

Fig.2.4. Microstructure arrangement of Photonic Crystal Fibers [12].

1.2.4. Multicore Fibers

Multicore fiber (MCF) is a type of optical fiber that contains multiple cores, allowing light to travel within a single cladding. The light can travel independently or be coupled in a supermode. The supermode interference (SSI) property of MCFs makes them a great option for small, high-performance interferometry sensing applications. MCFs can also act as spatially multiplexed sensor channels. They perform well in both distributed and multi-parameter sensing tasks; common applications include structural health monitoring, environmental sensing, and biomedical diagnostics [13]. The design of MCFs minimizes inter-core crosstalk and stabilizes the signal, which are both important for precise interferometric measurements. Figures 1.5 and 1.6 are depictions of single-mode multicore fibers.

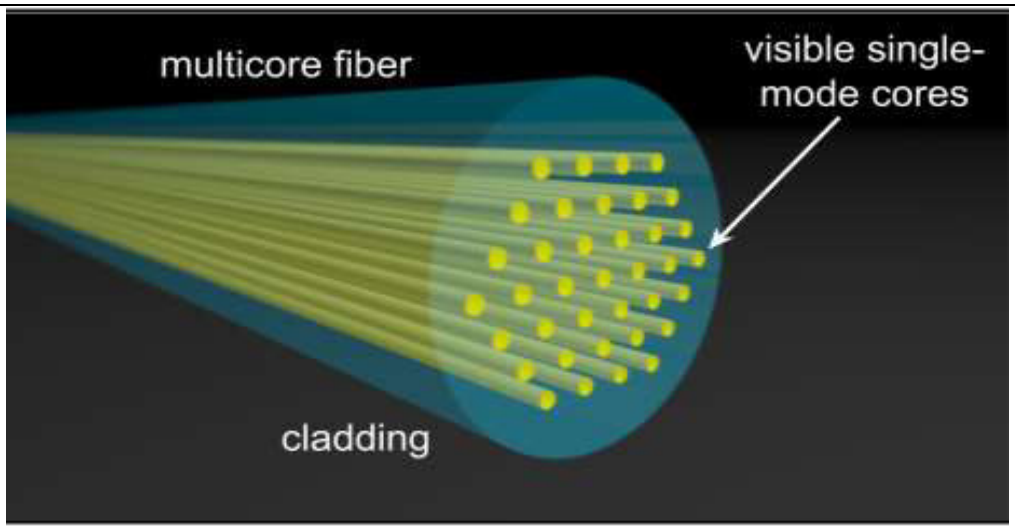

Fig.2.5. A single-mode multicore fiber [14].

Optical properties differ between Multicore Fibers (MCFs) and Standard Single-Mode Fibers (SMFs). MCFs have 2 to 19 or more cores within one cladding. In contrast, SMFs have only one core, which can support the basic LP_{01} mode. Each larger cladding of MCFs becomes a core caller and becomes capable of operating alone or able to work together through core-coupling, working as a supermode. It is possible to obtain a great deal of increase in transmission capacitance over SMFs that mainly do wavelength division multiplexing (WDM) by treating different cores as different channels.

However, MCFs may suffer from inter-core crosstalk, especially in cases where cores are too close to one another. By contrast, SMFs can minimize intercore crosstalk since their single kernel lacks any such paradoxes. An intensive, multi-parameter examination of any given environment becomes possible when MCFs are used with different cores simultaneously from which to take measurements. SMFs are preferred for single-parameter sensing and use with Fabry–Perot, Mach–Zehnder, or Michelson interferometers. The complexity of MCFs also affects the manufacture and fusion-splicing; it requires high precision ends and alignment.

MCFs offer flexible solutions for light-wave communication, high-bandwidth, and many types of space communication [15]. Table 1.1 summarizes the differences between Multicore and Single-mode Fibers.

Feature	**Multicore Fibers (MCFs)**	**Single-Mode Fibers (SMFs)**
Core structure	Multicore embedded within a single cladding	Single core with cladding
Mode propagation	Each core supports a mode. Cores support supermode when coupled	Supports the fundamental LP_{01} mode
Inter-Core Crosstalk	Occur between closely spaced cores; mitigated with trench-assisted designs	Not applicable, because there is only one core
Bandwidth & Capacity	Supports space-division multiplexing (SDM) for high-capacity transmission	Capacity enhanced by wavelength-division multiplexing (WDM)
Multiparameter Sensing	Enables simultaneous sensing of different parameters via different cores	Typically suited for single-parameter sensing
Interferometric Use	Used in advanced configurations	Common in Fabry-Perot, Mach-Zehnder
Code Coupling	Possible coupling between adjacent cores (intentional or accidental)	No coupling; single-mode only
Splicing Complexity	Requires precise core alignment across multiple channels	Standard, mature splicing techniques

Fabrication Complexity	Higher requires precise core symmetry and isolation	Lower, established, cost-effective manufacturing
Applications	Advanced sensing, high-speed communications, and imaging systems	Telecommunications, basic sensing, and medical instruments

Table 1.1. Difference between Multicore and Single-Mode Fibers [15]

1.3. Background

The evolution of optical sensors and interferometry was strongly influenced by technological advancements in light and lenses in the 17th century. The invention of the optical microscope and telescope paved the way for using light to observe physical properties. However, it was not until the 19th century that optical interferometry emerged as a powerful measurement technique [16]. One of these earliest breakthroughs was Thomas Young's double-slit experiment (1801), which demonstrated the wave nature of light and introduced the concept of interference [16]. Later still, Augustin Jean Fresnel and François Arago developed the theory of light interference, which laid the groundwork for interferometric measurement techniques [17].

The development of optical interferometry in the late 19th and early 20th centuries:

- Albert Michelson (1881-1887) developed the Michelson Interferometer, which became a fundamental device for high-precision measurements. The Michelson-Morley experiment (1887) helped disprove the existence of the luminiferous ether and later influenced Einstein's theory of relativity [18].

- Fabry and Perot (1899) introduced the Fabry-Perot Interferometer, which greatly improved spectral resolution and found wide use in spectroscopy and telecommunications [19].

As a result, these techniques allowed precise measurement, but they were limited in their application due to the amount of light available and the optical components.

In 1960, Theodore Maiman invented the laser. This invention has enormously improved optical sensors and interferometry [20]. The laser provided a coherently monochromic stable light source, which was extremely accurate and reliable for optical measurement techniques.

At:

- 1962: With the construction of the first laser Doppler velocimeter, the possibility of obtaining non-contact measurements of velocity and displacement [21,22].
- 1970: Developments in fiber optics, including the creation of low-loss optical fibers by Corning Inc., made it possible to send light over long distances [22].
- 1980–1990: Fiber optic sensors were developed that applied interferometry to obtain accurate measurements used in structural health monitoring, biomedical, and industrial sensors [23].

Thus, fiber optic sensors have become attractive and mature with the rapid development of optical fiber technology, and are widely used in telecommunication systems.

Major developments include:

- Bragg Gratings (1990s): Fiber Bragg Gratings (FBGs) provided distributed sensing along optical fiber sensing, advancing applications of strain and temperature measurements [24].

- Tunable Optical Interferometers (2000s): Developments in Michelson and Sagnac interferometers extended the performance of fiber optic measurement systems [25].
- Photonics Integration (2010s till now): Progress in photonic crystal fiber, plasmonic-based sensors, and laser-based spectroscopy has enhanced optical sensing technology [26].

However, on the other hand, various optical filter-type systems using special optical fibers have been intensively investigated in recent years. These sensors center around the uniform quantitative sensing of varying physical parameters [27,28]. The Fabry-Perot interferometers (FPI) [29,30], and the Bragg grating [31,32], with these interferometric devices, the key feature is the modulation of the input signal, which is generated by the broadband source. That is, the equilibrium between losses and gains allows us to obtain the principal features of the different optical configurations.

In addition to presenting different manufacturing techniques and multiple applications of fiber optic sensors in the literature, the physical analysis of the interferometric sensor prompted the scientific community to review its state of the art [33-36].

We can find applications such as filters capable of measuring humidity using photonic crystal fiber (PCF) under the MZI technique [37], developing interferometric bands in order to detect multiple polluting gases and reach the C, L, or U bands within the transmission spectrum [38,39].

Another area of interest and high impact is the development of fiber optic laser sources. We can combine interferometer sensors to modulate the laser emission output in this field. The search for laser emissions stands out for its characteristics, such as spectroscopic lines for optical processing, multiplexing of communication systems [40], high power, wavelength stability at room temperature, and low threshold operation.

Work has been carried out implementing various fiber lasers to monitor physical parameters such as temperature [41], bending [42], and torsion [43,44], among others.

Here, we highlight several studies that are closely related to the topic of this thesis:

In the reference [45], the author presents a compact, low-cost all-fiber Mach-Zehnder Interferometer (MZI) using a non-zero dispersion-shifted fiber (NZ-DSF) spliced between single-mode fibers (SMFs) with core-offset fusion. The NZ-DSF's core and cladding serve as the MZI arms, while the offset splices function as couplers. These authors have proposed and demonstrated a new Mach-Zehnder Interferometer based on a non-zero dispersion-shifted fiber. They implemented the MZI by a core offset splicing of a NZ-DSF between two segments of SMF, and several fringe contrasts of 2.25, 4.27, 5.22, and 20.54 dB were obtained, respectively.

Moreover, the MZI was tested for torsion sensing, and it was observed that the torsion effect induced a nonlinear behavior due to the shearing stress that is not uniform at the core-offset MZI structure. Here, by experimental measurements, they determined a sensitivity of 0.070 nm/° to a physical length of the NZ-DSF of 2.5 cm.

The following article presents a comprehensive review of interferometric sensors based on multicore fibers (MCFs), highlighting their unique advantages, including structural and functional diversity, high integration with compact form factors, space division multiplexing (SDM) capabilities, and robust yet straightforward fabrication processes. These features make MCF-based interferometric sensors highly versatile and effective for monitoring a wide range of physical and chemical parameters, such as temperature, strain, refractive index, vibration, flow, and torsion [46].

In this study, the author developed and demonstrated a low-cost method to produce an all-fiber, tunable, and wavelength-switchable erbium-doped fiber ring laser (EDFRL). The system was built using principal elements, adding a 3-meter-long erbium-doped fiber (EDF) as the gain medium, an arc-induced long-period fiber grating (LPFG) that acts as the wavelength-selective filter, a 980 nm laser diode (LD) as the pump source, a wavelength division multiplexer (WDM) for combining pump and signal wavelengths, and a section of DS/SMF fiber where the LPFG was inscribed. The LPFG was made with a commercial fusion splicer (S-176 from Fitel). The tunable and switchable tuning range of the EDFRL was 1526 – 1538 nm and 1568 – 1557 nm, with a maximum separation between two lasing wavelengths of approximately ~42nm, which is one of the maximum separations reported for an individual LPFG.

These results demonstrate that bent LPFGs can be used as efficient, reconfigurable wavelength-selective devices for WDM communication systems, fiber sensors, and photonic device characterization [47].

One other such example is given in [48]. In this paper, the authors demonstrate a new technique to achieve SLM operation in erbium-doped fiber ring lasers employing an MFR structure. This MFR configuration successfully eliminates the multi-longitudinal-mode (MLM) oscillation that typically occurs due to the bandwidth limitation of erbium gain and long cavity length. This configuration also allows the laser to tune from C-band into portions of the L-band.

The researchers tested optical signal-to-noise ratio (OSNR), output power, laser linewidth, and operational stability. The results showed that the MFR method successfully produces a stable and tunable SLM erbium-doped fiber laser.

In-fiber interferometric-based sensors are an emerging area in optical sensing, providing high precision in measuring physical and chemical parameters like temperature, pressure, and refractive index.

These sensors rely on light interference, where changes in the environment affect the optical path and phase difference, enabling accurate detection. Fabry–Perot interferometers (FOFPIs) are known for their high sensitivity and simple structure. They come in intrinsic and extrinsic forms, suitable for various uses, including biomedical and gas sensing. Mach–Zehnder interferometers (FOMZIs) are more complex but also offer high sensitivity by manipulating core and cladding modes in the fiber. Both FOFPIs and FOMZIs support multiplexing and multi-parameter sensing, which makes them crucial in areas such as environmental monitoring, structural health, and diagnostics [49].

1.4. Objectives

1.4.1. General objective

The main goal of this thesis is to create and study a fiber laser system that can monitor several physical parameters through dynamic modulation using embedded interferometric structures.

1.4.2. Specific Objectives

1. Study and understand the various components in a fiber laser. This point aims to grasp the basic parts that make up a fiber laser system.
2. Build different interferometers using multicore fibers and standard single-mode fibers. This goal involves designing and putting together interferometric structures for sensing within the laser system. Two main types will be created:
   - Multicore Fiber Interferometers: Using coupled cores to create Supermode Interferometers (SMIs).
   - Standard Single-Mode Fiber Interferometers: Such as Mach-Zehnder interferometers, built with techniques like core-offset splicing. The method of fabrication will use fusion splicing, precision alignment, and controlled displacement. The resulting structures will be tested for their spectral behavior, interference fringe quality, and insertion loss.

3. Test and evaluate the manufactured interferometers against various physical parameters. Each interferometer will undergo controlled changes in environmental and mechanical factors to determine its sensing capabilities: Strain, Temperature, Torsion, and Stability.
4. Create and implement a fiber optic laser that uses interferometers as wavelength selection filters. This ultimate goal brings together all previous efforts. A fiber laser system will be built, where the embedded interferometers act as filters, controlling the emission wavelength based on environmental conditions.

   The laser will serve both as a light source and a sensor, allowing the measurement of multiple parameters within a compact, all-fiber design.

Thus, Single-Mode Fibers (SMFs) are ideal for applications that need simplicity, lower cost, and high spectral purity, making them suitable for basic sensing systems. In contrast, Multicore Fibers (MCFs) offer higher sensitivity, multiparameter sensing, and spectral tunability through supermode interference. However, they require more complex fabrication and signal processing, making them more appropriate for advanced, high-performance sensing applications.

1.5. Justification

In recent years, fiber-optic sensors have attracted considerable interest because of their distinctive advantages. They offer a wide free spectral range (FSR), high fringe contrast, and a low lasing threshold. They are naturally immune to electromagnetic interference. With these attributes, they have become the best option for high-performance sensing systems and optical communication technologies [50]. Moreover, their compatibility with compact, all-fiber designs ensures their durability and flexibility in harsh environments. In tunable laser systems, fiber-optic interferometric structures commonly serve as wavelength-selecting filters (WSFs) [50,51], which are crucial for determining the laser's operating wavelength. They help suppress unwanted modes and improve spectral

purity. However, when WSFs are incorporated into fiber lasers, several technical difficulties arise, particularly with broad-spectrum gain media such as erbium-doped fiber (EDF).

A major challenge in EDF-based fiber lasers is maintaining a stable and selective lasing wavelength. This involves carefully balancing intracavity losses and gain saturation dynamics. In multimode cavities, there's an increased risk of multi-wavelength lasing because of the EDF's broad amplification bandwidth.

To address these instabilities, various strategies have been suggested in the literature. These include:

- Polarization controllers to manage spectral fluctuations caused by birefringence.
- Dispersion-shifted fibers (DSF) to change the phase-matching condition and lessen mode competition.
- Interferometric filters like Mach-Zehnder interferometers (MZIs), and supermode interferometers (SMIs) to improve selectivity [52,53].

In this thesis, we propose designing, fabricating, and implementing a fiber laser system based on a Supermode Interferometer (SMI) made from multicore fiber (MCF). The MCF-based SMI has two roles:

- Wavelength selection filter (WSF), determining the lasing wavelength with high accuracy.
- Optical transducer, converting changes in the environment, like strain, temperature, and torsion, into measurable spectral shifts.

The inter-core coupling in the MCF allows the excitation of optical supermodes. These supermodes can interfere constructively or destructively based on external effects and geometry. The interference patterns create periodic transmission spectra that can be finely adjusted by changing factors such as fiber length, core

separation, or surrounding index. This makes the SMI a strong structure for both filtering and multi-parameter sensing.

1.6. Organization of the thesis

This thesis is separated into five Chapters. Chapter 1, Theoretical Framework, introduces the fundamental concepts necessary to understand the investigation context, including the importance of sensors, the objectives, and the justification for the study. Chapter 2, Interferometry, presents the theoretical and practical foundations of fiber optic interferometry, laser systems, and related optical components used in the design. Chapter 3 details the experimental procedures, component characterizations, and fabrication methods employed to develop the laser system and interferometric sensors. Chapter 4 presents and analyzes the experimental results, including the sensor's response to different stimuli and the stability and spectral behavior of the laser, and Chapter 5 summarizes the achievements of the investigation, identifies limitations, and proposes directions for future work. Then will follow the references.

Chapter 2: Interferometry

Interferometry is a highly sensitive optical technique that measures small changes in optical path length, phase, or frequency by analyzing the interference of coherent light waves. When two or more light beams are combined, they produce an interference pattern (fringes) resulting from constructive and destructive interference, which depends on their phase difference. Several interferometer configurations exist, including the Mach-Zehnder (MZI), Fabry-Perot, Michelson, and Sagnac Interferometers [[54]. Details will be provided in the development of this thesis.

With interferometry, scientists observe interactions between waves to gain useful physical knowledge. Interferometers operate by splitting coherent light into two or more paths that are later recombined to produce an interference pattern. The resulting signal depends on the optical path difference (OPD), which can be affected by changes in refractive index, path length, temperature, or mechanical strain. Because of their high sensitivity to phase changes, interferometers can detect extremely small variations in environmental conditions, which makes them highly suitable for high-precision sensing and metrology [55].

2.1. Interference

Interference is a phenomenon that happens when two coherent light waves intersect. The waves overlap both spatially and temporally and thus create a new wave pattern in space. The intensity distribution of the resulting waves is used to measure physical changes.

In optics, interference is definitely one of the basic physical principles behind a whole range of precise measuring systems and instruments, such as interferometers [56,57].

2.1.1. Two-Wave Interference

Several characteristics are sine qua non for creating interference in an optical fiber system. They are:

- High Temporal and Spatial Coherence: The light source should have high temporal and spatial coherence. Coherence is important because it allows light waves to remain in a fixed phase relationship, which is necessary for stable and visible interference patterns. Usually, narrow-linewidth lasers or broadband sources that have been appropriately filtered to ensure coherence are used.
- Optical Path Length Difference: Another essential feature is having an optical path length difference between two beams, or modes, resulting in a phase shift upon addition that brings about constructive or destructive interference [57].

$$\Delta \mathrm{OPD} = |n_1 L_1 - n_2 L_2| < Lc \quad (2.1)$$

Where:

- n_1, n_2 are refractive indices
- L_1, L_2 are physical path lengths
- *L*c is the coherence length of the source [57].

The Interference is the result of the superposition of two or more coherent light waves. The total intensity is given by:

$$I = I_1 + I_2 + 2\sqrt{I_1 I_2 cos(\Delta \emptyset)} \quad (2.2)$$

Where I_1, I_{12} are the intensities of the two waves, and $\Delta\emptyset$ is the phase difference between them [57].

In addition, the polarization state of the two interfering waves should be matched or controlled. If they are not, that will cause visibility to decline and interfere with observation. On the other hand, structural symmetry and stability in the interferometric system are needed to keep constant phase relationships over time.

The physical overlap of light modes, especially in multimode or multicore systems, ensures both proper mixing and on-the-spot interaction among system fields. A pattern of interference is shown in Figure 2.1.

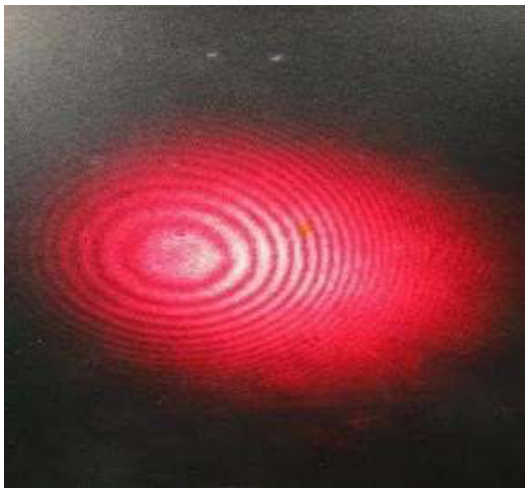

Fig.2.1. Example of the pattern of interference.

Thus, the spacing in wavelength between two consecutive interference maxima (free spectral range, FSR) is given by:

$$FSR = \lambda 2 / n\Delta L \quad (2.3)$$

Where:

- λ is the center wavelength

- *n* is the refractive index of the fiber core
- *ΔL* is the optical path difference between the interferometer arms [58].

This equation is especially useful for evaluating the spectral resolution of Fabry–Perot and Mach–Zehnder interferometers. With Supermode Interferometers (SMIs) in Multicore Fibers (MCFs), it is necessary to include:

$$\Delta\phi = 2\pi . \Delta n . L/\lambda \quad (2.4)$$

Where:

- *Δn* is the difference in effective refractive indices of the supermodes supported by coupled cores [58].

The Free Spectral Range (FSR) is crucial for different optical systems such as fiber optic sensors, lasers, and wavelength-division multiplexing (WDM) networks. In fiber optic sensors, it influences the spectral resolution and dynamic range, and it also determines the spacing between consecutive interference fringes. In lasers, the FSR, particularly in Fabry–Perot laser cavities, determines the spacing between longitudinal modes. This spacing affects both the stability and spectral purity of the laser. In WDM systems, the FSR is required to keep wavelength channels separated so that efficient multiplexing can be made.

With a smaller FSR, the distance between spectral peaks is smaller. This increases the resolution of measurements but also makes it more difficult to distinguish between peaks. However, a bigger FSR means fewer peaks are generated over a given wavelength range. This property is useful for multi-parameter sensing and dense WDM applications, as it reduces spectral overlap and crosstalk [59,60].

2.1.2. Interferometers

Interferometers are superior as sensors of physical parameters because they convert very small variations in parameters into measurable phase changes in light.

Interferometric sensors offer very high sensitivity to phase changes, high resolution, multiparameter sensing capability, compact and distributed sensing, compatibility with laser sources, and immunity to electromagnetic interference, making them ideal for precision sensing applications. Common interferometer configurations, including the Mach-Zehnder, Michelson, Fabry-Perot, and Sagnac, are capable of detecting phase variations smaller than one optical wavelength for accurate environmental monitoring. [60]. Figure 2.2 illustrates a schematic diagram of a typical interferometer.

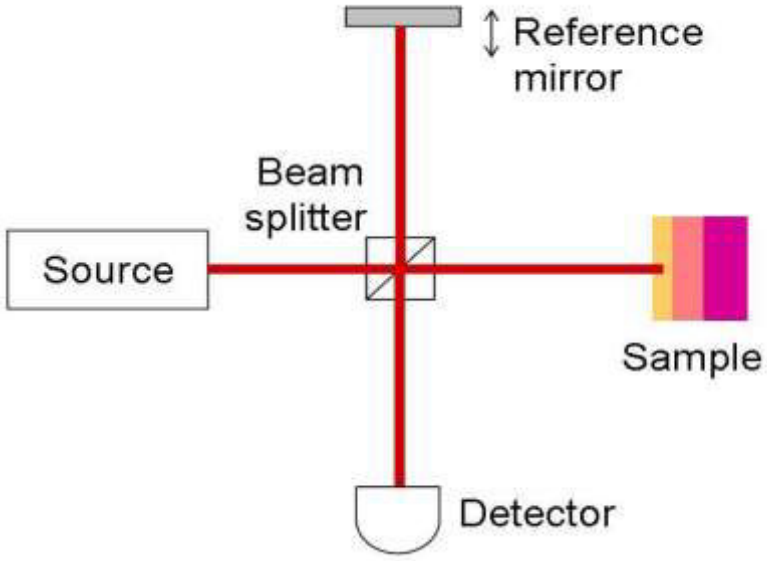

Fig.2.2. Sample of interferometer [61].

2.1.3. Type of interferometers

1. Tunable Optical Fiber Interferometers

Fiber Optical Interference is an interferometric system based on fiber that can adjust the optical path difference (OPD) between interfering light beams. This

tunability makes them great for optical sensing, signal processing, and wavelength filtering.

It's achieved by various methods, such as piezoelectric stretchers, thermal tuning, electro-optic or acousto-optic modulation, pressure or strain control, and variable-delay lines. Types of Tunable Fiber Interferometers:

- MZI: Two-arm Mach-Zehnder Interferometer (MZI), where both arms are individually modified and widely applied in the sensing field.

- FPI: The cavity length of a Fabry–Perot Interferometer is tuned to shift away from resonance peaks, or one end of the cavity portion may be moved out to achieve a suitable balance between the two mirrors.

- Michelson Interferometer: Tuning requires changing both the length of what it's named after as well as its mirror positions.

- Sagnac Interferometer: Uses rotation to give phase shifts; can be tuned using thermal or strain devices.

Applications [62]

- Optical Sensing: Tunability can give us the means to measure temperature accurately, strain, pressure, vibration, and more.
- Tunable Filters: Tunable FPIs are used in DWDM (Dense Wavelength Division Multiplexing) to choose or block particular wavelengths; this is vital if you want any part of a network to be visible without jamming out everything else.
- Optical Signal Processing and Photonic Integrated Circuits: Phase Modulation and Switching are essential operations in these applications.
- Laser Stabilization: Interferometers capable of fine-tuning wavelengths help make sure the laser gets sent only where it needs to go.

A. Mach-Zehnder Interferometer (MZI)

A Mach–Zehnder (MZI) Interferometer is an optical device used to measure the phase shift caused by environmental changes. It works by splitting one coherent light beam into two paths, known as “arms”. These two arms are independent, whether they are physically distinct or optically distinct, and may be subject to different outside conditions, such as temperature changes due to regional variances; force load deformation created under loads from stretching forces, pressure applied on an area of interest along its surface with high pressures per unit volume against exterior surfaces. After being exposed to their respective paths, the two light beams are then brought together once again. Any difference in the length of an optical path between these two arcs is caused by environmental perturbations, which leads to a phase shift among the beams. Owing to their configuration, Mach-Zehnder interferometers (MZIs) exhibit high sensitivity to phase variations, making them widely used in sensing applications for structural health monitoring and environmental monitoring, such as measuring temperature or strain simultaneously. The latter half of the 1980s saw the use become progressively widespread as researchers readily utilized low-loss optical fiber links (both single-mode and multimode) [63,64]. The schematic of the Mach-Zehnder Interferometer is given by diagram 2.3:

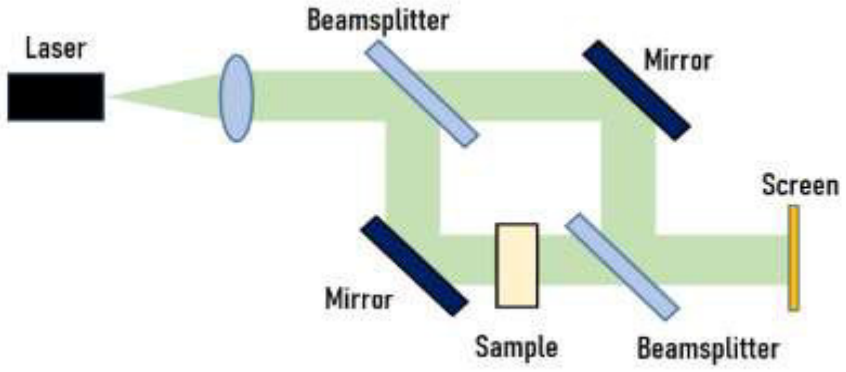

Fig. 2.3. Schematic of Mach–Zehnder Interferometer [65].

B. Sagnac Interferometer

The Sagnac Interferometer is an optical device used to detect rotational motion based on the Sagnac effect. In this system, a coherent light beam is split into two beams that propagate in opposite directions around a closed loop. When the system is stationary, both beams travel identical paths and recombine in phase, producing an interference pattern.

However, when the loop rotates, the counter-propagating beams acquire different effective path lengths, resulting in a phase shift between them. This phase shift changes the interference pattern, and the magnitude of the shift is proportional to the rotation rate and the area enclosed by the loop. This principle is used in a Fiber Optic Gyroscope (FOG), which contains no moving parts and is widely used for navigation of aircraft, spacecraft, and submarines. Increasing the fiber length or the number of loops improves sensitivity, while the use of single-mode optical fiber enhances measurement accuracy [66]. Diagram 2.4 details the experimental setup for what we have come to call the Sagnac Fiber Interferometer.

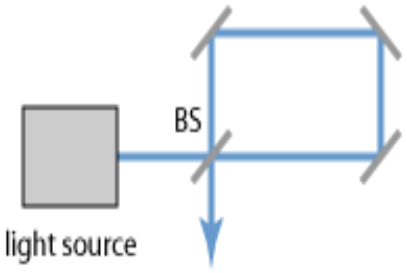

Fig. 2.4. Sagnac Interferometer [66]

C. Michelson Interferometer

The Michelson Interferometer creates an interference pattern by splitting a light beam into two arms, reflecting them with mirrors, and recombining them. Because the light travels each arm twice (forward and back), any change in optical path length is amplified. Variation in strain, temperature, or refractive index in either arm causes a phase shift in the interference pattern. Due to its simple design and robustness, the Michelson interferometer is widely used for high-precision sensing, including structural health monitoring, temperature measurement, and stress detection in engineering and geographical systems. [66]. Diagram 2.5 shows how a recording device works with a Michelson Interferometer.

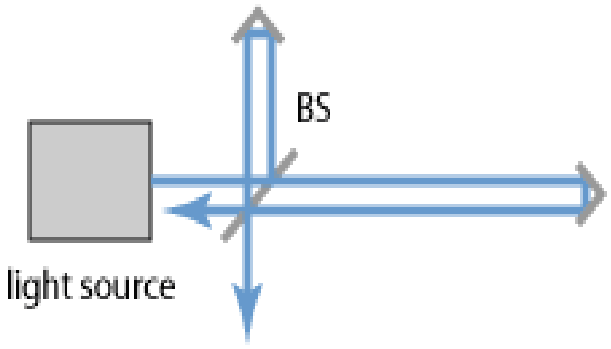

Fig. 2.5. Schematic of Michelson Interferometer [66].

D. Fabry-Perot Interferometer

The Fabry-Perot Interferometer (FPI) consists of two parallel, partially reflective mirrors that create multiple reflections of light between them. Interference depends on the light's wavelength and the distance between the mirrors, producing sharp and periodic transmission peaks. Because of its high spectral resolution, the FPI is widely used in high-resolution spectroscopy and wavelength filtering.

Fabry-Perot interferometers are applied in spectrometers, telecommunications, laser analysis, and optical research. In fiber-optic sensing, Fabry-Perot cavities can also measure changes in temperature or pressure, as these variations shift the interference fringes and allow precise monitoring [67]. The Fabry-Perot interferometer is pictured in Figure 2.6.

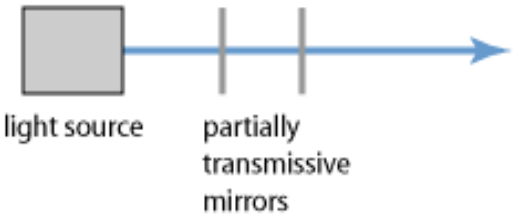

Fig. 2.6. Image of Fabry-Perot Interferometer [68]

2.2. Sensors

Sensor technologies have significantly transformed daily life by enabling the detection and monitoring of environmental changes such as light, temperature, sound waves, and vibrations.

These technologies are widely applied in fields such as medicine and industry, where they monitor physical, chemical, and biological parameters, and provide real-time data for diagnosis, control, and optimization [69].

A Sensor is a device that detects and measures physical, chemical, or biological changes in the environment and converts them into signals that can be processed, interpreted, or recorded by computers or other systems [69]. Basically, a sensor receives information from the environment, such as temperature, light, pressure, motion, etc., and translates that information into an electrical output like voltage, current, resistance, or a digital signal that can be interpreted by electronics or control systems.

The basic working process of most sensors follows this sequence:

1. Detection: a physical quantity, such as temperature, light, or force, interacts with a sensitive element inside the sensor.
2. Transduction: that interaction causes a change in an electrical parameter (for example, resistance, capacitance) through effects like thermoelectric, piezoelectric, photoelectric, or electromagnetic induction.
3. Signal conditioning: the raw electric effect is converted and conditioned into a readable signal (for example, voltage or digital data), often using circuits that amplify, filter, and linearize the output.
4. Processing: the conditioned signal is sent to another system (OSA, controller, etc.) for measurement, monitoring, control, or decision-making.

Generally, sensors have the following essential components:

- Sensitive element: The component of a sensor that interacts directly with a physical property being measured.
- Transducer/Conversion element: Changes the physical variation from the sensitive element (such as strain, displacement, etc.) into an electrical signal.
- Signal conditioning circuit: The circuit that adjusts (e.g., amplifying, filtering, analog-to-digital conversion) the electrical signal to make it suitable for use in measurement systems.
- Output Interference: The device that provides the final, conditioned signal either in an analog or digital form to the outside, such as a display, recording, or OSA [69].

2.2.1. Different types of sensors

Sensors can be classified in many ways, including by what they measure, how they operate, and how they output signals.

a. By measured quantity, we have temperature sensors, Light sensors, Proximity sensors, etc. They are detecting physical quantities.
b. By operating principle, resistive sensors and capacitive sensors rely on physical effects.
c. By signal output format, analog and digital sensors.
d. By energy usage, active and passive sensors [70].

We will focus on light sensors because this thesis is dedicated to the study of optical fiber sensors, which rely on changes in light propagation within the fiber to measure physical quantities such as strain, torsion, and temperature.

2.2.1.1. Optical fiber sensors

Optical fiber sensors are devices that use optical fibers as the sensing medium to detect changes in physical, chemical, or environmental parameters and convert them into measurable optical signals. When an external perturbation, such as temperature, strain, torsion, or refractive index variation, interacts with the fiber, it alters the properties of the guided light, for example, its phase, wavelength, intensity, or interference pattern. The changes will be measured with the Optical Spectrum Analyzer.

Optical fiber sensors are well known for their high sensitivity, immunity to electromagnetic interference, compactness, and multi-parameter measuring capabilities. New developments, such as multi-sensor devices based on multicore optical fibers, provide accurate and reliable measurements in critical applications [71].

2.2.1.2. Multicore fiber sensors

Multicore optical fibers (MCFs) are a special class of optical fiber where multiple cores are embedded within a single cladding. This design allows light to propagate in several special channels simultaneously. The proximity of the cores and their optical coupling properties determine light fluidity.

Light can either remain largely confined in each core (weakly coupled multicore fiber) or interact strongly between cores, forming supermodes (strongly coupled multicore fiber), collective mode patterns that extend across multiple cores. The multicore

structure provides several advantages for sensing, such as space division multiplexing, differential sensitivity, and simplified fabrication [72].

2.2.1.3. Supermode interferometer

A supermode interferometer (SMI) based on multicore fiber is a sensor architecture that exploits the strong coupling between cores to generate collective mode patterns known as supermodes. In a strongly coupled MCF, the distance between cores is reduced so that light can couple efficiently between them.

A set of supermodes with different propagation constants is excited by the injected light when a brief segment of strongly coupled MCF is spliced between standard single-mode fibers (SMF–MCF–SMF). There is a production of an interference spectrum with distinct peaks and valleys. The interference pattern is shifted by changes in the effective refractive indices or optical path differences of the supermodes caused by external physical perturbations like temperature changes or variations in refractive index. The sensor will determine the strength of the external disturbance by tracking these spectral shifts. Supermode multicore sensor provides compact, robust, and multi-parameter measurement capability with relatively simple fabrication and readout method [73].

2.3. The Laser

A laser, or "Light Amplification by Stimulated Emission of Radiation," is an instrument that creates a single, highly focused beam of light. In contrast, ordinary light sources emit incoherent light. Lasers are characterized by being:

- Coherent: All the light waves are in sync with each other - the peaks and troughs of one wave correspond exactly to those of another.
- Monochromatic: This single wavelength of light appears as one color only.

- Directional: The beam is narrow and concentrated, with very little scattering.
- Intense: The output can be greatly strengthened, making it suitable for uses in medicine, communications, and cutting materials [74].

2.3.1. Types of Lasers

Lasers are typically classified according to the type of gain medium used to amplify light. For example, gas lasers use gases such as helium-neon, carbon dioxide (CO_2), or argon to produce laser light. Semiconductor lasers, such as laser diodes, use semiconductor materials as the gain medium. Another important type is the fiber laser, which uses optical fibers doped with rare-earth elements like erbium or ytterbium to generate amplification. Among these types, fiber lasers are particularly well-suited for sensing applications. They offer advantages such as compact integration, high beam quality, efficient heat dissipation, and strong compatibility with fiber-optic components. Table 2.1 explains different characteristics of laser types and their applications.

Laser Type	Active Medium	Wavelength (nm)	Power Range	Class	Typical Applications
Gas Laser (He-Ne)	Helium-Neon gas	632.8	Low (mW)	II–III	Alignment, Holography
Gas Laser (CO_2)	Carbon Dioxide gas	10,600	High (W–kW)	IV	Cutting, Welding
Solid State Laser (Nd: YAG)	Neodymium-doped Yttrium Aluminum Garnet	1064	Medium–High (W–kW)	IV	Surgery, Materials Processing

Diode Laser	Semiconductor junction	630–1600	Low–Medium (mW–W)	I–IIIb	Optical Communication, Pointers
Fiber Laser	Doped optical fiber (e.g., Erbium)	1060–1560	Medium–High (W– kW)	IV	Sensing, Telecommunications
Excimer Laser	Excimer gas mixture	193–351	High (pulse)	IV	Eye Surgery, Lithography
Dye Laser	Organic dye in solution	400–700	Low–Medium (mW–W)	IIIb–IV	Spectroscopy

Table 2.1. Laser type and application [75].

2.3.1.1. Fiber Laser

A fiber laser is a type of solid-state laser in which an optical fiber doped with rare-earth elements, such as ytterbium, erbium, or neodymium, serves as the active gain medium, the part that amplifies light. In this case, we will use erbium.

The fiber laser works on this principle: the pump light is injected into the optical fiber using laser diodes. The erbium receives energy from this light. Pump light is absorbed by erbium, and its electrons rise in energy. Excited electrons release photons when they settle back to lower energy levels.

These photons cause stimulated emission and amplification because they have the same wavelength and phase as incoming light. The fiber extremities serve as mirrors for reflection. These Optical fibers itself produces and amplify the laser light and direct the beam to the desired location. [76].

2.3.2. Basic Components of a Laser

Lasers work by amplifying light through stimulated emission in a gain medium that is energized by a pump source, like an electrical current or optical pumping. The optical cavity, usually made of mirrors or reflective ends of optical fibers, traps the light. This allows it to move back and forth, stimulating more emissions and creating coherent light. Laser emission relies on three basic physical processes that involve the interaction of light with matter: absorption, spontaneous emission, and stimulated emission. Here's a clear explanation of how laser light is generated:

1. Energy Absorption (Excitation): Atoms or molecules in the gain medium, which is the active laser material, absorb energy from an external pump source. This source can be optical, electrical, or chemical. The energy raises electrons in the atoms to a higher excited energy state.

   Example: In a semiconductor laser, an electrical current provides this energy; in a gas or solid-state laser, a flash lamp or another laser may serve as the pump.

2. Spontaneous Emission: After excitation, electrons do not remain in the excited state forever. Finally, they return to lower energy states and release energy in the form of photons. This process occurs randomly in direction and phase.

   While spontaneous emission initiates the laser process, it does not produce coherent light on its own.

3. Stimulated Emission (Core Laser Mechanism): If an electron in an excited state meets a photon with exactly the right energy, matching the energy difference between the excited and ground states, it can drop to a lower energy level and emit a second photon. This second photon has the same

wavelength, phase, direction, and polarization as the incoming one. This leads to coherent light amplification.

4. Population Inversion: There must be more atoms in the excited state for stimulated emission to exceed absorption. This situation is called population inversion and is achieved through enough and continuous pumping. Without population inversion, the medium would absorb more light than it emits, stopping laser action.
5. Optical Resonator (Feedback Mechanism): The laser setup includes an optical resonator, usually made of two mirrors placed at opposite ends of the gain medium, one is fully reflective, and the other is partially reflective, permitting light to escape as the laser beam. - Light bounces back and forth, stimulating more emissions and amplifying the beam each time it passes through the gain medium.
6. Laser's Beam Emission: As the light is amplified repeatedly and its intensity increases, a part of it exits through the partially transparent mirror as a coherent, monochromatic, collimated laser beam. In fiber lasers, the gain medium is an optical fiber treated with rare-earth elements such as erbium, ytterbium, or neodymium. These setups offer benefits such as compact size, high efficiency, and easy integration into optical sensing systems.

Adding interferometers to fiber laser systems offers several benefits: improved sensitivity in sensing applications due to the laser's coherent and stable output; compact design and seamless integration, since all components are fiber-based; and high versatility, with adjustable spectral filtering that suits various applications, including telecommunications and distributed optical sensing [77-79]. Figure 2.7 illustrates these benefits. The laser components are presented in Figure 80.

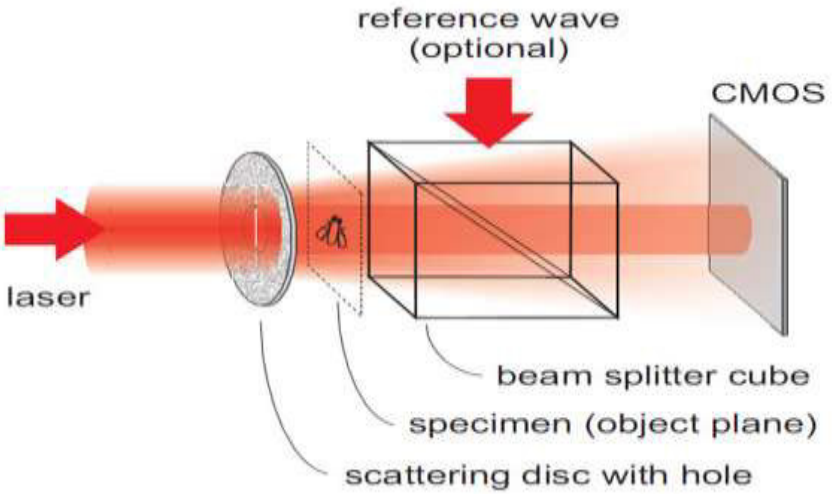

Fig. 2.7. The laser components [80].

2.4. Wavelength Division Multiplexing (WDM)

Wavelength Division Multiplexing (WDM) is a fundamental technique in fiber-optic communication that dramatically increases the throughput and transmission capacity of a single fiber by using various optical-carrier signals to simultaneously send each at different wavelengths. Those carriers are all 'colors' of laser emission: wavelength [81].

2.4.1. WDM Functionality

WDM's technology makes it possible for each wavelength to carry its own data stream. This increases the fiber's capacity to carry information. WDM systems work by using multiplexers at the transmitter end to combine different wavelength channels into a single fiber and demultiplexers at the receiver end to separate them for processing.

There are two principal types of WDM:

- Coarse WDM (CWDM): Uses fewer channels with wider spacing (usually around 20 nm apart) and is suitable for shorter range transmission.
- Dense WDM (DWDM): Provides dozens to hundreds of closely spaced channels (about 0.8 nm spaced), making it ideal for long-haul and high-capacity networks.

The WDM applications are extensive and include telecommunications and Internet backbones, where it greatly increases data throughput without the need to lay more fiber. In fiber optic sensing, WDM makes it possible to use several sensors along one fiber, each operating at a different wavelength to monitor parameters such as temperature, strain, or pressure. WDM is also valuable in data centers, where it makes efficient use of infrastructure by transmitting multiple high-speed signals through a single fiber.

WDM optimizes the use of existing fiber infrastructure and supports scalable, flexible network designs. It permits remote and distributed sensing over long distances [81,82]. At the receiving end of a Wavelength Division Multiplexing (WDM) system, the multiplexed optical signal is split into its constituent components by an optical demultiplexer. Each one of these signals can then be received as an independent wavelength. Diagram 2.8 illustrates the Wavelength Division Multiplexing in multicore fibers transmitting multiple data streams, each on a different wavelength, through multiple cores within a single fiber.

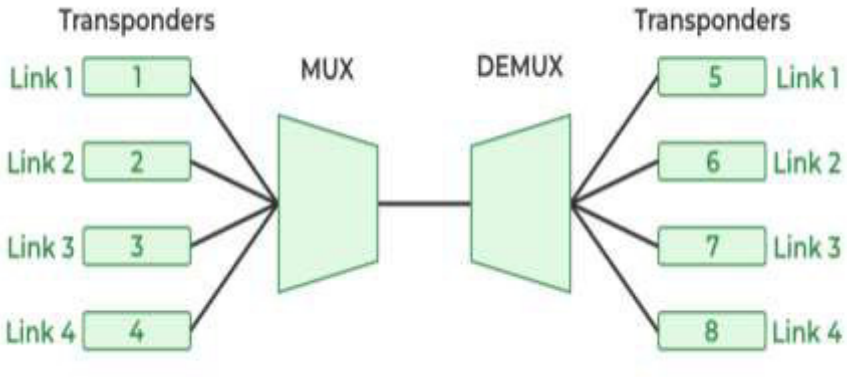

Fig.2.8. Basic WDM Technology Diagram [83].

2.5. Doped Fiber Amplifiers

Erbium-Doped Fiber Amplifiers (EDFAs) are important constituents of advanced communication systems, particularly for long-distance data transfer.

2.5.1. Erbium-Doped Fiber Amplifier (EDFA)

In the first studies to amplify light in the C-band from around 1530 to 1565 nm, this part of the spectrum has low transmission loss in well-established single-mode fibers, making it ideal for long-distance communications. EDFAs consist of a length of optical fiber that is doped with erbium ions. An external pump laser of typically 980 nm or 1480 nm pumps up these ions to place them in an excited state. As the signal light moves through the doped fiber in the C-band, it's absorbed by the excited ions, causing them to release more photons and thus amplify the signal without converting it into an electrical form. As well as functioning as amplifiers in communication systems, fiber lasers often use EDFAs as the gain medium. Here, they pump light and provide sources of Amplified Spontaneous Emission (ASE). This ASE can be used either as a kind of broad light source or filtered into narrow-band laser signals, depending on whether they are to be used for experimental purposes or for application within the system.

This ASE can be presented as a more standardized broad light source, or it can be filtered to give narrow-band laser signals [84]. The EDFA has a simplified block-diagram configuration with input and output pump lasers and an erbium-doped optical fiber between them in Figure 2.9.

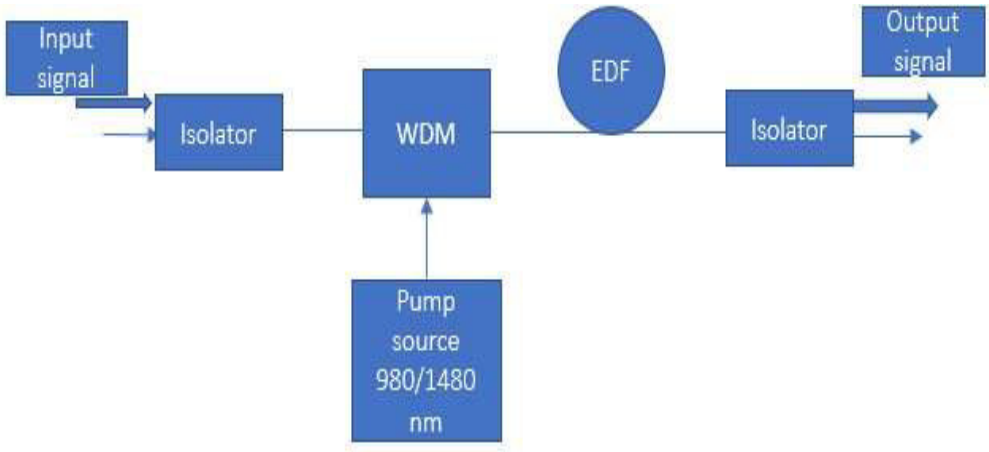

Fig.2.9. The basic block diagram of an EDFA

2.5.2. Ytterbium-Doped Fiber Amplification

Ytterbium-doped fibers (YDFs) are essential in modern fiber laser and amplifier technologies. They are valued for their high gain and efficiency in the 1 μm wavelength range, typically between 1030 and 1100 nm. These fibers contain the rare-earth element ytterbium (Yb^{3+}), which has a simple two-level energy structure. This structure reduces non-radiative decay and improves optical efficiency. Because of this simplicity, YDFs have low quantum defect and generate less heat, making them suitable for high-power applications. They are commonly used to build high-power fiber lasers for industrial tasks such as cutting, welding, and engraving. They also find use in medical, military, and scientific fields that need strong and efficient laser sources.

Furthermore, ytterbium-doped fiber lasers often act as pump sources in two-stage amplification systems, especially when pumping erbium-doped fiber amplifiers (EDFAs). In this setup, a high-power ytterbium laser operating around 1064 nm pumps the erbium-doped fiber, which amplifies optical signals in the C-band, approximately 1530 to 1565 nm. This method increases the overall gain and output power of the system, facilitating long-distance optical communication and high data-rate transmission.

The ability of YDFs to provide high output power with excellent beam quality and thermal stability makes them a key element in modern photonic systems [85]. Figure 2.10 shows the fiber doped with Ytterbium.

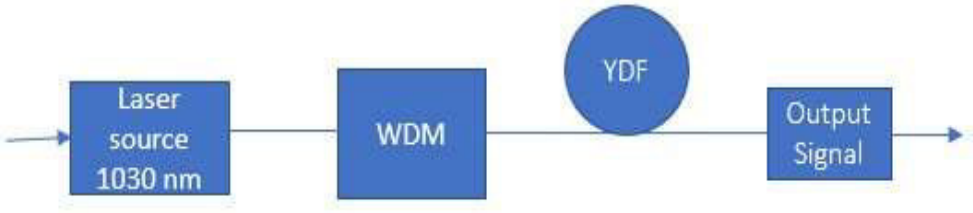

Fig. 2.10. The fiber doped with Ytterbium.

2.6. Optical Isolator

An optical isolator is typically a passive component in photonic systems that prevents unwanted back reflections or backscattering of light traveling from a laser to other sensitive components. This shielding ensures stable operation as well as protection for sensitive parts of optical systems, such as fiber optic cables, where disruption from external noise could cause catastrophic failure.

Isolation circuits cook waste heat and clean power supplies. All drives in the circuit are independent of each other. The circuit keeps waste going out of the box. It detects feedback voltage from the metal detection system and sends an inverted signal back to it.

For example, interocular crosstalk inside the eyewear itself interferes with the 3D effect. Another problem is that the electronics that process 3D information are not easy to integrate. Most scanners and projectors today cannot yet handle stereo input [86]. Diagram 2.11 illustrates a simple schematic of an optoisolator.

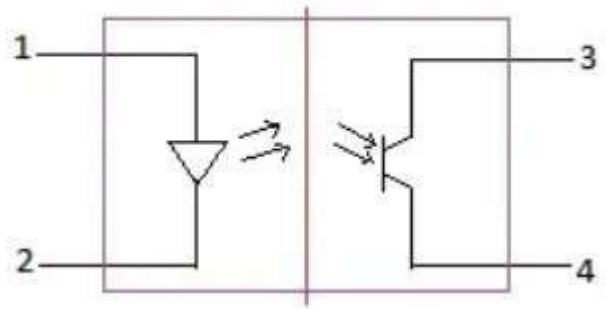

Fig.2.11. Simple schematic of an optoisolator [86].

2.6.1. Characteristics of an Optical Isolator

Isolation is essential in interferometric sensing systems, such as those that use Supermode Interferometers in multicore fibers. Optical isolators help maintain signal quality and system stability by removing feedback that can damage interference patterns or measurement precision. An isolator usually operates on the Faraday effect. This effect causes a one-way rotation in the polarization of the light, so that light from only one direction can pass through.

An optical isolator is a component that plays a vital role in photonic systems. For a start, it ensures that light can go in only one direction. It effectively cuts off any light traveling in the opposite direction. This function has special significance in laser systems where reflected light can produce instability, noise, or even damage to the laser cavity. An optical fiber coupler is a passive component used in fiber optic systems to combine optical signals. It allows light from one or more input fibers to be sent to two or more output fibers.

Depending on the design, couplers can be bidirectional and may work as splitters, which distribute light, or combiners, which merge signals [87]. The optical fiber coupler is shown in Figure 2.12.

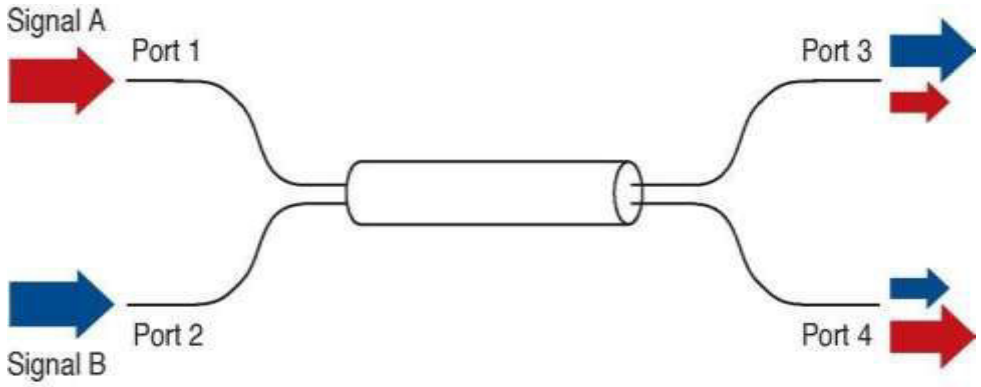

Fig.2.12. optical fiber coupler [88].

In interferometric networks, such as Mach-Zehnder or Supermode Interferometers and fiber couplers are used to split the optical power between two different arms of the interferometer and then recombine the light to create an interference pattern. Coupling ratio, insertion loss, and wavelength dependency are parameters that describe the performance of a coupler. Couplers generally are formed either by fusing one or more fibers and tapering, such that a propagation of the light occurs between the cores due to essentially evanescent field coupling.

2.7. Characteristics of an Optical Fiber Coupler

An optical fiber coupler is a passive device used to split or combine light signals in fibers. It typically has two or more input and output ports and operates based on evanescent wave coupling, where light transfers between closely spaced fibers through overlapping evanescent fields. Optical fiber couplers are widely used in interferometers to divide the input light into different arms and later recombine it to produce interference.

The splitting ratio (such as 50/50 or 90/10) determines how much light is directed into each path, which directly influences the resulting interference pattern. Couplers can be manufactured using methods such as fused biconical tapering, planar light-wave circuit (PLC) technology, and waveguide integration. Key performance parameters include insertion loss, excess loss, coupling ratio, and wavelength dependence. High-quality couplers with low losses and accurate power distribution are essential for fiber-optic sensors, communication systems, and laser applications [89,90].

2.8. Polarization Controllers

Polarization controllers are devices for adjusting the direction and quality of light waves as they pass through a fiber or optical system. Light can vibrate in different ways; a property often called its polarization or mode of vibration. However, when light travels through a fiber, factors like bending, twisting, or temperature changes may affect the light's polarization. This affects signal performance in sensitive systems such as sensors, lasers, and interferometers.

By employing a polarization controller, the light's polarization can be restored to the state required. This is done in one of three ways: mechanically (by bending the fiber slightly), optically (using special crystals or waveplates), or electrically (using quickly varying electrical signals). For example, in experiments or systems where the direction of light influences performance, stability, or precision (such as fiber-optic sensors, interferometers, and lasers), adjusting the direction and properties of light in accordance with the changing state of the system can be crucial [91]. Now, polarization controllers can ensure that the direction of light is right, helping everything run smoothly and reliably. Figure 2.13 shows polarization controllers.

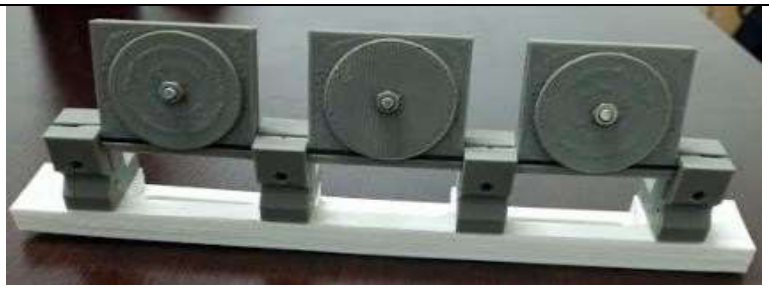

Fig. 2.13. The polarization controller.

2.8.1. Polarization of an electromagnetic wave.

Light waves are electromagnetic waves that are transverse. This means their electric and magnetic fields move at right angles to the direction that they are traveling. These waves can be polarized in different ways, including linear, circular, or elliptical polarization. In linear polarization, the electric field stays in a fixed direction. In circular polarization, it rotates evenly around the direction of travel. In elliptical polarization, it forms an ellipse in the transverse plane. Polarization greatly influences the contrast and visibility of interference patterns in optical interferometers. When two light beams interfere, the degree to which their electric fields align affects the interference contrast.
Maximum contrast occurs when the beams are co-polarized [92].

2.9. Types of Polarization

Because of birefringence and mode coupling, linearly, circularly, and elliptically polarized light behave differently in optical fibers. In birefringent fibers, linearly polarized light can split into two orthogonally polarized modes that travel at different speeds. This leads to polarization mode dispersion (PMD). Circularly and elliptically polarized light, which has a mix of linear components, will have different phase shifts. These shifts can distort the state of polarization and affect the coherence of interference patterns.

In addition, random mode coupling from core asymmetries, external pressure, or temperature changes can lead to polarization-mode internal energy exchange. This makes waveform analysis more complex and reduces measurement accuracy. Managing polarization behavior is important for maintaining high-performance sensing in fiber-optic systems. It is a key factor in designing and operating interferometric sensors, especially in fiber-based systems where birefringence and environmental changes can change the polarization state of light [93]. Figures 2.14 show the linear, circular, and elliptical polarized states.

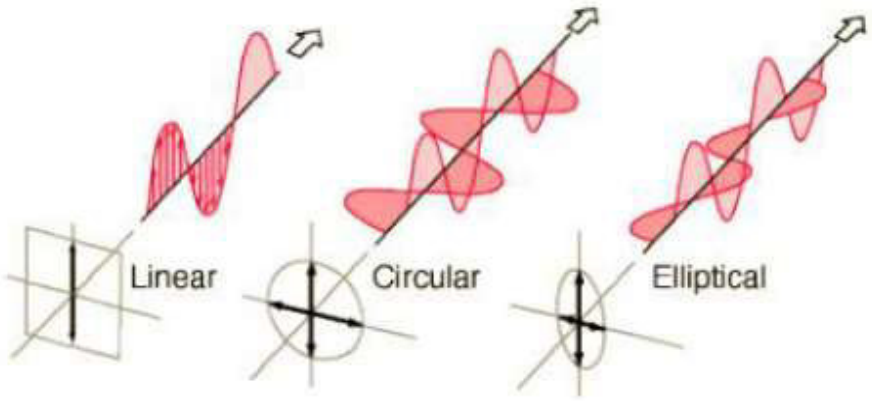

Fig.2.14. Linear, circular, and elliptical polarization states [94].

2.10. Functionality of Polarization Controllers

By changing the polarization angle of light in optical fiber systems, polarization controllers ensure an interference edge. These controllers can increase the visibility with which you interfere and decrease the error caused by polarization mode dispersion reduction techniques. That one exists as a postscript: of some interest, their benefits are coming into wider prominence nowadays. They are especially valuable in environments that change, where the state of polarization might otherwise be altered by outside factors and thus degrade signal quality [95].

Chapter 3. Methodology

This chapter details the procedure to be employed and the manner by which a Supermode Interferometer (SMI) structure-based fiber optic sensor will be designed, manufactured, and tested. The design methodology integrates theoretical modeling and experimental verification to ensure applicability in the multi-parameter sensing fields.

3.1. Introduction

The first considerations when developing the optical fiber sensor system concern defining the measurement targets and what physical parameter is to be observed. The parameters being probed for this study are:

- Temperature: This affects the refractive index as well as the physical length of the fiber. These variations manifest in the phase delay in the interferometric setup. The goal is to monitor thermal expansion or overheating in critical components, such as electrical transformers or engines.
- Torsion: This alters the symmetry and the distribution of stress in the fiber and causes observable optical path length variations. The goal is the detection of the twisting forces that might indicate structural strain or early mechanical failure.
- Strain: This beam-type structure, particularly the stress in the main infrastructure. It prevents some failures early and enables scheduled service. It is also useful for material testing to determine properties such as elastic behavior and strength.

This goal of multi-parameter sensing requires an interferometric arrangement, such as a Supermode Interferometer (SMI) with multicore fiber (MCF) [96].

3.2. Characterization of the Semiconductor Laser Diode

The semiconductor laser diode is used extensively in optical systems that require narrow linewidth, stable output, and accurate wavelength. In the following, we assess the laser diode to determine if it can be included in the fiber optic sensor system.

1. Setup

The laser diode is integrated on a temperature-controlled stage to ensure stable temperature operation. Current is injected into the diode via a laser driver with accuracy, and the forward bias voltage is measured using a digital multimeter. We connected the laser diode to a single-mode Erbium-doped fiber acting as an optical input source. The optical signal is passed through an erbium-doped fiber (EDF), which amplifies the optical signal. An EDF is pumped with a 980 nm pump laser to excite erbium ions in the EDF and power an optical signal. The excited ions then lase in the optical signal by stimulated emission. The schematic shows the Pump Laser Source and the Temperature Controller as in Fig. 3.1.

Fig.3.1. a. Temperature-controller b. Pump Laser Source: Wavelength 980 nm.

We measure the output power of the laser as a function of injection current using an optical power meter. The threshold current is the point where the optical output starts to increase sharply. We calculate linearity and slope efficiency (mW/mA) to evaluate the laser's performance.

2. Device Turn-On

The fiber laser diode QPhotonics QFBGLD-980-500 is a fiber laser diode intended for applications that require narrow spectral width emission at 980 nm wavelength, which is frequently applied in erbium-doped fiber amplifiers (EDFAs) and other telecommunication and photonics treatments [97]. Typical Operating Characteristics:

- The Central wavelength emission is 980 nm, and it is tuned with a Fiber Bragg Grating (FBG) to improve temperature stability and wavelength accuracy.
- Output power: Typical optical power up to 500 mW (as specified by the "500" specification on the model).
- Operations: CW (Continuous) or modulated operation, depending on the control design.
- Spectral stability: The Bragg grating ensures wavelength stability.
- Temperature: Usually between 0°C and 70°C, depending on the cooling system (thermoelectric cooler or passive heatsink).
- Connection and packaging: Usually with integrated thermoelectric cooling and a photodiode monitor for power control in a 14-pin butterfly package.
- Operating current: The maximum current recommended for delivering 500 mW of power, which is typically 300-600 mA, and depends on efficiency.
- Electrical protection: Sensitive to electrostatic discharge (ESD); requires care in handling.

We used a current range of 20-400 mA in this experiment; at each input current value of 20 mA, we received an output power in watts (W) that was quantified with a photodetector. The curve is shown in the next figure. Fig. 3.2. Investigation of the laser diode with respect to the output power.

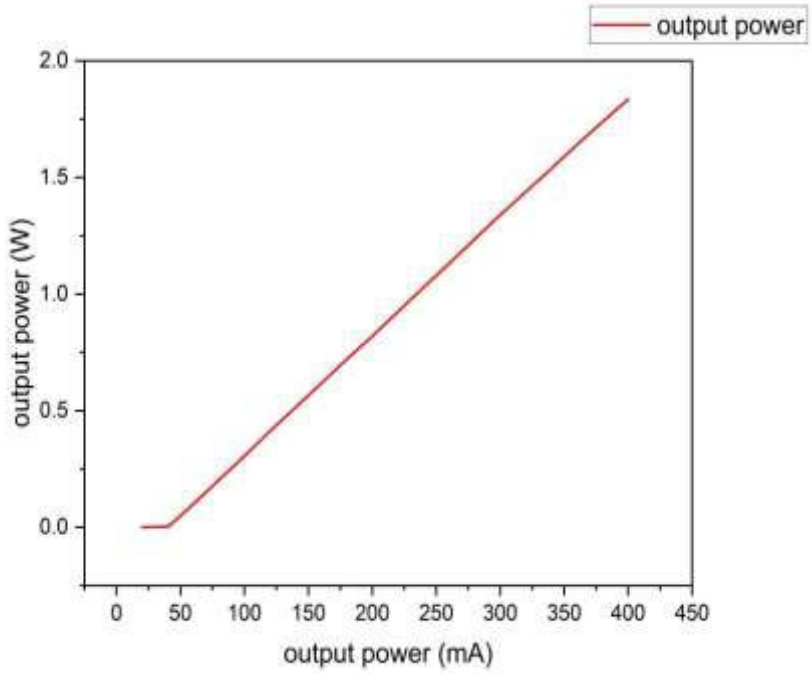

Fig. 3.2. Characterization of the laser diode in output power.

For high-quality signal output, the laser diode current requires calibration for a constant input signal level. The pump laser was then tuned to an appropriate power level to excite the erbium ions without saturating the system. The amplified optical signal was then characterized with an Optical Spectrum Analyzer (OSA) to compare the intensity of light before and after amplification. The values of system parameters, such as gain based on the wavelength and the optical power, are plotted in Figure 3.3.

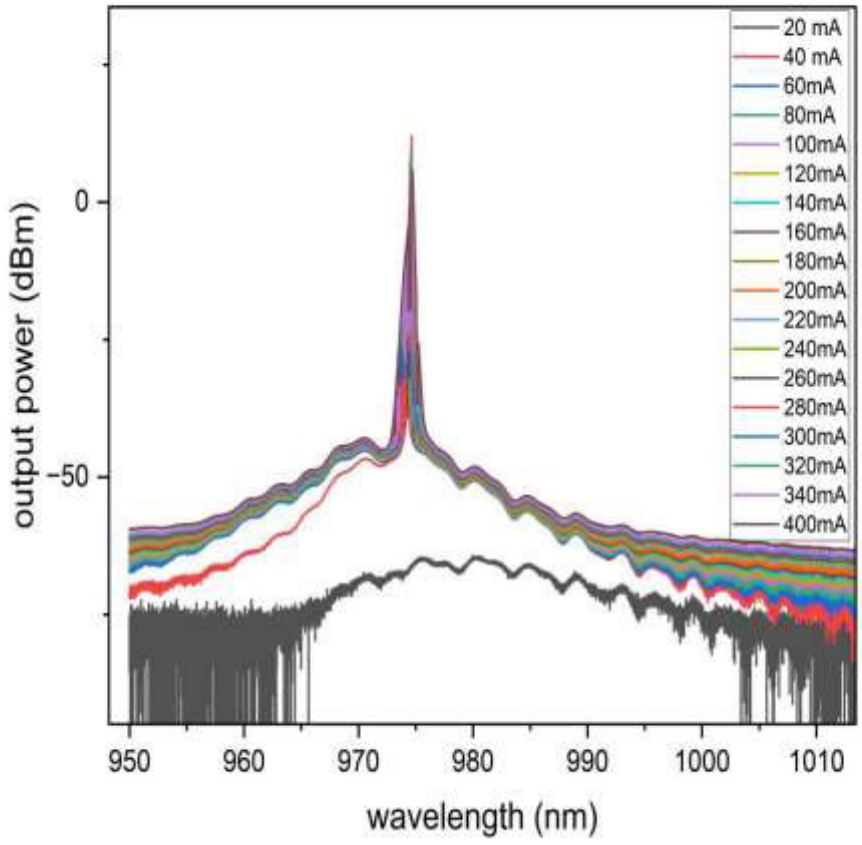

Fig. 3.3. Characterization of the laser diode (output spectrum).

By cutting the pump diode and varying the input current from 20 mA to 400 mA in increments of 20 mA, we can observe its typical form and saturation at the OSA. In this case, the diode characterization was only performed up to 400 mA for safety reasons. From 350 mA to 400 mA, the diode is in saturation, meaning it has reached its maximum output power limit and no longer shows an increase in output power with increasing current, so the behavior remains essentially the same, as shown in Figure 3.3. The signal gain varies linearly with pump laser power until saturation, as shown in Figure 3.3.

3. Spectral Characterization

The emission spectrum of the laser diode can be seen by using an Optical Spectrum Analyzer (OSA). The values of the center wavelength, the spectral fullwidth at half-maximum (FWHM), and SMSR (side-mode suppression ratio) are measured.

These are important parameters in applications for which a high level of coherence is required, such as interferometric sensing. The OSA that we used in the lab is shown in the following figure, Fig. 3.4. Optical Spectrum Analyzer (OSA)

Fig.3. 4. Optical Spectrum Analyzer (OSA)

4. Wavelength Stability and Tuning

In Wavelength Division Multiplexing (WDM) systems, multiple data channels can be sent together on a single fiber by using different wavelengths at each end of the system. EDFAs can amplify all the wavelengths of light at once, which makes them suitable for WDM networks, as their capacity and efficiency will increase with the number that they carry. This has led to a substantial increase in the capacity for transmission. We investigate how current and temperature affect the emitted wavelength. A temperature controller changes the heat sink in small steps (usually 10 °C), and we record its varying effect upon wavelength.

We calculate the wavelength tuning coefficient (nm/°C or nm/mA) so that we can understand how responsive our device is to tuning. Image 3.4 represents the wavelength division multiplexer used during our trial in the laboratory.

Fig. 3.5. Wavelength Division Multiplexer

5. Polarization and Beam Quality

The polarization of the laser is evaluated using a polarization analyzer. We measure the beam profile using a beam profiler to evaluate the beam divergence and mode quality. The polarization controller is shown in Figure 3.6.

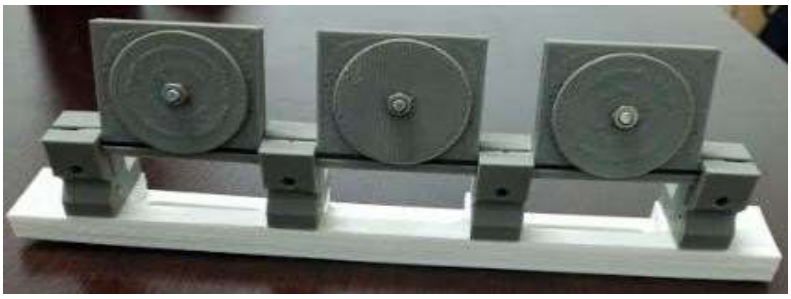

Fig.3.6. Polarization Controller

3.3. Characterization of the Erbium-Doped Fiber Amplifier (EDFA)

Erbium-Doped Fiber Amplifiers (EDFAs) are essential in modern optical telecommunications. They allow for efficient, high-quality data transmission over long distances.

Their common use in backbone networks, Wavelength Division Multiplexing (WDM) systems, access networks, and submarine communication systems shows their important role in meeting the rising global demand for data. EDFAs offer strong optical gain, which makes them perfect for long-distance and high-capacity applications. EDFAs operate by creating a population inversion between energy levels 2 and 1. A pump source excites erbium ions from energy level 1 to energy level 2. This process enables the amplification of incoming optical signals through stimulated emission. Figure 3.7 shows the schematic diagram of an EDFA.

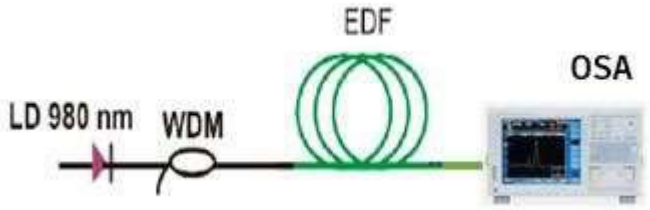

Fig.3.7. Schematic diagram of Erbium Doped Single-mode Fiber (EDFA).

Signal Gain

The input power of the laser diode signal reaching the erbium-doped optical fiber was 9.3 dBm; after amplification, it reached 21 dBm peak power. However, within the wavelength range, this increased from just 3 nm to over 100 nm due to amplification. Figure 3.8 shows the single-mode fiber doped with erbium.

Fig.3. 8. Image of EDFA.

The erbium-doped fiber was characterized to examine its performance. The fiber thus exhibited gain at 1500–1600 nm, which is consistent with the characteristics of erbium-doped fibers at this wavelength. A visible green fluorescence is evident as an indication that the system is working and amplifying correctly. The schematic diagram of the Erbium Doped Fiber is shown in Figure 3.7. This experiment meant defining an EDFA to see how it operates with an OSA. We utilized two primary instruments: a temperature controller and a laser power supply. The pump laser was operated at 980 nm. It passed through a WDM coupler and an Er-doped optical fiber. Finally, Fig. 3.9 shows the amplified signal on the OSA.

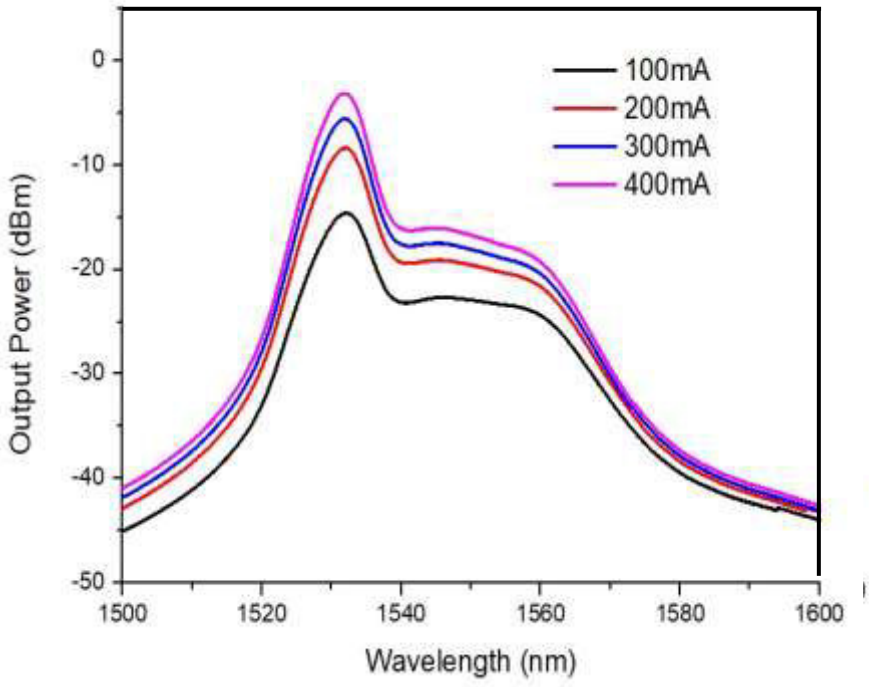

Fig.3.9 EDFA behavior in OSA

Erbium-Doped Fiber Amplifiers (EDFAs) directly amplify optical signals. This process removes the losses and complexities related to converting optical signals to electrical ones and back again. They perform well over a wide range of wavelengths, especially in the 980 nm and 1480 nm bands.

When you adjust the power controller, the Optical Spectrum Analyzer (OSA) evaluates various signal characteristics. Notably, increasing the power leads to an increase in the observed curvature.

3.4. Fabrication Methodology of the Mach-Zehnder Optical Filter

In our experiment, we use both manual and automatic splicers. This equipment is a tool used to splice optical fibers precisely. Its main function is to join the two ends of the optical fiber. The image 3.10. a and 3.10.b illustrate the splicer machine.

Fig. 3.10. a. automatic splicer Fig. 3.10. b. manual splicer

The following point illustrates the different steps of the fabrication process of a Mach-Zehnder Interferometer Optical Filter.

1. Design the Interferometer Layout: The MZI consists of two arms: one reference arm and one sensing arm. The path length difference between these arms will determine the filtering characteristics.
2. Prepare the Substrate: Selection and preparation of optical fiber. Remove contaminants, clean, and ensure precise alignment.
3. Forming the couplers, the MZI requires two couplers (also known as beam splitters) to split and then recombine the optical signals.
4. Precisely control the lengths of the two arms during patterning to achieve the desired phase difference. This length difference sets the free spectral range and filtering wavelength.
5. Cladding Deposition: After waveguide and coupler fabrication, deposit a cladding layer over the waveguides to protect and stabilize the optical paths.
6. Facet Preparation or Fiber Coupling: Polish the input and output facets of the chip for efficient coupling of light into and out of the device.
7. Testing and Characterization

Use a laser source and an OSA to characterize the filter's spectral response.

Table 3.1 summarizes the various steps involved in the fabrication process of a Mach-Zehnder Interferometer Optical Filter.

Step	Action
1.	Select SMF-28
2.	Strip coating at splicing/coupling sections
3.	Clean the core with alcohol
4.	Cut with precision
5.	Splice to form MZI (2x2 couplers)
6.	Manage fiber routing
7.	Characterized with a laser source + OSA.

Table 3.1: Different steps of a Mach-Zehnder Interferometer Optical Filter process.

Figures 3.11 show the manufacturing process of an MZI interferometer. a) alignment between the MZI arm and the sensitive part, b) 30 µm offset for the generation of the splitter/combiner, c) splicing between fibers generating the splitter/combiner.

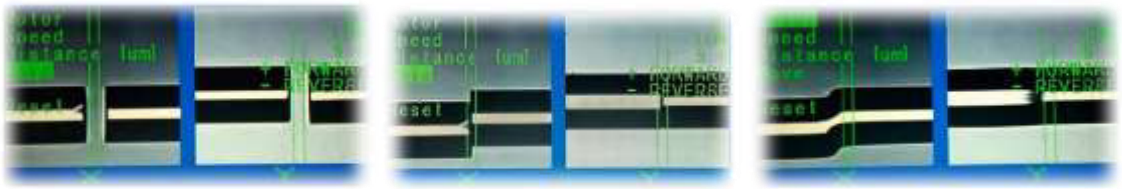

a. b. c.

Fig.3. 11. Describe the fabrication process of MZI

1. Precise alignment: Uses core or coating alignment technology to properly align fibers.

2. Arc Flash Fusion: Emits at an arc flash power of 175, with a duration of 1450 msg and a pre-fusion time of 330 ms, which heats and melts the two fiber points, creating a robust, low-loss bond.
3. Precision cutting: to make the splicing between fibers, we used a standard fiber single-mode, and multicore single-mode, in addition, manual cuts (made with a silica plate) to guarantee straight and clean cuts. The splicing was performed with a 30 μm offset (X-alignment). The automatic splicer automatically measures losses after melting.

3.5. Characterization of the Mach-Zehnder Optical Filter

The purpose of this section is to characterize a Mach-Zehnder Optical Filter experimentally. We characterize its spectral response, extinction ratio, insertion loss, and tunability. Let's break down the important performance aspects of this optical filter.

1. Spectral Behavior: First, we examine how the filter transmits light across different wavelengths. The transmission spectrum reveals a repeated pattern of peaks and valleys due to light wave interference within the filter. This pattern, often referred to as fringes, is characterized by the Free Spectral Range (FSR), which is the distance between two adjacent peaks or valleys and can be calculated using this formula:

$$FSR = \frac{\lambda 2}{n\Delta L} \tag{3.1}$$

Where:

- λ is the central wavelength of interest.

- n represents the effective refractive index of the filter material.

- ΔL is the difference in path length between the two optical paths within the filter.

To measure this, we use an Optical Spectrum Analyzer (OSA) to capture the filter's output over a range of wavelengths, such as from 1520 to 1580 nm.

2. Extinction Ratio: The Extinction Ratio (ER) shows how well the filter blocks light at wavelengths it should reject. It measures the filter's ability to reduce unwanted signals. It is calculated using this equation:

$$ER = 10log_{10}\left(_{Pmax/Pmin}\right) \quad (3.2)$$

Where:

- Pmax is the maximum power transmitted by the filter.

- Pmin is the minimum power transmitted by the filter (near zero).

For a high-performing filter, we usually want to see an ER greater than 20 to 30 dB. Lower ER values might indicate issues like an imperfect splitting ratio in the filter, mismatches in light polarization, or errors during manufacturing.

3. Insertion Loss: Finally, we consider the Insertion Loss (IL). This represents the amount of optical power lost as light passes through the filter, even at wavelengths the filter is designed to pass. It is calculated using this equation:

$$IL = 10log_{10}\left(_{Pin\ /Pout}\right) \quad (3.3)$$

Where:

- Pin is the input optical power.

- Pout is the output optical power.

Ideally, we want to minimize insertion loss to keep a strong signal. The insertion loss can occur due to several factors, including losses at connection points, losses from bending the optical path, or scattering of light at interfaces inside the filter. Generally, Modern MZOFs are designed to be adjustable, altering their spectral characteristics based on external factors. Figure 3.12 represents a block diagram of the implemented system to test the interferometers.

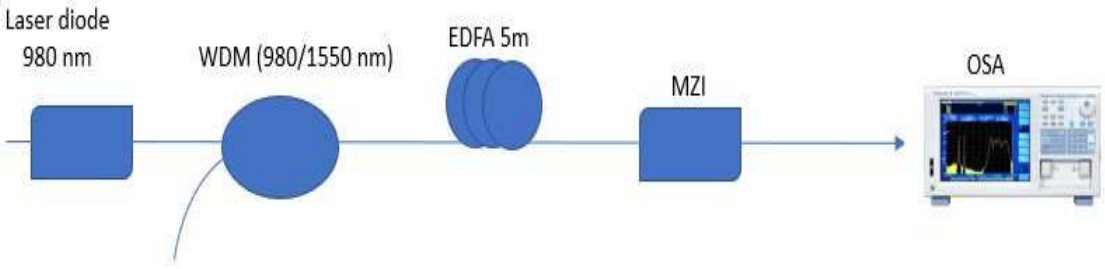

Fig. 3.12. Characterization diagram block of the Mach-Zehnder Optical Filter.

Some examples of MZI can be seen in Figure 3.13, where we can observe a traverse contraction for two interferometers; the same setup is used to test two interferometers with multicore fibers. The results of characteristic graphics are shown in Figure 3.13, for MZI core offset single-mode fiber, and in Figure 3.14 for MZI multicore fiber.

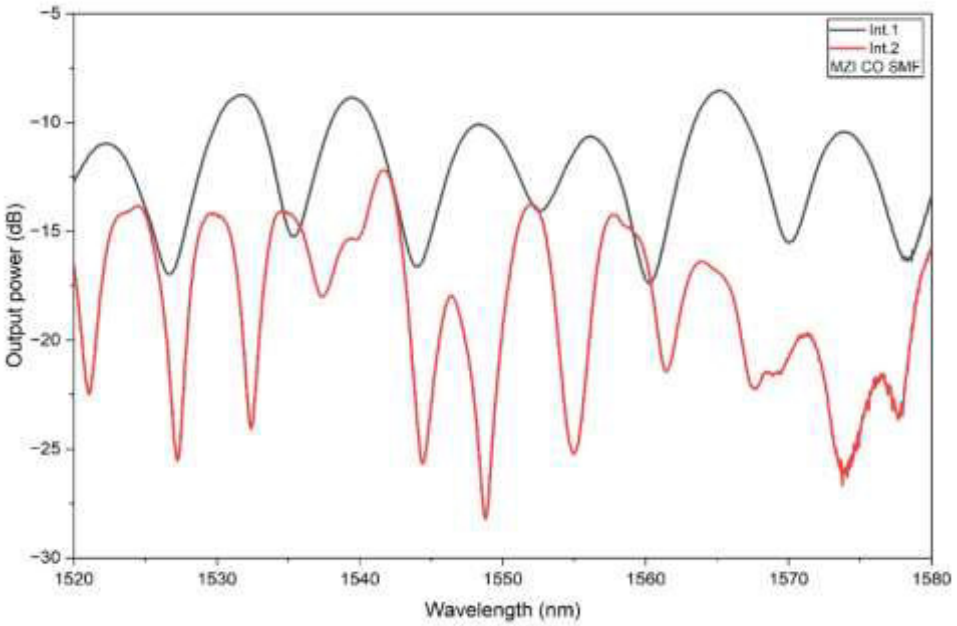

Fig. 3.13. Characteristic graphics of MZI core offset single-mode fiber.

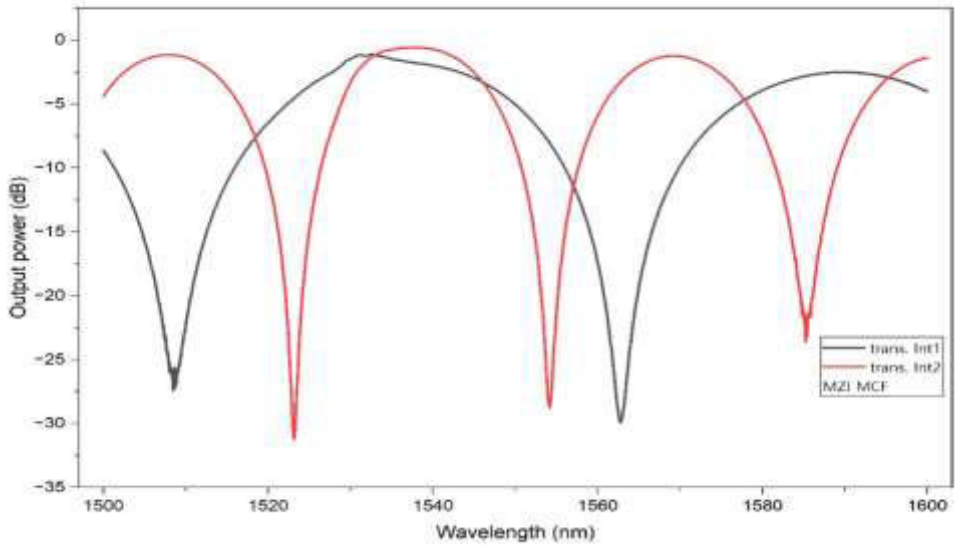

Fig. 3.14. Characteristic graphics of MZI multicore fiber.

3.5.1. Strain Characterization

Strain characterization examines how stretching or compressing affects the optical behavior of the interferometer. This process is important for understanding and using the device as a sensor for mechanical quantities such as tension or deformation. When strain is applied to an optical fiber interferometer, the length L increases and the refractive index n may change due to the photoelastic effect. This alteration changes the optical path length (OPL) of the light traveling through it. The optical path length is given by:

$$\varepsilon = \frac{\Delta x}{D} \tag{3.4}$$

where:

- $\boldsymbol{\varepsilon}$: is the OPL of the light
- $\boldsymbol{\Delta x}$ is the variation of refractive index of the fiber core,
- D is the distance between two fiber clamps (30 cm)

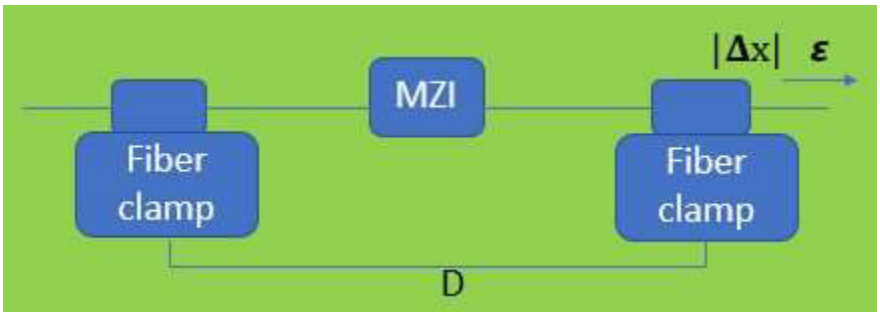

Fig. 3.15. Strain characterization.

Strain characterization not only shows how mechanical deformation influences the interferometer's optical output but also emphasizes its potential as a highly sensitive and precise strain sensor.

Figure 3.15 represents the strain characterization. And the figures 3.16 and 3.17 represent the strain characterization of MZI SMF and MZI MCF.

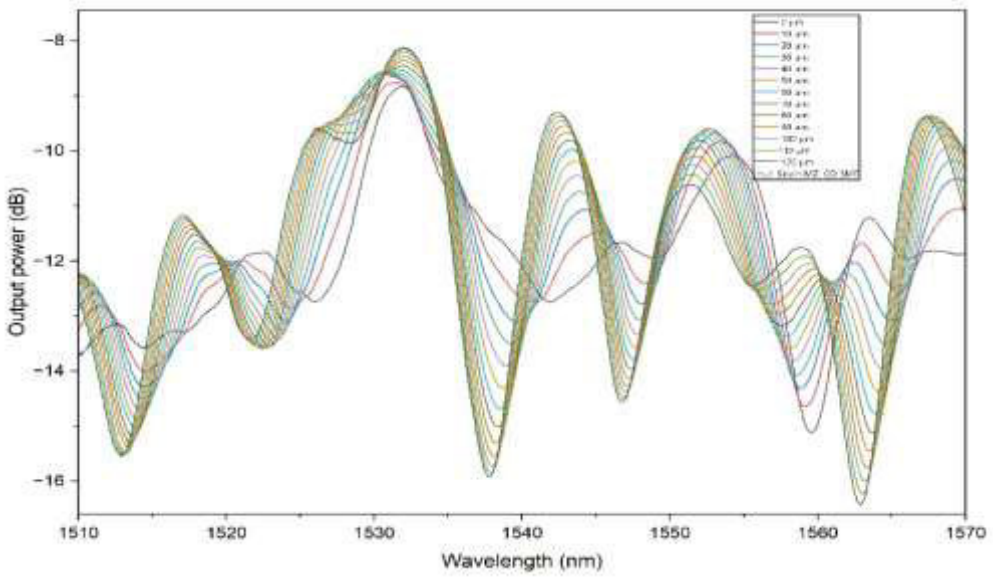

Fig. 3.16.a. Strain characterization of MZI (1) core offset SMF

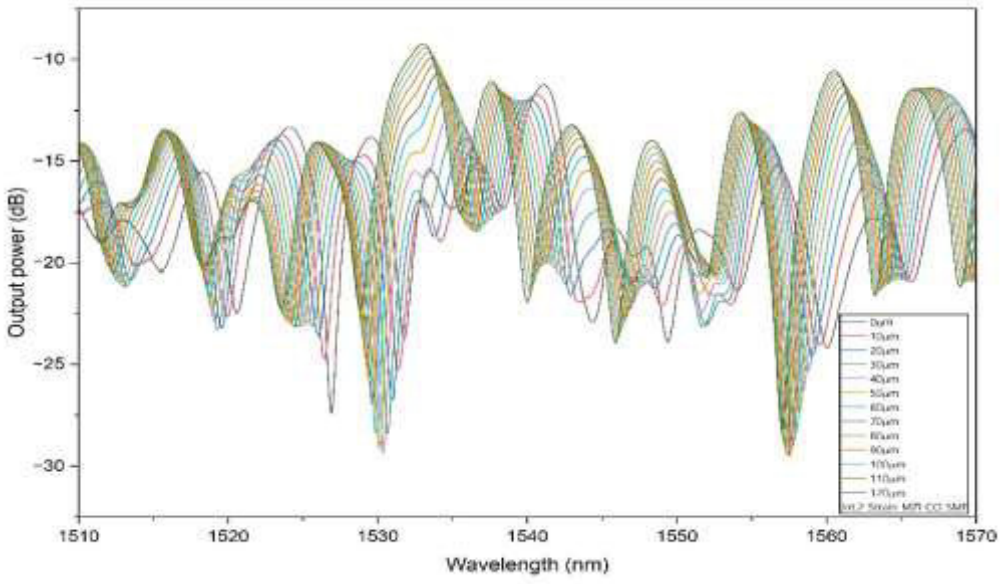

Fig. 3.16.b. Strain characterization of MZI (2) core offset SMF

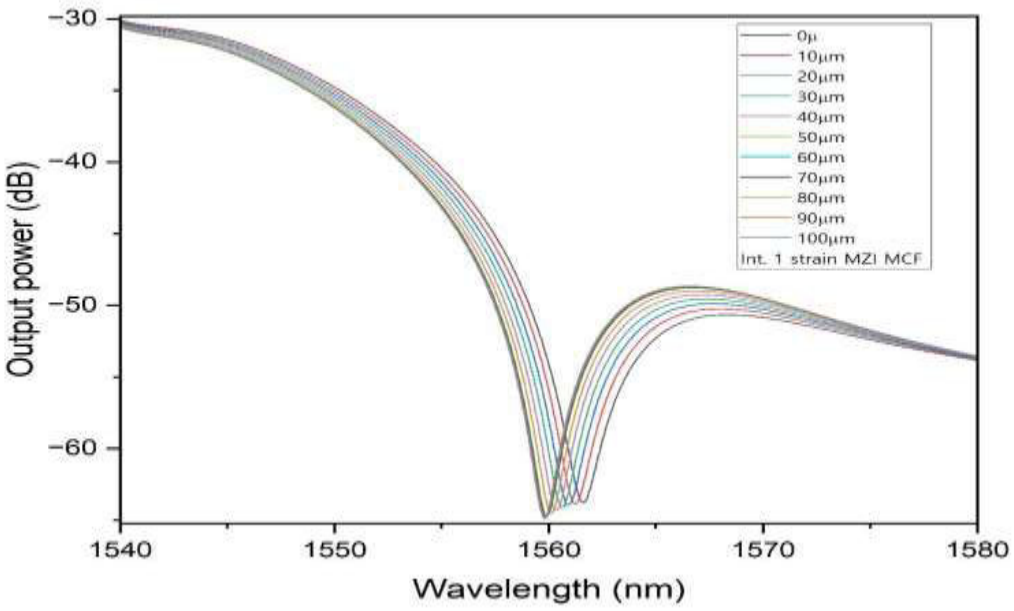

Fig. 3.17. Strain characterization of MZI MCF

3.5.2. Torsion Characterization

Torsion characterization aims to demonstrate how to induce a twist in the optical fiber, with implications for the interferometric system's optical properties. This study is crucial for establishing the interferometer's value as a torsion sensor, particularly when evaluating rotation or angular deformation. Twisting modifies the fiber's birefringence. It introduces asymmetry to the fiber's internal structure and alters the way that each of the two polarization modes propagates within the fiber. This change in birefringence results in the phase difference between the interfering modes, which results in a change in the interference pattern (fringes visibility, spectra shift, and intensity). The mode coupling between cores or different propagation modes induced by the torsion in multicore fibers could also contribute to the transmission spectrum.

The interferometric physical quantity, $\Delta\phi$, between two modes of the interferometer is expressed as:

$$\Delta\phi = \frac{2\pi}{\lambda} (\Delta n. L) \quad (3.5)$$

Where λ is the operating wavelength, Δn is the induced birefringence, and L is the length of the twisted fiber.

Under torsion, Δn is observed to be a function of the twist rate in radians/m. As the torsion increases, the birefringence-induced phase difference also increases, allowing for spectral tracking. By plotting the spectral response at a series of torsion levels, a calibration curve that relates changes in intensity to a known angle of twist can be constructed. The result makes the fiber interferometer a high-sensitivity torsion sensor. We can observe the spectral response in Figures 3.18 for MZI MCF and 3.19 for MZI CO SMF.

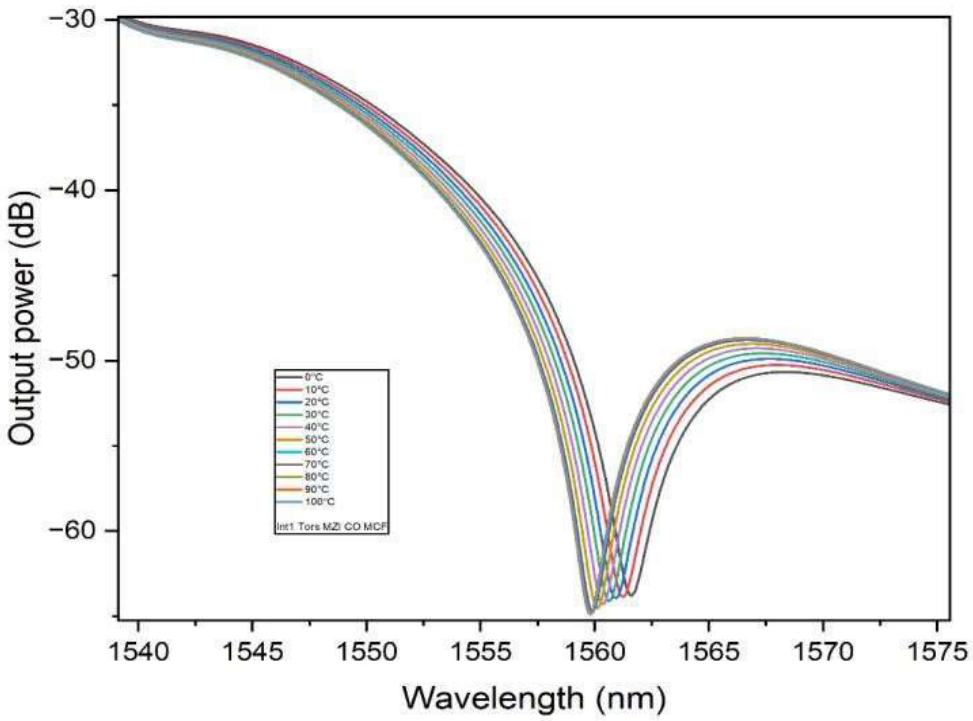

Fig. 3.18.a Torsion characterization of MZI (1) MCF

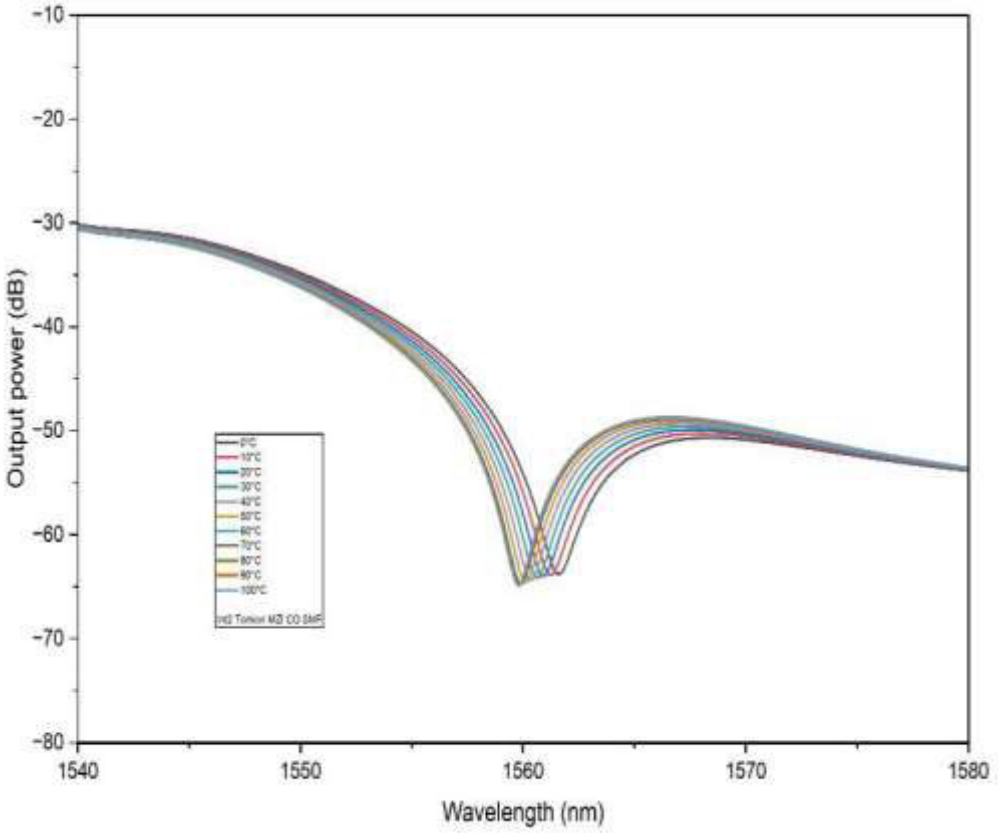

Fig. 3.18.b Torsion characterization of MZI (2) MCF

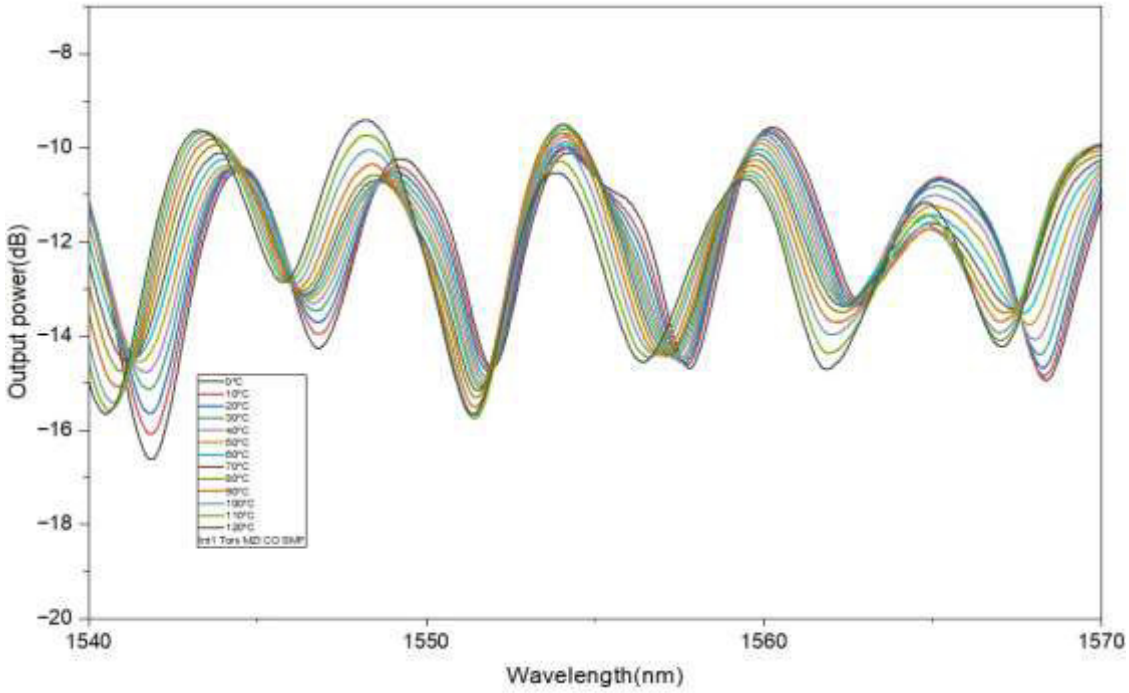

Fig. 3.19.a. Torsion characterization of MZI (1) core offset SMF

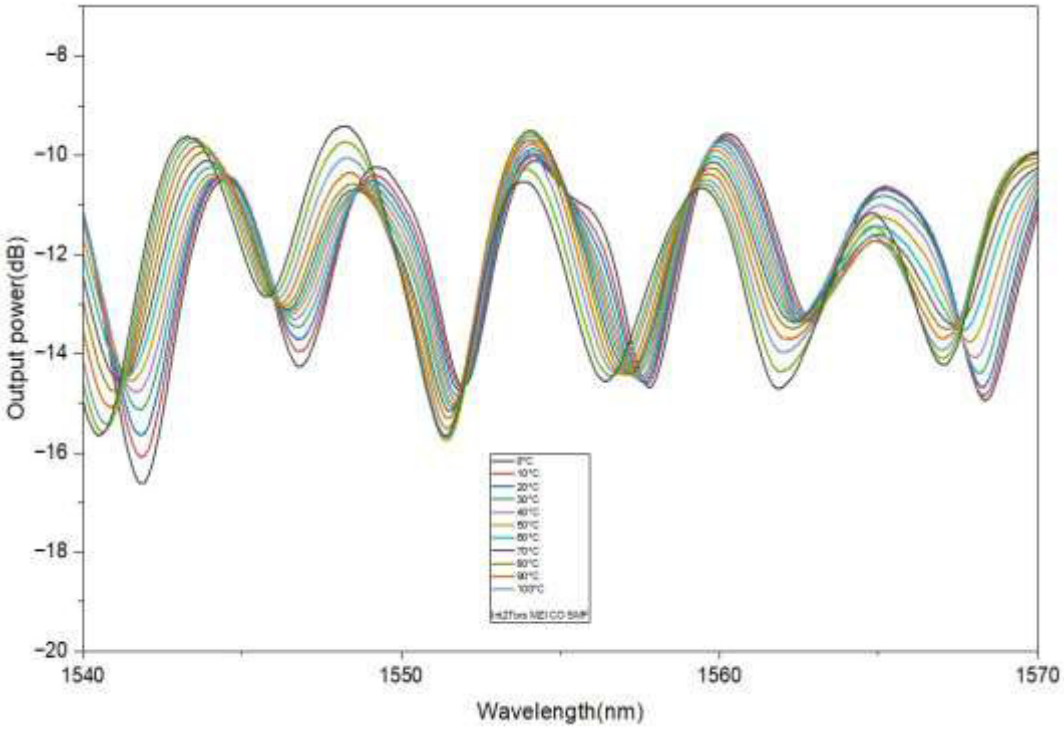

Fig. 3.19.b Torsion characterization of MZI (2) core offset SMF

3.5.3. Temperature Characterization

Thermal characterization studies the changes in the optical response of the interferometric system, which are due to variations in the ambient temperature. Optical fibers are intrinsically sensitive to temperature, and thus, this analysis is also essential for temperature sensing and thermal cross-sensitivity in measurements of multiple parameters [98].

a) Thermal Tuning

One arm of the interferometer is then heated in a controlled manner to introduce a phase delay of the fiber due to temperature-induced modification of its optical properties. These alterations are primarily caused by variations in the refractive index (n) due to the thermo-optic effect. In the case of silica, the refractive index rises with increasing temperature, with a positive thermo-optic coefficient:

$$\frac{dT}{dn} = 1 \times 10^{-5}\ °C^{-1} \tag{3.6}$$

The fiber expands slightly in length with temperature. But the physical length (L) that is dependent on the thermal expansion coefficient of silica is short, so it is not very effective because it occurs in a low ratio as compared to the thermo-optic effect.

$$\alpha = \approx 5 \times 10^{-7}\ °C^{-1} \tag{3.7}$$

These two effects in concert produce a shift in the optical path length (OPL) of the fiber:

$$OPL = n(T).\ L(T) \tag{3.8}$$

$$\frac{d(OPL)}{d(T)} = L\,\frac{dn}{dT} + n\,\frac{dL}{dT} \tag{3.9}$$

The resulting optical phase shift $\boldsymbol{\Delta\phi}$ leads to a measurable change in the interference pattern.

b) Spectral Response and Sensitivity

In experiments, temperature is modulated by the thermal chamber elements to realize homogeneous heating, micro-heaters for localized tuning, and the OSA for real-time measurements, with the thermocouple as a reference.

Spectral tuning is monitored with an OSA. The temperature sensitivity is derived from the slope of the wavelength shift as a function of temperature and compared with theoretical values. The figure 3.20. and 3.21 shows the characteristics of temperature.

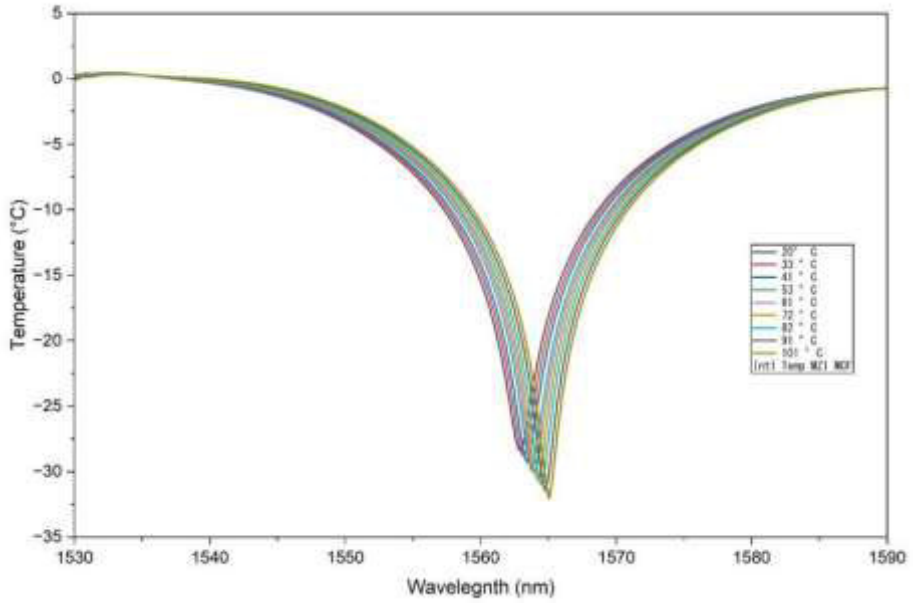

Fig. 3.20.a Temperature characterization of MZI (1) MCF

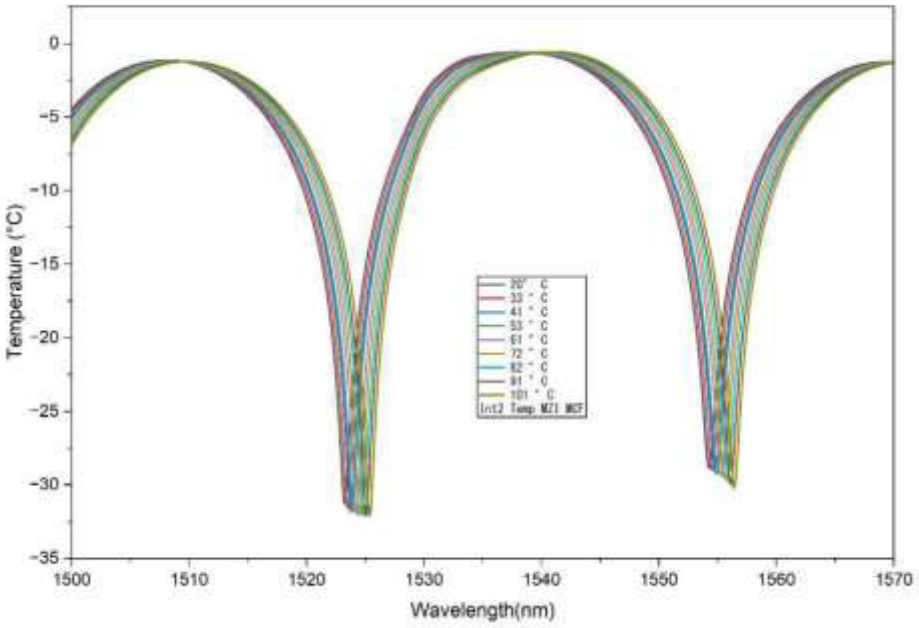

Fig. 3.20.b Temperature characterization of MZI (2) MCF

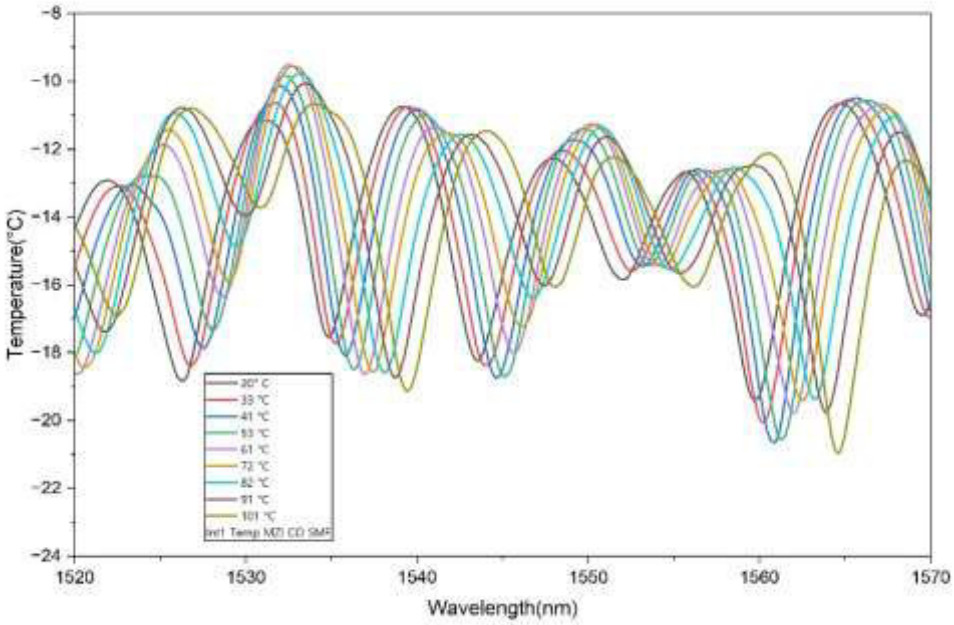

Fig. 3.20. a Temperature characterization of MZI (1) core offset SMF

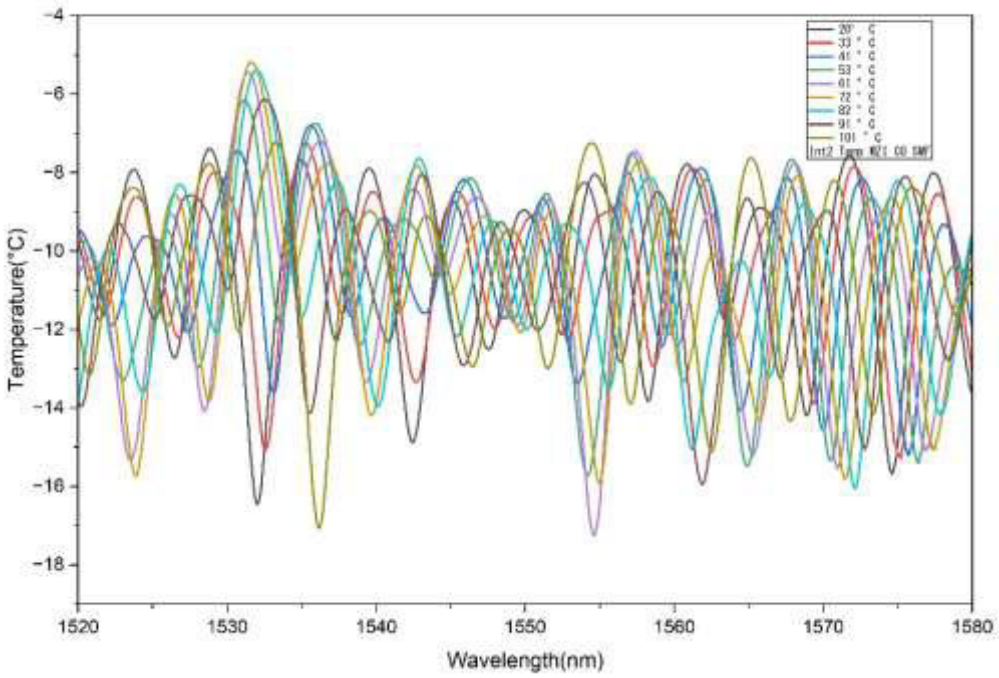

Fig. 3.20. b Temperature characterization of MZI (2) core offset SMF.

3.6. Laser Arrangement

In this section, we describe the configuration and enhancement of the laser source for investigating the interferometric sensor in the experiments. The stability, tuning range, and spectral characteristics of the laser have a direct influence on the clarity and renewability of the measurement [99].

1. Laser Source Selection

Experiments were performed with a single-frequency, narrow linewidth tunable laser. The main criteria considered in the selection included:

- Wavelength range: The laser operates in the C band (approximately 1520-1570 nm), single frequency, which is coincident with the low-loss band of ordinary single-mode fibers (SMF-28).

- Output power: It must be enough to maintain a high signal-to-noise ratio (SNR) by ensuring the optical signal is stronger than the system noise in the interferometer, but not high enough to saturate the detection optics.
- A narrow linewidth (100 kHz) yields high spectral resolution, which is important for determining small shifts in the spectrum due to strain or torsion.
- Tuning Ability: Either piezo-electric or thermal tuning is employed to realize high wavelength sweep rates and spectral measurements.

2. Optical Setup

The output of the laser is coupled to the interferometric sensing setup by means of fiber patch cords and optical connectors. The key elements in the setup were:

- Isolator: It is placed immediately after the laser to block the retroreflection into the laser.
- Polarization controller: It changes the polarization state of light to maximize fringe contrast in the interferometer, most noticeably in polarization-sensitive setups.
- Variable Optical Attenuator (VOA): For adjusting the optical power on the sensor, such that nonlinear effects are suppressed, and the detector is prevented from saturating.
- Couplers: They divide light according to the geometry of the sensor (Mach-Zehnder, for example).

3. Optimization Procedure

The laser setup was tuned to ensure a robust excitation of the sensor in the testing environment:

- Linearity of the wavelength tuning was calibrated versus a known reference (e.g., an OSA).

- The power stability was checked and adjusted with the VOA to keep an even input level during all the measurements.
- Polarization was aligned before each measurement to maximize interference contrast.

4. Data Acquisition

The phase of the interferometric signal was locked by sweeping the tunable laser across a defined wavelength range while tracking the interferometric output with a photodetector and an optical spectrum analyzer (OSA). The transmission spectra obtained from this sweep were recorded, and the sensor responses to tensile, torsional, and environmental variations were analyzed. Because the reference source is shared with the measuring interferometer, the coherence length of the laser source can be optimized to ensure accurate detection of the interferometric response under test [100].

The schematic of a generic laser system for interferometric sensing experiments is illustrated in Figure 3.21 with the successive positioning of the main devices.

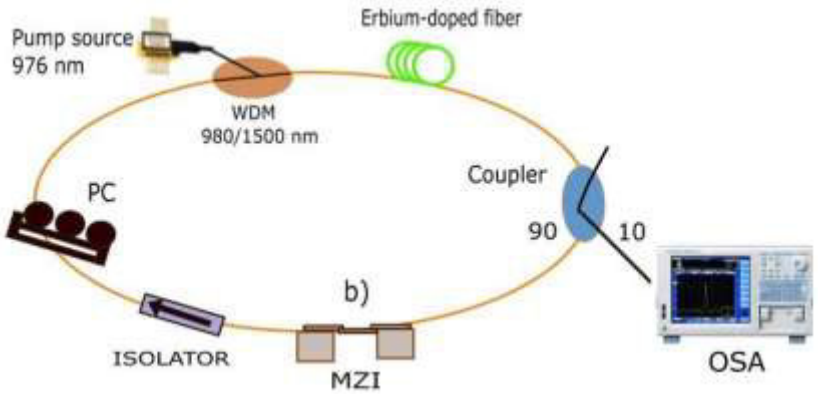

Fig. 3.21. Laser setup used in interferometric sensing experiments

Main experimental components:

- Laser Source
- Isolator, which protects the laser from back reflections.

- Polarization Controller, optimizes the polarization state for maximum interference.
- WDM: increases data transmission capacity.
- Coupler, splits, and guides the light to the sensor.
- Interferometric Sensor, the sensing element.
- Optical Spectrum Analyzer (OSA) is a multiport interferometer that does not damage the laser.

Chapter 4: Results

4.1. Introduction

This section discusses how the fiber laser system was examined and tested by incorporating interferometric structures. Let's consider the tests arranged one by one, allowing the separate characterization of individual components to precede system integration, followed by performance analysis, thereby maintaining a logical sequence and formality in our research. This section explains the process and analyzes spectral signals by integrating the interferometers into the fiber laser cavity.

The overall system's effectiveness is discussed in terms of laser stability and its ability to respond simultaneously to various environmental changes. The results presented here support the practicality of the proposed technique in terms of high-performance multi-parameter optical sensing.

4.2. Laser Stability

A laser source must maintain a stable output power and wavelength. Any alterations will introduce noise into the interferometric spectrum, reducing sensitivity and resolution. This study examined the stability of a laser-sensor operating under constant conditions. The aim was then to determine whether it would be suitable for incorporation into the complete fiber laser system. The stability tests of the Mach-Zehnder Interferometers (MZI1 and MZI2), built with single-mode fibers, and of MZIs with three-core and seven-core fibers were performed. The figure 4.2. shows the stability of a laser using MZI with three cores, seven cores, the MZI1, and the MZI2.

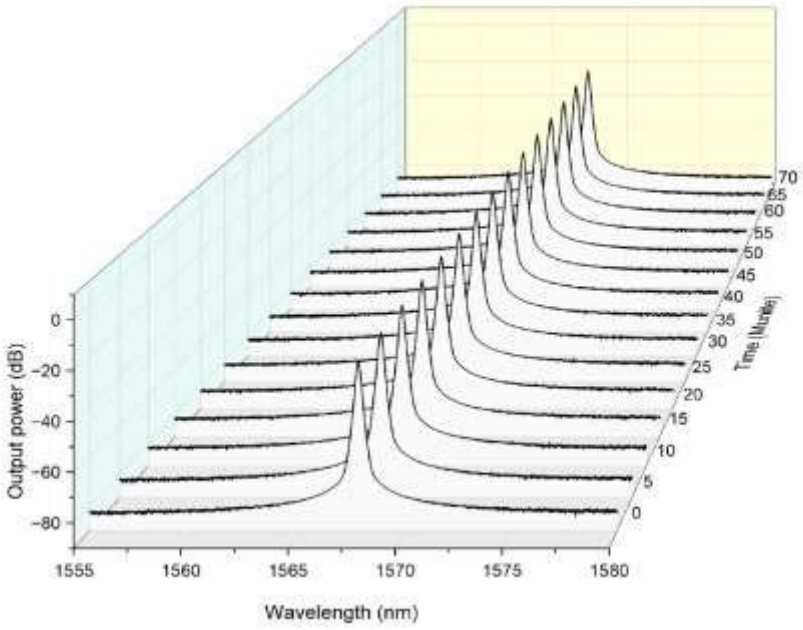

Fig. 4.2.a.1: Laser stability of MZI three-core fiber.

In this figure, the temporal results of the emission laser with the MZI three-core filter show stable operation with constant output power. This means that when the laser output power is monitored over time, the signal remains nearly constant, with no significant fluctuations. This stability indicates that the laser operates reliably. The following figure explains the table of Figure 4.2.a.1.

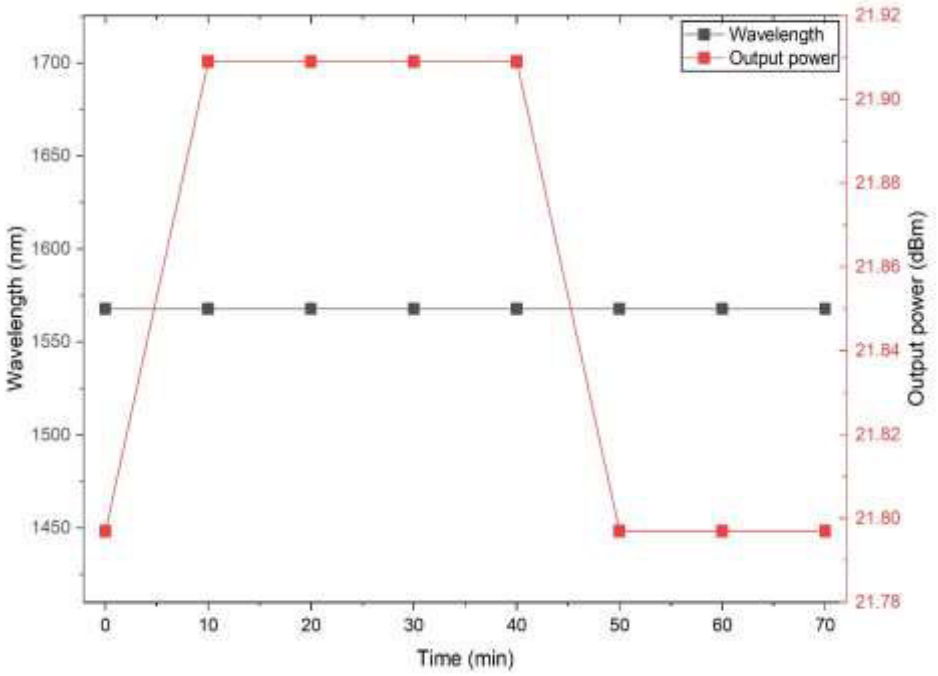

Fig. 4.2.a.2: Laser stability table of MZI three-core fiber.

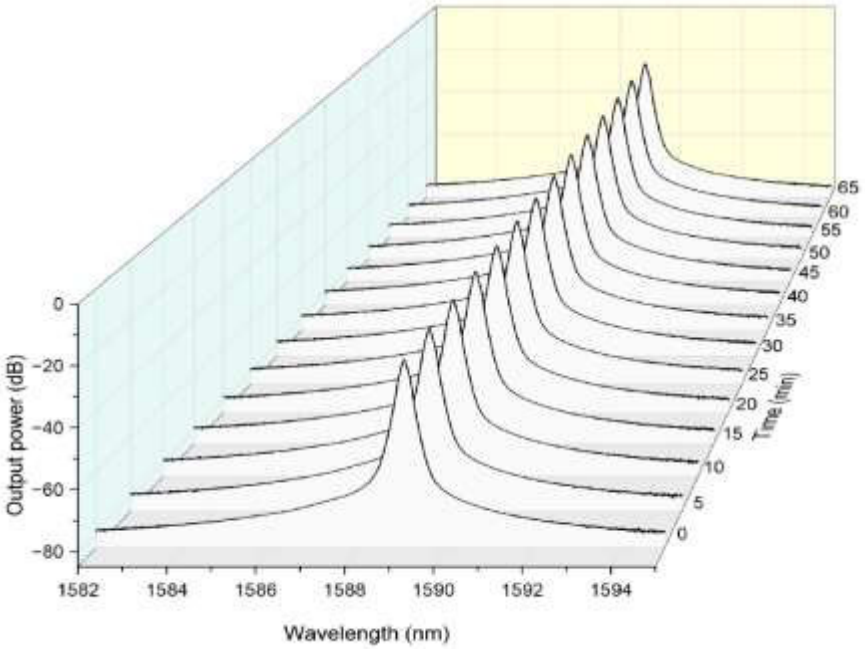

Fig. 4.2.b.1: Laser stability of MZI seven-core fiber.

The temporal spectral measurements show that the laser emission filtered by the seven-core fiber Mach-Zehnder interferometer remains highly stable over time. The interferometer peaks maintain constant amplitude and shape, while only a slight wavelength drift is observed, indicating reliable laser operation and stable cavity filtering. The following figure explains the table of Figure 4.2.b.1.

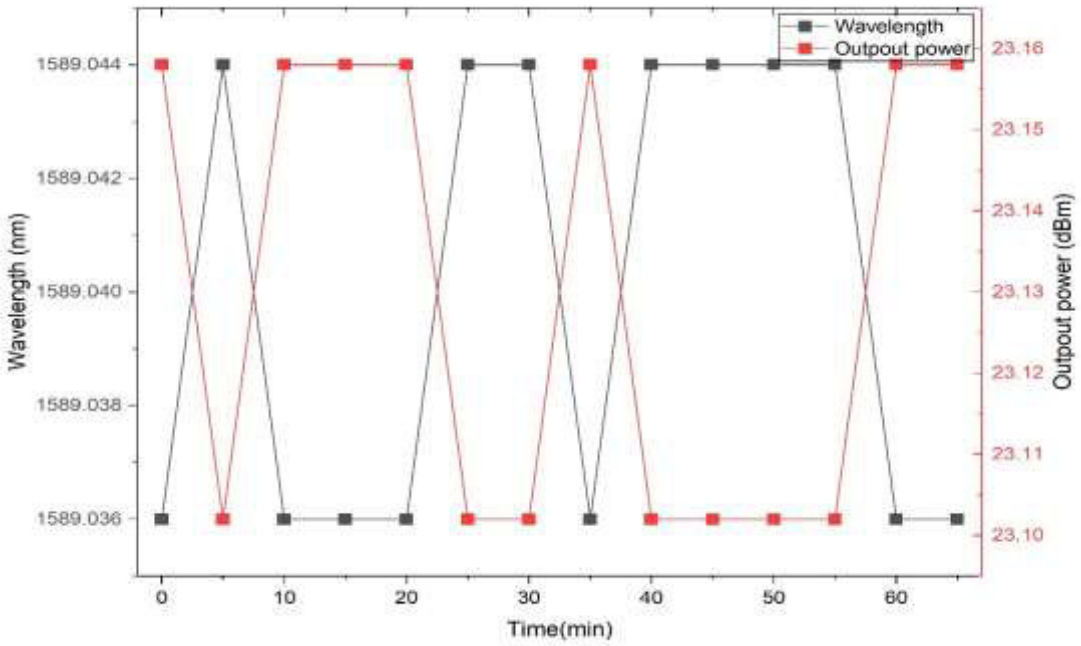

Fig. 4.2.b.2: Laser stability table of MZI seven-core fiber

The simultaneous stability of both the wavelength and the output power demonstrates that the fiber laser system operates in a highly stable lasing state. The results confirm that the interferometric filter inside the cavity provides robust spectral selection and stable laser operation over time.

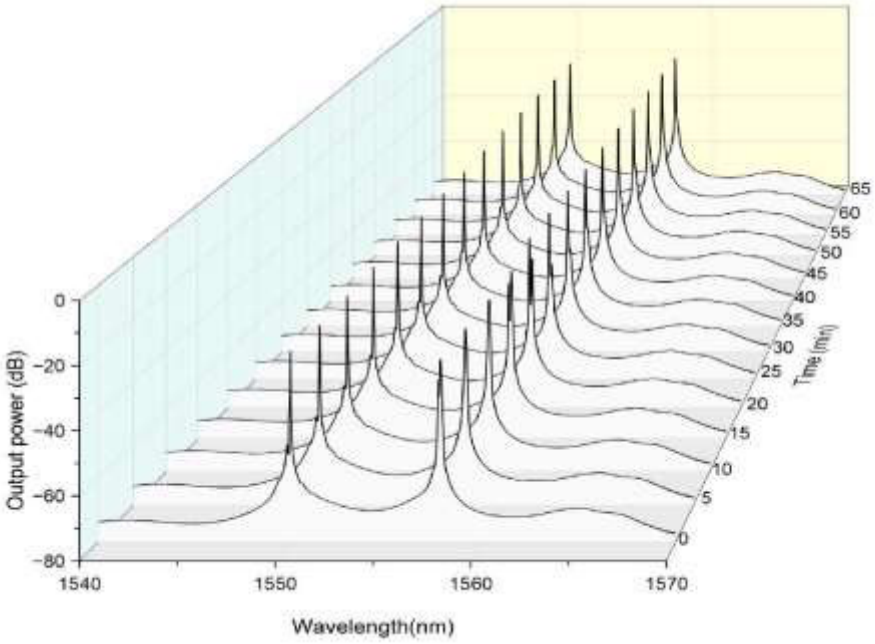

Fig. 4.2.c.1: Laser stability of MZI 1 single-mode fiber.

Figure 4.2.c.1 presents the temporal evolution of the laser emission spectrum obtained using an MZI single-mode filter. The output spectrum is monitored over time, with the wavelength ranging approximately from 1540 nm to 1580 nm and the measurement lasting about 65 minutes. The spectra exhibit sharp and narrow peaks, indicating that the interferometer acts as a wavelength-selective filter inside the laser cavity. These peaks correspond to the resonant wavelengths that satisfy the interference condition between the two optical paths of the interferometer.

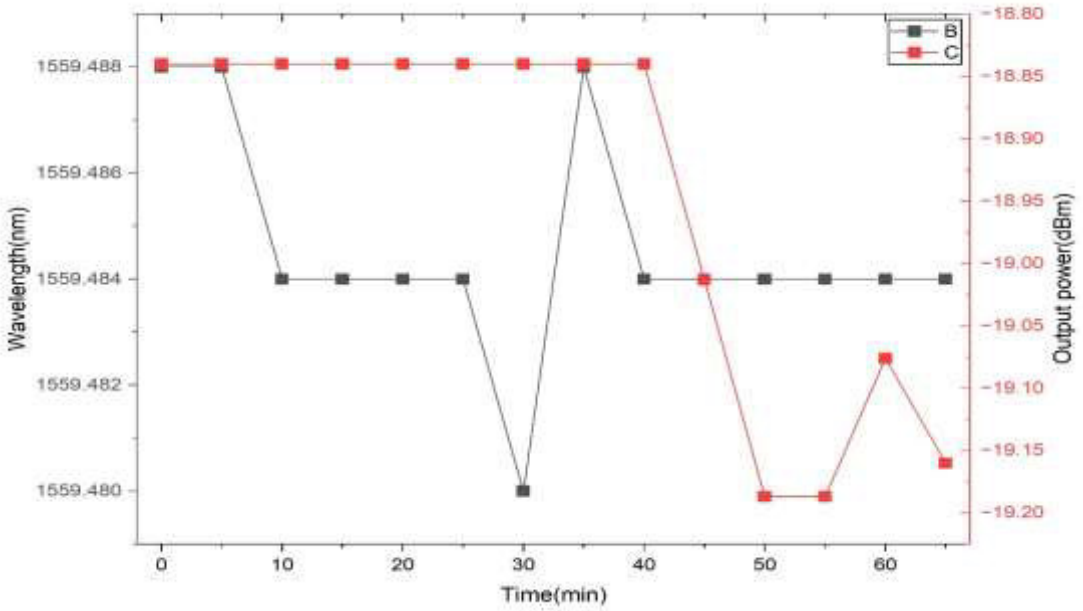

Fig. 4.2.c.2: Laser stability table of MZI 1 single-mode fiber

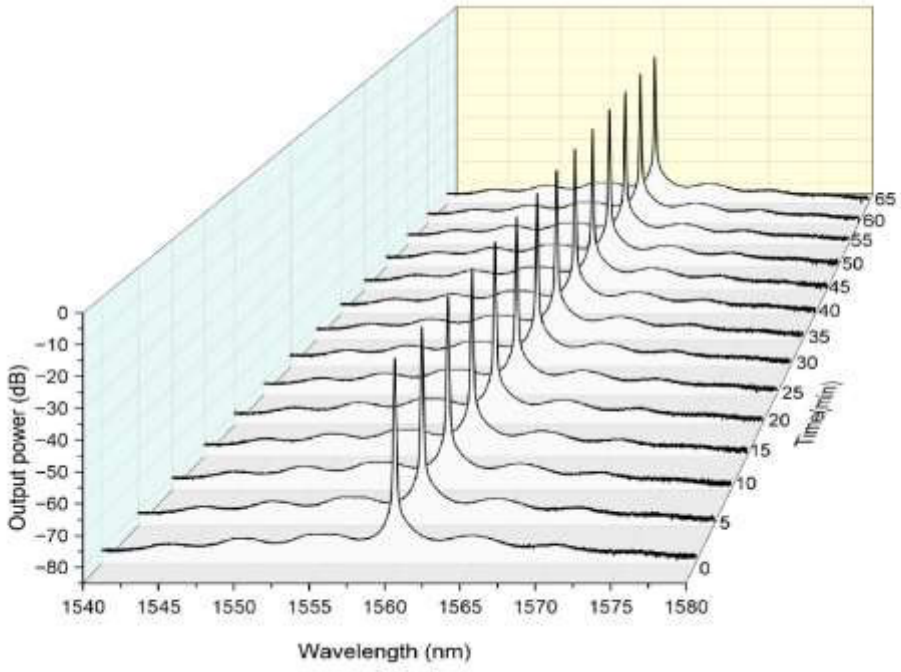

Fig. 4.2.d.1: Laser stability of MZI 2 single-mode fiber.

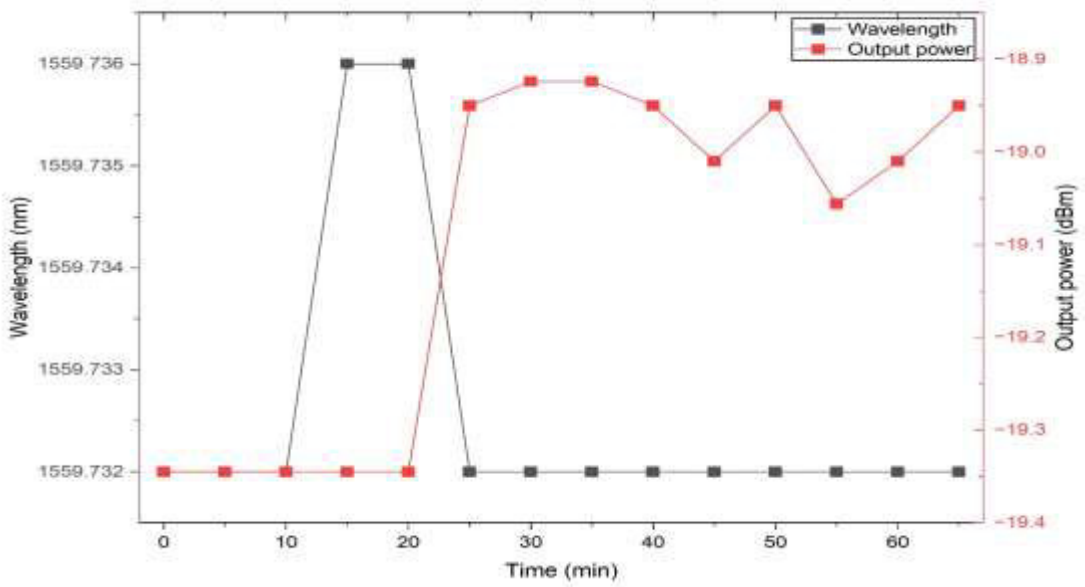

Fig. 4.2.d.2: Laser stability table of MZI 2 single-mode fiber

Figures show a multi-wavelength output, with several sharp spectral peaks in each trace. The overall peak power remains stable, with the maximum production consistently reaching about 0 dB during all measurements. The results from the time-lapse spectral analysis demonstrate that the resonant wavelength exhibits excellent stability over 5 minutes.

4.3. Laser Strain

The study is based on how the laser radiation properties change under a strain mechanism. In a laser using fiber optics, when the cavity or related devices are stressed, the optical path and refractive index are varied. This can cause wavelength drift as well as fluctuations in light output.

For the present experiment, the laser output was connected to a fiber segment on a precision translation stage, offering controlled elongation. The strain varied from 0 to 100 μm in 10-μm increments for three cores and from 0 to 210 μm for seven cores, in 10-μm increments.

At each step, the emission spectrum was recorded with the details on an optical spectrum analyzer (OSA) to monitor the output power. The strain results of a laser using an MZI with three cores, seven cores, the MZI1, and the MZI2 are shown in Figure 4.3.

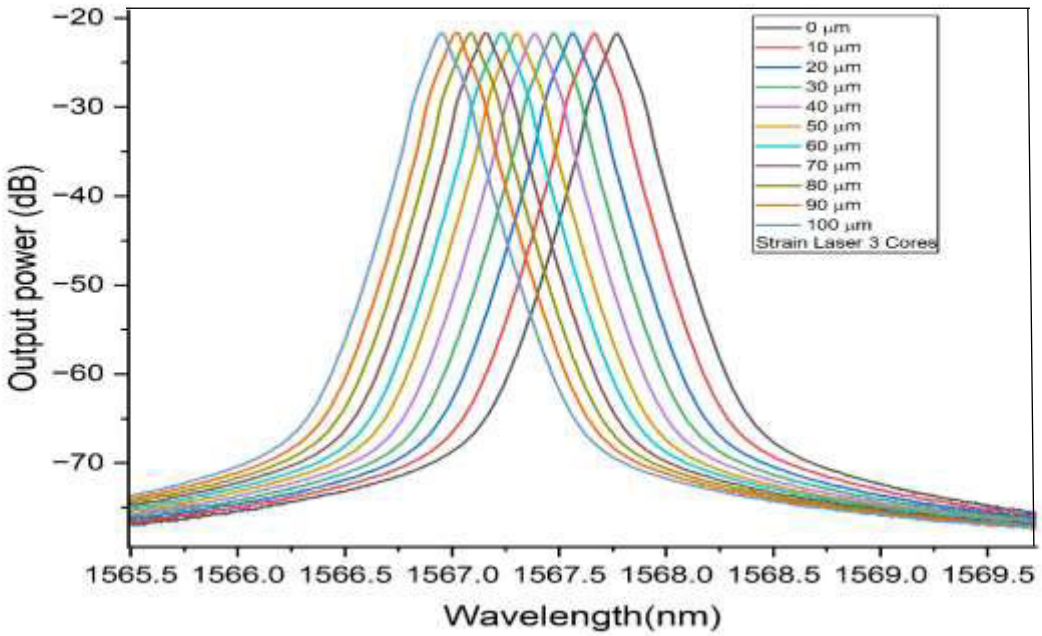

Fig. 4.3.a. Strain laser of MZI 3 cores

The figure shows the laser emission spectra under different applied strain levels for a fiber laser filtered by a Mach–Zehnder interferometer based on a multicore optical fiber with three cores. The strain applied to the fiber varies from 0 µm to 100 µm, and the corresponding output spectra are recorded in the wavelength range around 1566–1569 nm. As the strain applied to the fiber increases, the following behavior is observed:

- The laser peak shift progressively toward shorter wavelengths.
- The spectral shape remains nearly unchanged.
- The output power level is relatively stable.

This behavior indicates that the interferometer maintains a stable spectral filtering effect while responding sensitively to the applied strain.

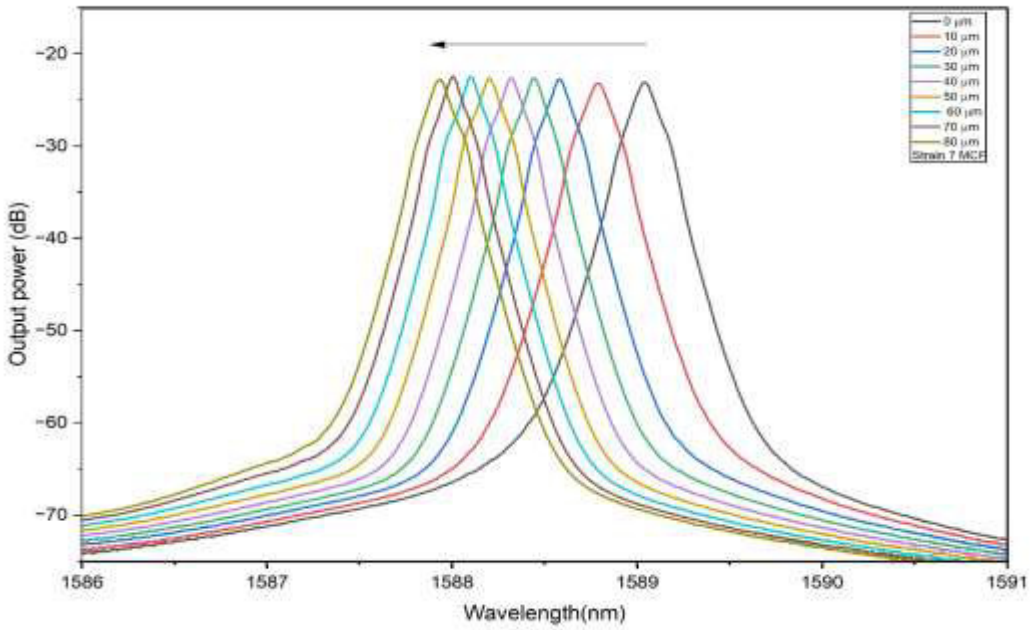

Fig. 4.3.b.1. Strain laser of MZI 7 cores

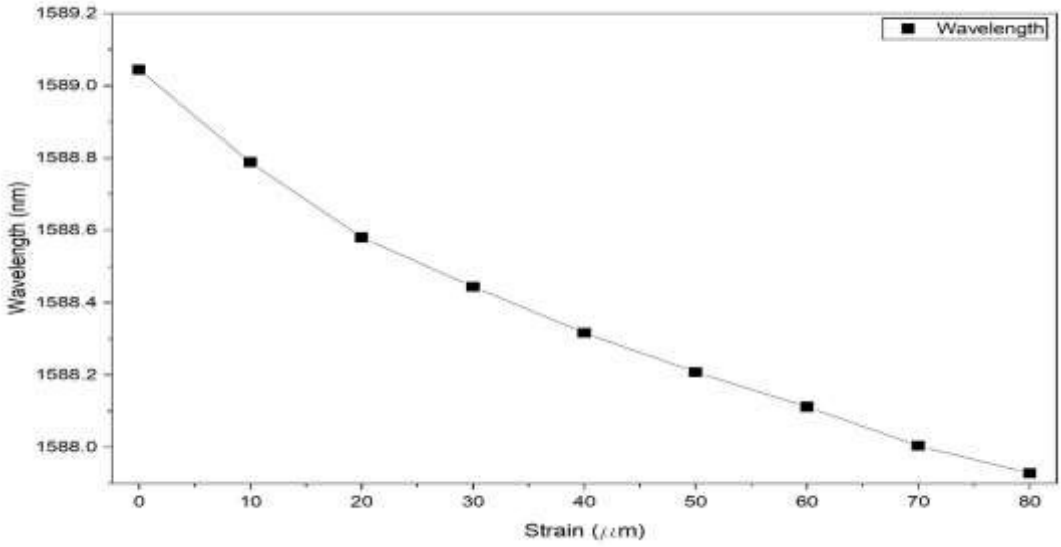

Fig. 4.3.b.2. Strain laser table MZI 7 cores

The figures display a seven-core sensor arrangement for this measurement. They trace a set of distinct bell-shaped spectral peaks, each one for an individual displacement level of 10 μm. These results demonstrate that, at each step, the output power exhibits distinct wavelength shifts with displacement, confirming high sensitivity and reliability. The experiment clearly shows that the laser output wavelength is a monotonic, approximately linear function of the applied displacement and, as such, is an excellent transducer for measuring strain.

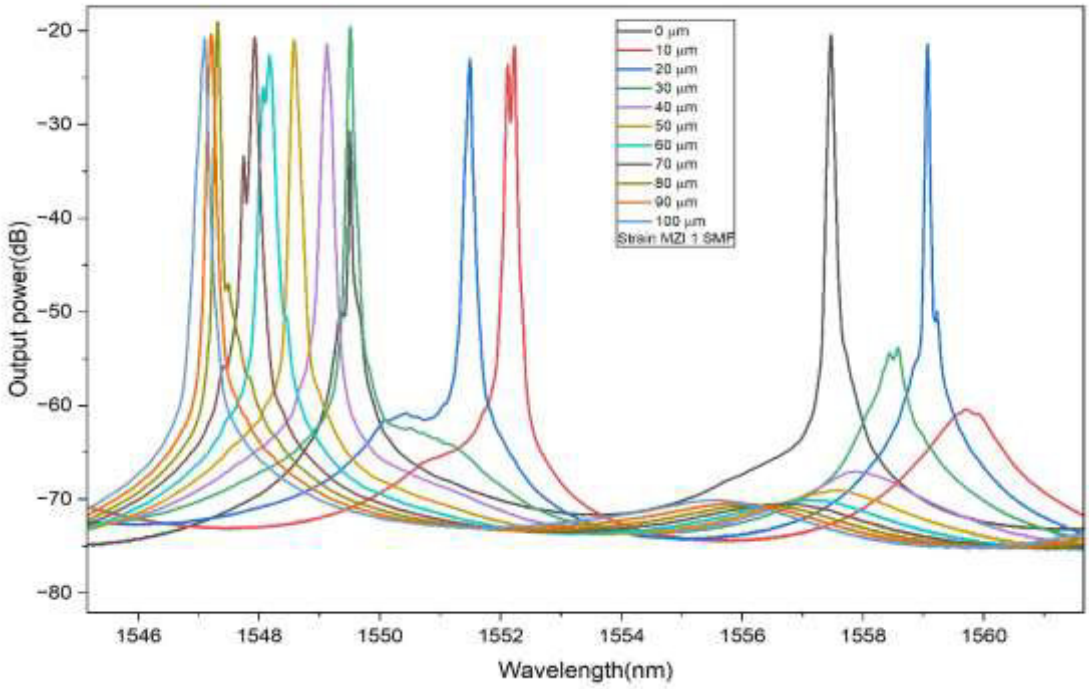

Fig. 4.3.c. Strain laser of MZI 1 SMF

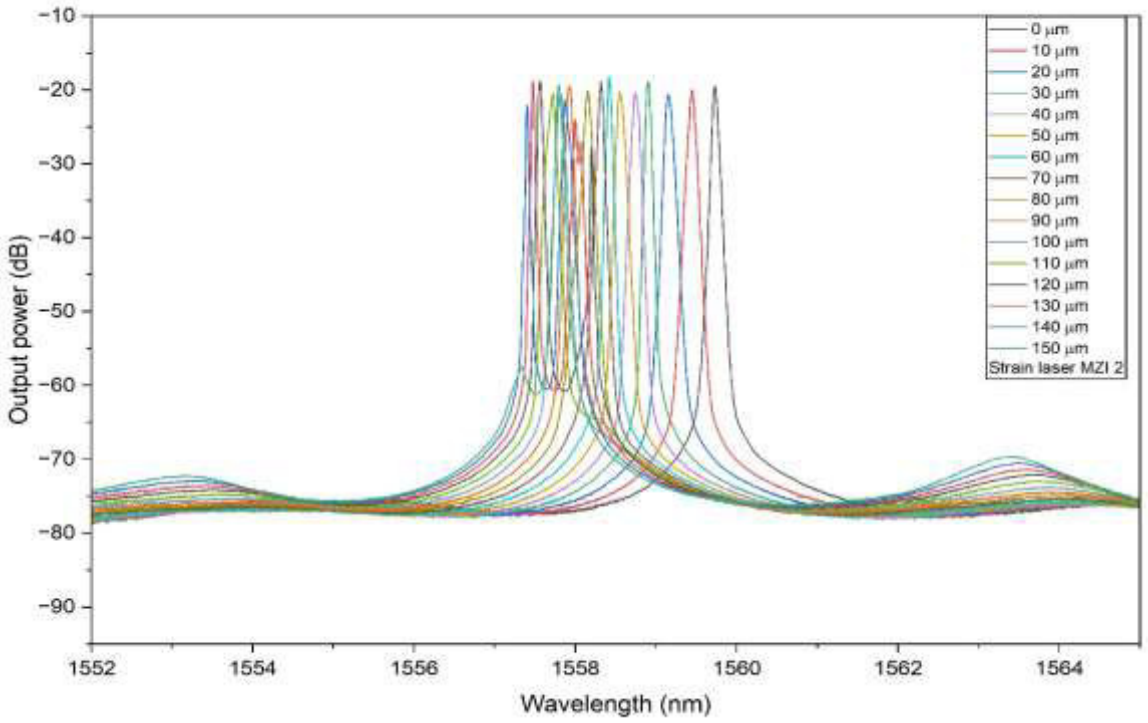

Fig. 4.3.d.1. Strain laser of MZI 2 SMF

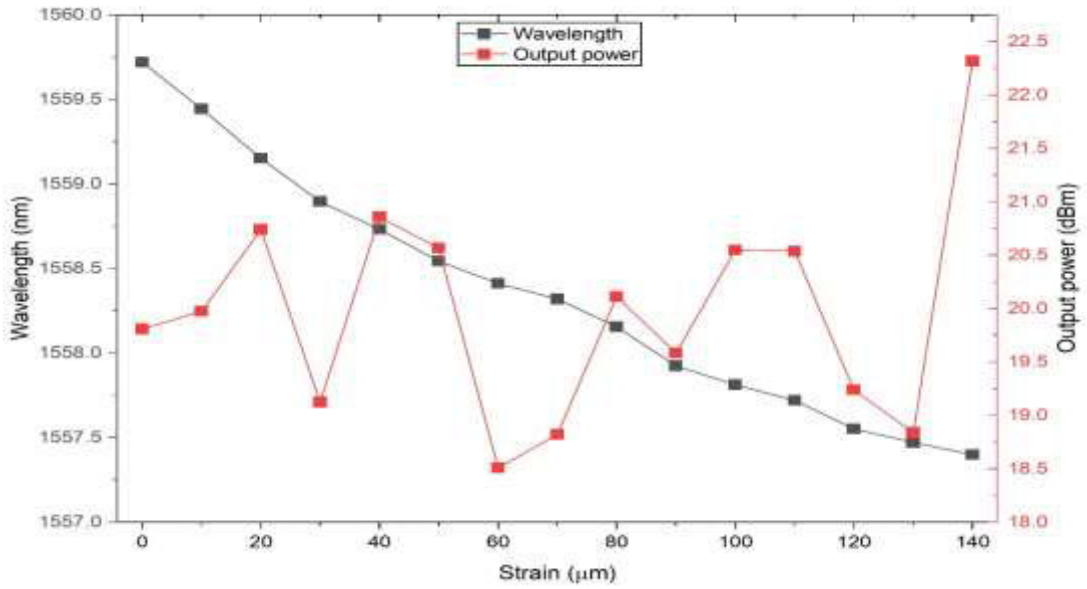

Fig. 4.3.d.2. Strain laser table of MZI 2 SMF

The plots show the MZI1 and MZI2 arrangements of single-mode fiber laser sensors. For this measurement, the data confirm that the strain laser MZIs 1 and 2 function as highly effective linear-displacement strain sensors based on wavelength encoding. Their high sensitivity and wide dynamic range are excellent. The primary trade-off observed is a decrease in output power at higher strain levels, which must be considered in practical sensing applications.

4.4. Laser Torsion

When torsional stress is applied to a fiber laser system, the interferometric pattern helps us to understand its effect on wavelength stability, fringing visibility, and as a sensing parameter. For this test, the fiber segment with the interferometer was clamped between two rotational mounts. This configuration allowed controlled torsion to be applied. **The twist level was varied from 0°C to 120°C. At each torsion stage, an optical spectrum analyzer (OSA) recorded the output spectrum and data derived from spectrum measurements.** The torsion results of a laser using a Mach-Zehnder Interferometer with three cores, seven cores, the MZI1, and the MZI2 are shown in Figure 4.4.

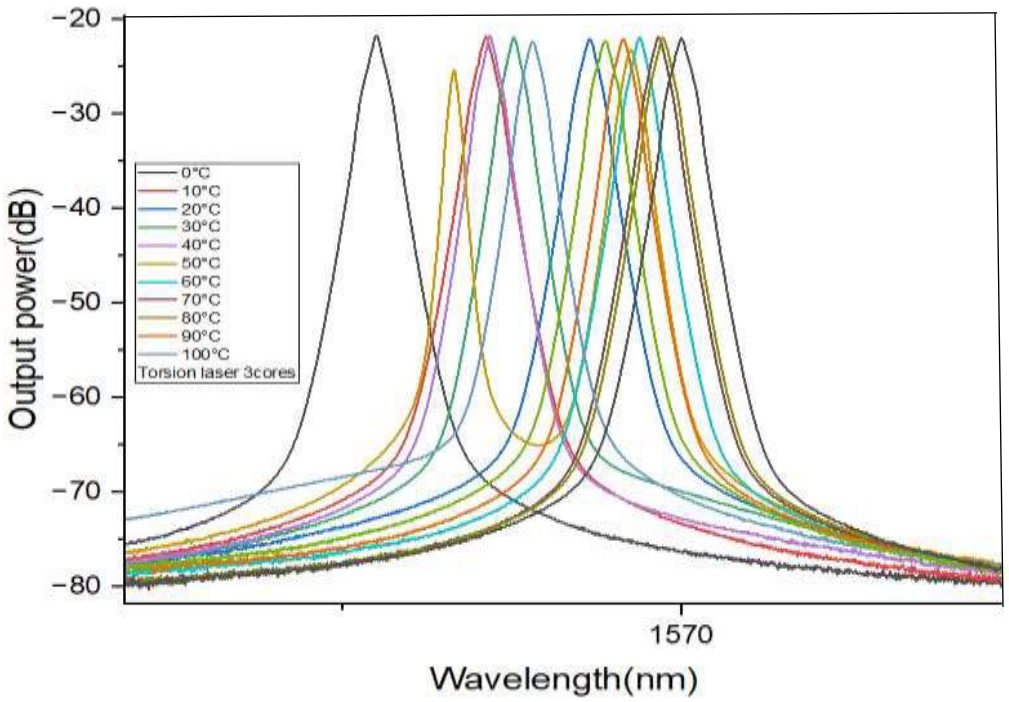

Fig. 4.4.a. Torsion laser of MZI 3 cores

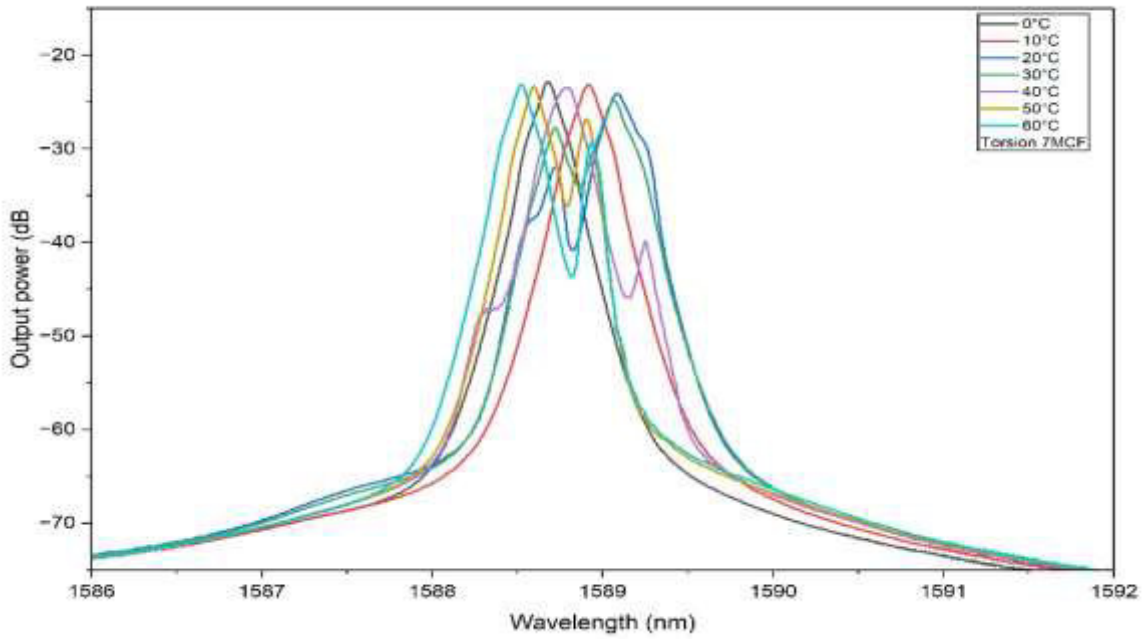

Fig. 4.4.b. Torsion laser of MZI 7 cores

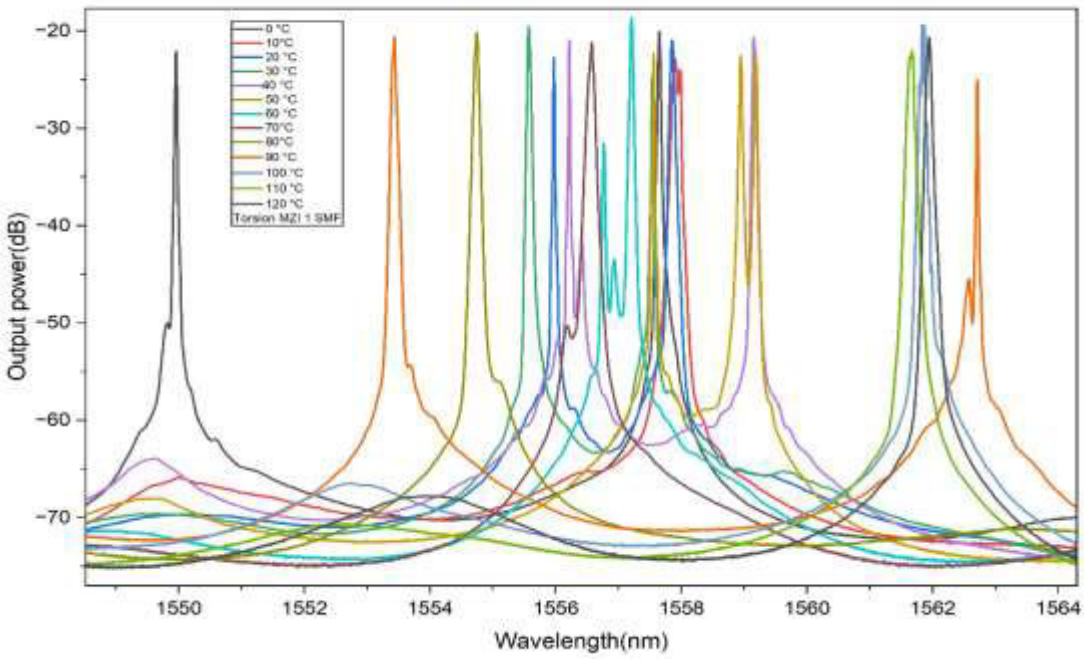

Fig. 4.4.c. Torsion laser of MZI 1 SMF

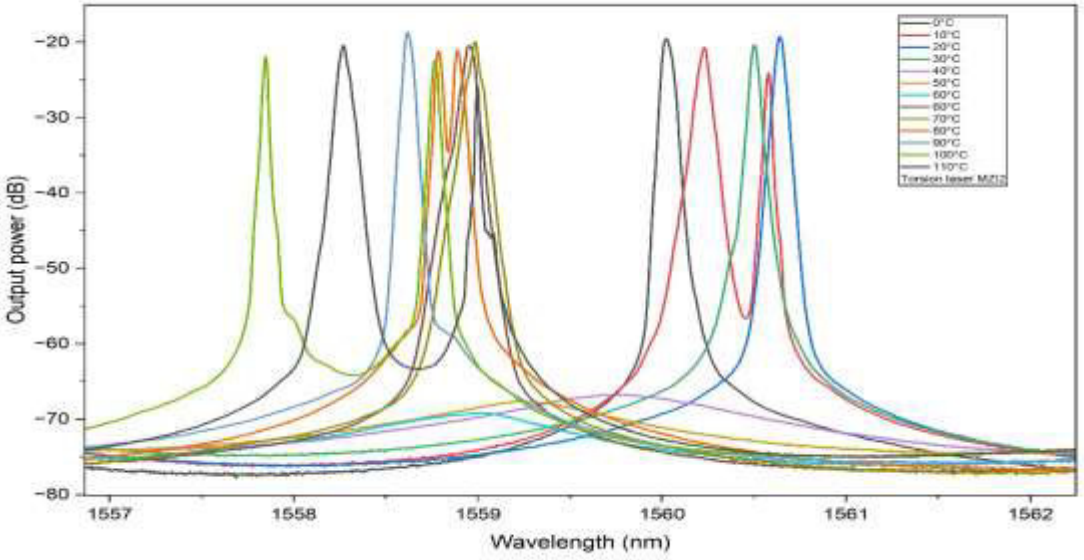

Fig. 4.4.d. Torsion laser of MZI 2 SMF

With the torsion test, every 30◦ produces a wavelength shift. We start with a power of 5 dB, with a peak wavelength. Applying 60◦, the output signal doubles, indicating that torsion also affects mode coupling strength and polarization states. Thus, it's important to reinforce interference fringes because torsion changes birefringence and polarization faster than it changes physical length. These results suggest that twisting can serve as a standalone measure of sensitivity. However, the sensitivity trends observed in this research align with the theoretical predictions from the model, which couples modes and alters birefringence under torsional strain.

4.5. Laser Temperature

The investigation aimed to explore the effects of temperature on the optical response of a fiber laser system. This study primarily focuses on thermal sensitivity and its impact on stability and sensing applications. Temperature variations in fiber interferometric systems can alter the refractive index due to the thermo-optic effect and change the fiber's modal length due to thermal expansion. These changes can cause notable spectral shifts in the interference fringe patterns and, in some cases, may even influence output power.

In this study, the section of the laser cavity containing the interferometer was placed in a temperature-controlled chamber. The temperature was increased from 20 °C to 120 °C in steps of 10 °C, with 5 minutes allowed at each temperature for stabilization. During the tests, the laser's output spectrum was measured using an OSA (Optical Spectrum Analyzer), and power was monitored with an optical power meter. The results showed a linear shift in wavelength as temperature increased. While temperature can be used to tune the interferometer wavelength in fiber lasers, it also highlights the importance of temperature stabilization for any application that requires precise wavelength control. The temperature results of a laser using an MZI with three cores, seven cores, the MZI1, and the MZI2 are shown in Figure 4.5.

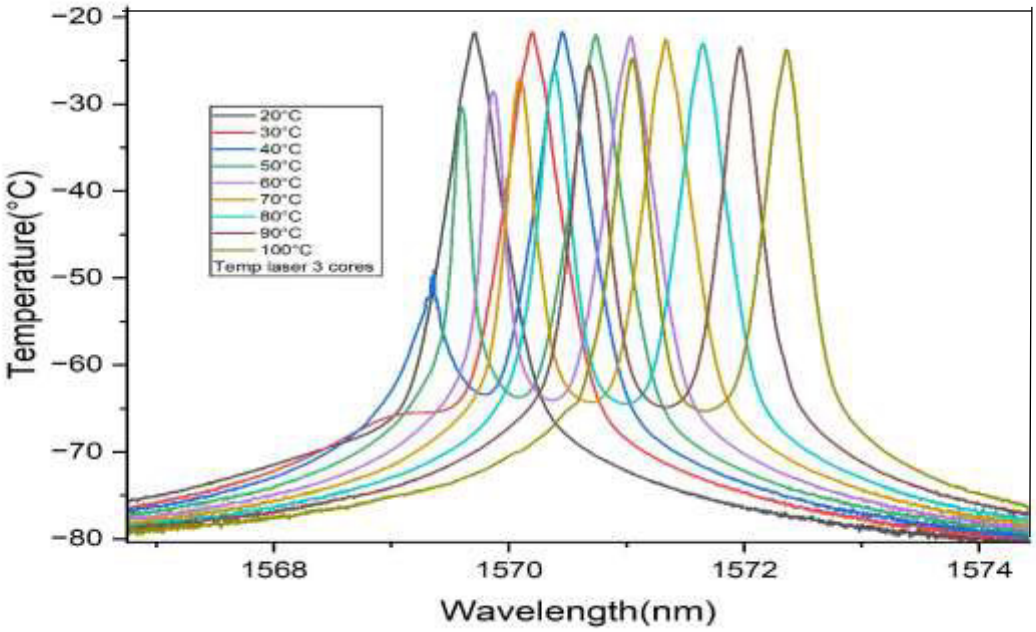

Fig. 4.5.a. Temperature laser of MZI 3 cores

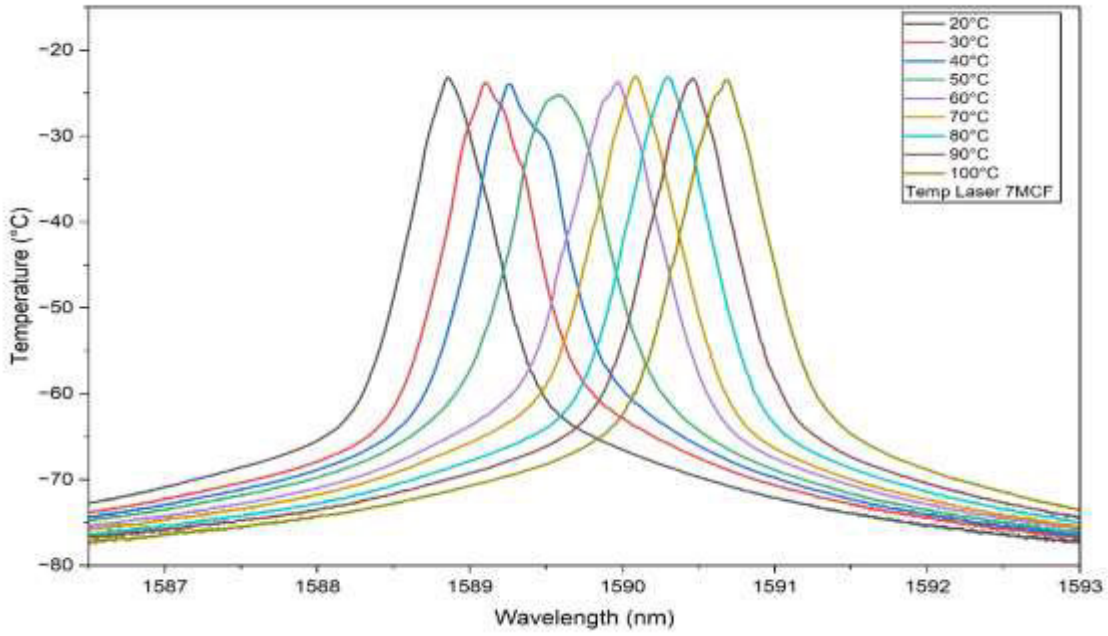

Fig. 4.5.b.1. Temperature laser of MZI 7 cores

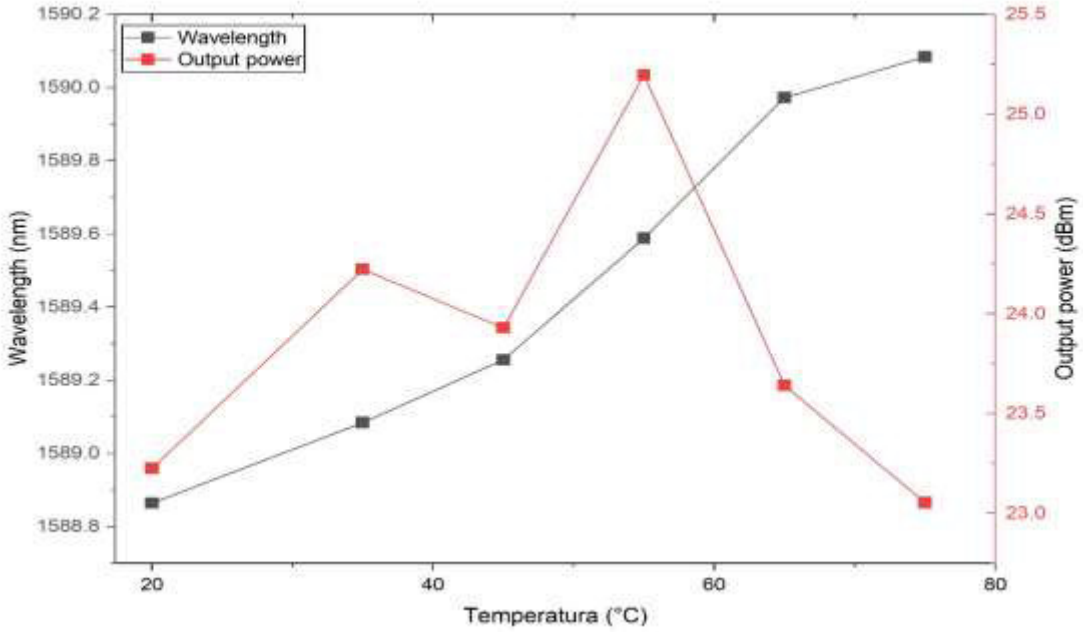

Fig. 4.5.b.2. Temperature laser table of MZI 7 cores.

In this trial, we observe that each temperature is associated with a distinct spectral peak, which represents the characteristic wavelength where the device is most sensitive to the specific temperature. As the temperature increases, the spectral peak shifts to a longer wavelength. This is a clear demonstration of the thermo-optic effect and high sensitivity over a moderate range, ideal for precision temperature measurement. There is a continuous shift, making temperature determination straightforward via calibration.

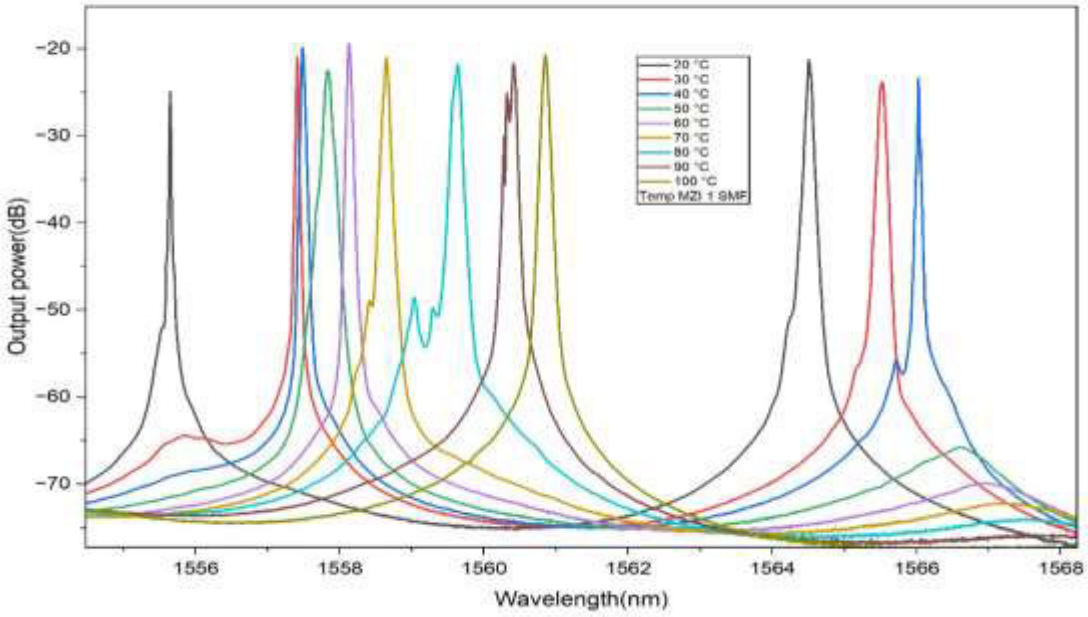

Fig. 4.5.c. Temperature laser of MZI 1 SMF

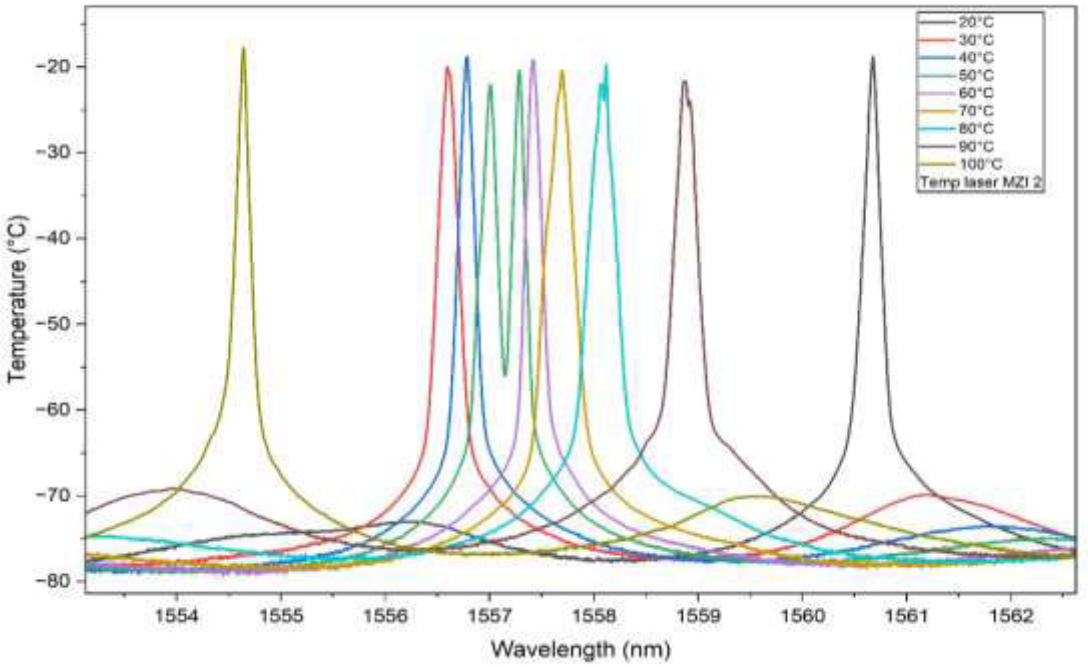

Fig. 4.5.d.1. Temperature laser of MZI 2 SMF

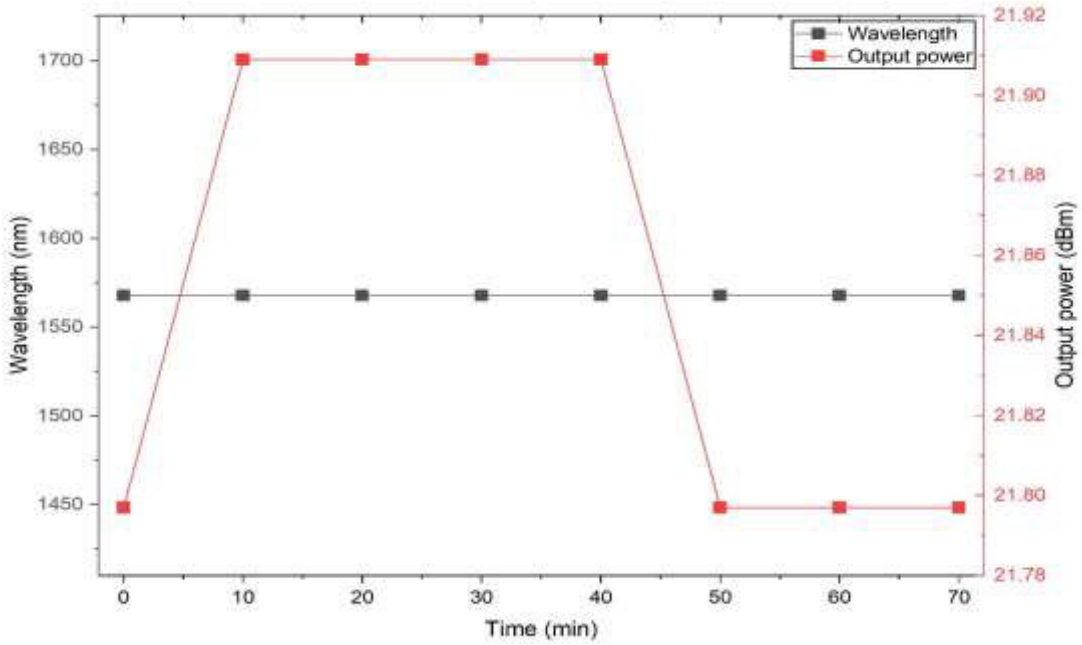

Fig. 4.5.d.2. Temperature laser table of MZI 2 SMF

In this trial, the MZI using standard single-mode fiber is significantly more complex, exhibiting mode structure and discontinuous peak shifts, which makes it challenging to use for simple, single-point temperature sensing without advanced spectral tracking. It shows a non-linear, modal shift, which would necessitate a much more complex interrogation system to accurately track temperature across the entire range.

4.6. Spectral Analysis of Laser Emissions

This section gives details on the spectral measurements of the laser's emission, highlighting important features such as line width, central wavelength, and spectral stability. The Emission Spectrum Analysis allows us to judge coherence and wavelength stability.

These spectral characteristics have a direct impact on the resolution and accuracy of the sensor. Several similarities and differences are seen during the

trial of a laser system with a Mach-Zehnder Interferometer (MZI) using standard single-mode fiber (SMF) or multicore fiber (MCF).

1. Similarities

Main Observation:

- Basic Principle of Interference: They both depend on splitting light into two optical paths and then re-combining them to create interference fringes, which will shift with changes like temperature or stress.
- Incorporation into the Laser System: In both cases, the MZI is placed inside the laser cavity as a spectral filter, which allows single and multi-wavelength lasing out of the same source.
- Vulnerability to External changes: Both react with the change of refractive index or optical path length and phase difference and, thus, can be used for sensing things like temperature or stress.
- Polarity Control Required: Both of them require regulated polarization states for operation, and this is done by using a polarization controller to control the light effectively and keep fringes from disappearing completely.
- Spectral Response Characteristics: The same parameters are observed, including free spectral range (FSR), extinction ratio, insertion loss, and fringe visibility.

2. Differences

Parameter MZI with SMF:

- Structurally, a path separation is needed. Optical path separation uses fiber couplers; distinct fiber arms are created when multiple cores within a single fiber serve as pathways for light.
- Easier splicing: use a standard fusion splicer.

- In environmental terms, the two arms face similar conditions in general, which limits differential phase unless deliberate asymmetry is imposed.
- Larger and much less firm, partly due to its physical separation.
- Multi-Parameter Sensing: Mostly measures one parameter at a time. In this MZI, each arm primarily operates in the fundamental mode and only with little crosstalk.
- Insertion Loss is often lower because the SMF couplers are well optimized and there is minimal inter-core crosstalk.

Parameters MZI with MCF

- Multicore geometry requires fine-tuning to align correctly. Different cores can be designed to possess different sensitivities; this improves fundamentally multiparameter sensing. Compact, integrated geometry containing multiple paths within one cladding.
- Can measure a plurality of different parameters at once, such as strain, torsion, and temperature, among the responses from different supermodes.
- Strong coupling between cores can produce supermodes, turning the MZI into a supermode interferometer with more spectral features.
- If inter-core coupling is poor, or if splicing between MCF and regular components isn't quite perfect, you may experience slightly more loss.
- More thermal stability and mechanical integrity due to the common cladding, but it is still sensitive to twisting.

Chapter 5. Conclusion

5.1. Conclusions

A new fiber laser system, designed, fabricated, and tested for high-sensitivity multi-parameter optical sensing, is described in this thesis. The system employs single-mode multicore fiber interferometers as wavelength-selective filters, making it the first compact and flexible platform to provide real-time monitoring in multiple channels.

Experimental results show that the laser's emission stability remains unchanged despite variations in the environment. The stability, combined with high-resolution measurements of strain, torsion, and temperature effects, greatly enhances sensor performance. Spectral analysis reveals narrow linewidth and steady wavelength operation. Both are essential to practical sensing applications, which demand high resolution and reliability.

Furthermore, all-fiber sensing systems have been successfully used with single-mode fibers to achieve high-purity spectral responses efficiently and with excellent sensitivity, using multi-core fibers. It demonstrates the practicality and potential of an all-fiber multi-functional sensing system. The findings provide a solid foundation for improved supermode interferometers based on multicore fibers, enabling future high-resolution monitoring technology.

In sum, this study provides scalable, robust, yet accurate solutions that are appropriate for complex and dynamic environments, hence making a significant contribution to the field of optical sensing.

5.2. Future work

Based on these initial results, in the future, we will concentrate on constructing a fiber laser sensing system that is more powerful and flexible. Potential improvements could come from incorporating signal processing techniques and perhaps even machining operations to reduce noise levels. We may also consider new multicore fiber designs to enhance the sensitivities and selectivity for specific parameters. Furthermore, we can examine methods for packaging and miniaturizing the system to make it practical for field use.

From a practical viewpoint, the system sketched above could be employed for real-time monitoring in industry, medicine, and the environment, where simultaneous multiparameter sensing is mandatory. Giving the system greater capabilities in terms of wireless data transmission and remote operation will help extend its use in intelligent sensing networks.

References

[1] Senior, J. M. (2009). *Optical fiber communications: Principles and practice* (3rd ed.). Pearson Education.

[2] Snell's law worksheet: Refraction and refractive index practice problems. (n.d.). *Scribd*. https://es.scribd.com/document/594872566/Snell-s-Law-Worksheet

[3] Hecht, E. (2017). *Optics* (5th ed.). Pearson Education.

[4] Agrawal, G. P. (2012). *Fiber-Optic Communication Systems* (4th ed.). Wiley.

[5] Snyder, A. W., & Love, J. D. (1983). *Optical Waveguide Theory*. Springer.

[6] Kao, C. K. (2002). *Fiber optics handbook: Fiber, devices, and systems for optical communications*. McGraw-Hill.

[7] Khanna, V. (2023, April 16). *Everything you need to know about multimode fiber*. Retrieved from https://www.fiberoptics4sale.com

[8] DINTEK. (2024, June 22). *Fiber optic cable image*. DINTEK. https://dintek.com.tw/images/2024/06/22/2024-06-17_14-09-12z.webpKnight, J. C. (2003). Photonic crystal fibres. *Nature*, 424(6950), 847–851. https://doi.org/10.1038/nature01940.

[9] Russell, P. (2006). Photonic-crystal fibers. *Journal of Lightwave Technology*, 24(12), 4729–4749. https://doi.org/10.1109/JLT.2006.885266

[10] The Office of the CTO. (n.d.). *MKS Instruments handbook: Principles & applications in photonics technologies*. MKS Instruments. https://www.mksinst.com

[11] Agrawal, G. P. (2019). *Nonlinear fiber optics* (6th ed.). Academic Press.

[12] Yermakov, O., Zeisberger, M., Schneidewind, H., Lorenz, A., Wieduwilt, T., Schwuchow, A., Khosravi, M., Tiess, T., & Schmidt, M. A. (2025). Fiber-based angular demultiplexer using nanoprinted periodic structures on single-mode multicore fibers. *Nature Communications, 16*, Article 2294. https://doi.org/10.1038/s41467-025-20179-9

[13] Zhang, Y., Wang, Y., Zhang, Y., & Zhang, Y. (2023). Advances in multicore fiber interferometric sensors. *Sensors, 23*(7), 3436. https://doi.org/10.3390/s23073436

[14] IEEE Spectrum. (2023). *Novel 19-core fiber hits 1.7 petabits per second*. https://spectrum.ieee.org/multicore-fiber Fresnel, A. J. (1819). *Mémoire sur la diffraction de la lumière*. Mémoires de l'Académie des Sciences de l'Institut de France. 2. Schmidt, M. A. (n.d.). *We did it: High-density, low-crosstalk multicore fiber—now for visible light*.

[15] Michelson, A. A., & Morley, E. W. (1887). *On the Relative Motion of the Earth and the Luminiferous Ether*. American Journal of Science, 34(203), 333–345.

[16] Fabry, C., & Perot, A. (1899). *Theory and applications of the Fabry-Perot interferometer*. Annales de Chimie et de Physique, 16, 115–144.

[17] Maiman, T. H. (1960). *Stimulated Optical Radiation in Ruby*. Nature, 187(4736), 493– 494.

[18] Yeh, Y. S., & Cummins, H. Z. (1964). *Localized Fluid Flow Measurements with an He-Ne Laser Spectrometer*. Applied Physics Letters, 4(9), 176–178.

[19] Liu, Y., Li, X., Zhang, Y. N., & Zhao, Y. (2021). Fiber-optic sensors based on Vernier effect. *Measurement*, *167*, 108451.

[20] Kapron, F. P., Keck, D. B., & Maurer, R. D. (1970). *Radiation Losses in Glass Optical Waveguides*. Applied Physics Letters, 17(10), 423–425.

[21] G. Meltz, W. W. Morey, and W. H. Glenn, "Formation of Bragg gratings in optical fibers by a transverse holographic method," *Optics Letters*, vol. 14, no. 15, pp. 823–825, 1989.

[22] B. Lee, "Review of the present status of optical fiber sensors," *Optical Fiber Technology*, vol. 9, no. 2, pp. 57–79, 2003.

[23] J. C. Knight, "Photonic crystal fibres," *Nature*, vol. 424, no. 6950, pp. 847–851, 2003.

[24] M. Bianchetti, M. S. Avila-Garcia, R. I. Mata-Chavez, J. M. Sierra-Hernandez, L. A. ZendejasAndrade, D. Jauregui-Vazquez, J. M. Estudillo-Ayala and R. Rojas-Laguna,"

Symmetric and Asymmetric core-offset Mach-Zehnder interferometer torsion sensors," IEEE Photon. Technol. Lett. vol. 29, 1521-1524 (2017).

[25] M. S. Avila-Garcia, M. Bianchetti, R. I. Mata-Chavez, J. M. Sierra-Hernandez, D. Jauregui-Vazquez, J. R. Reyes-Ayona, J. M. Estudillo-Ayala and R. Rojas-Laguna, "High sensitivity strain sensors based on single-mode-fiber core-offset Mach-Zehnder interferometers" Opt. and Laser in Eng., vol. 107, 202-206 (2018).

[26] Ch. Tu, W. Guo, Y. Li, S. Zhang and F. Lu, "Stable multiwavelength and passively modelocked Yb-doped fiber based on nonlinear polarization rotation," Optics Communications 280, 448-452, 2007.

[27] W. G. Chen, S. Q. Lou, S. C. Feng, L. W. Wang, H. L. Li, T. Y. Gou and S. S. Jian, "Switchable multi-wavelength fiber ring laser based on a compact in-fiber Mach-Zehnder interferometer with photonic crystal fiber," Laser Physics 19, 2115-2119, 2009.

[28] F. F. Zhong, Y. Xu, Y. J. Zhang and Y. Ju, “Widely ultra-narrow linewidth 104 nm tunable all-fiber compact erbium-doped ring laser,” Laser Physics 21, 219-221, 2011.

[29] A. Hamzah, M. C. Paul, S. W. Harun, N. A. D. Huri, A. Lokman, M. Pal, S. Das, S. K. Bhadra, H. Ahmad, S. Yoo, M. P. Kalita, A. J. Boyland and J. K. Sahu, “Compact fiber laser at L Band region using erbium-doped zirconia fiber,” Laser Physics 21, 176-179, 2011.

[30] Contreras-Teran, M. A., Berganza, A., Lindner, F., Bierlich, J., Wondraczek, K., & Villatoro, J. (2024). Multipoint temperature-independent vector bending sensing with coupled-core fibers. *IEEE Sensors Journal*.

[31] Villatoro, J., Arrizabalaga, O., Diez, M., Arrospide, E., Antonio-Lopez, E., Zubia, J., ... & Amezcua-Correa, R. (2018, July). Simple multi-core optical fiber accelerometer. In Optical Sensors (pp. SeW3E-4). Optica Publishing Group.

[32] Flores-Bravo, J. A., Madrigal, J., Zubia, J., Sales, S., & Villatoro, J. (2022). Coupled-core fiber Bragg gratings for low-cost sensing. *Scientific Reports*, *12*(1), 1280.

[33] Villatoro, J., Antonio-Lopez, E., Zubia, J., Schülzgen, A., & Amezcua-Correa, R. (2017). Interferometer based on strongly coupled multi-core optical fiber for accurate vibration sensing. *Optics express*, *25*(21), 25734-25740.

[34] Amorebieta, J., Pereira, J., Durana, G., Franciscangelis, C., Ortega-Gomez, A., Zubia, J., ... & Margulis, W. (2022). Twin-core fiber sensor integrated in laser cavity. *Scientific Reports*, *12*(1), 11797.

[35] Lopez-Torres, D., Elosua, C., Villatoro, J., Zubia, J., Rothhardt, M., Schuster, K., & Arregui, F. J. (2017). Enhancing sensitivity of photonic crystal fiber

interferometric humidity sensor by the thickness of SnO2 thin films. *Sensors and Actuators B: Chemical*, *251*, 1059-1067.

[36] Wang, Z., Zhang, H., Wang, J., Jiang, S., Gao, S., Wang, Y., ... & Ren, W. (2022). Photothermal multi-species detection in a hollow-core fiber with frequency-division multiplexing. *Sensors and Actuators B: Chemical*, *369*, 132333.

[37] Zhao, P., Zhao, Y., Bao, H., Ho, H. L., Jin, W., Fan, S., ... & Wang, P. (2020). Modephase-difference photothermal spectroscopy for gas detection with an anti-resonant hollow-core optical fiber. *Nature communications*, *11*(1), 847.

[38] M. N. Mohd Nasir, M.H. Al-Mansoori, H.A. Abdul Rashid, P.K. Choudhury, Z. Yusoff, Multiwavelength Brillouin-erbium fiber laser incorporating a fiber Bragg grating filter, Laser Phys. 18 (2008) 446–448.

[39] Gonzales-Reyna, M. et al. “Sensor de temperatura basado en un interferómetro modal de tipo Mach-Zehnder de fibra óptica”. Universidad de Guanajuato, Campus Irapuato-Salamanca. 2015.

[40] Kuhlmey B T., et al. “Multipole analysis of photonic crystal fibers with coated inclusions”. 2006 Opt. Express 14 10851–64

[41] Sierra-Hernandez, J. M., et al. “Torsion sensing setup based on a three beam path Mach–Zehnder interferometer”. Microwave and Optical Technology Letters, 2015, vol. 57, no 8, p. 1857-1860.

[42] Huerta-Mascotte, Eduardo, et al. A Core-Offset Mach Zehnder Interferometer Based on A Non-Zero Dispersion-Shifted Fiber and Its Torsion Sensing Application. Sensors, 2016, vol. 16, no 6, p. 856.

[43] E. Huerta-Mascotte, J. M. Sierra-Hernandez, R. I. Mata-Chavez, D. JaureguiVazquez, A. CastilloGuzman, J. M. Estudillo-Ayala, A. D. Guzman-Chavez and R. RojasLaguna, “A core-offset Mach-Zehnder interferometer based on a non-zero dispersionshifted fiber and its torsion sensing application,” Sensor, vol. 16, 856 (2016).

[44] Advances in Multicore Fiber Interferometric Sensors de Y Yao · 2023 · Cité 22 fois, MCF interferometric sensors have been developed to measure various physical and chemical parameters such as temperature, strain, curvature, refractive index, ...

[45] E. Huerta-Mascotte, J. M. Sierra-Hernandez, R. I. Mata-Chavez, D. JaureguiVazquez, A. CastilloGuzman, J. M. Estudillo-Ayala, A. D. Guzman-Chavez and R. RojasLaguna, “A core-offset Mach-Zehnder interferometer based on a non-zero dispersionshifted fiber and its torsion sensing application,” Sensor, vol. 16, 856 (2016).

[46] Rojas Hernandez, P. G., Belal, M., Baker, C., Pidishety, S., Feng, Y., Friebele, E. J., Shaw, L. B., Rhonehouse, D., Sanghera, J., & Nilsson, J. (2020). Efficient extraction of high pulse energy from partly quenched highly Er^{3+}-doped fiber amplifiers. *arXiv preprint arXiv:2002.04356*. https://arxiv.org/abs/2002.0435G. Anzueto-Sanchez, A. Martinez-Rios, and J. Castrellon-Uribe, “Tuning and wavelength switching erbium-doped fiber ring lasers by controlled bending in arc-induced long-period fiber gratings,” Opt. Fiber Technol., vol. 18, 513-517 (2012).

[47] Tsai, CJ., Chen, HZ., Wang, WC. *et al.* A single-mode wavelength-selectable erbium laser based on multiple-fiber-ring design. *Opt Quant Electron* 54, 814 (2022). https://doi.org/10.1007/s11082-022-04205-6

[48] Amalia Miliou *Photonics* 2021, *8*(7), 265; https://doi.org/10.3390/photonics8070265 In-Fiber Interferometric-Based Sensors: Overview and Recent Advances

[49] B. Yao, Y. Wu, Y. Cheng, A. Zhang, Y. Gong, Y.-J. Rao, Z. Wang, and Y. Chen, "All-optical Mach-Zehnder interferometric NH3 gas sensor based on graphene microfiber hybrid waveguide," Sens. and Actuators B, vol. 194, 142-148 (2014).

[50] Fernández-Hinestrosa, A., Luque-González, J. M., Cheben, P., Schmid, J. H., Wangüemert-Pérez, J., Molina-Fernández, I., Ortega-Moñux, A., & others. (2024). Nanophotonic Bragg grating assisted Mach-Zehnder interferometers for O-band add-drop filters. Scientific Reports, 14(1), 18492.

[51] ScienceDirect. (n.d.). *Mach-Zehnder interferometer – an overview*. https://www.sciencedirect.com/topics/engineering/mach-zehnder-interferometer

[52] Zhang, Y., Wang, Y., Zhang, Y., & Zhang, Y. (2023). Advances in multicore fiber interferometric sensors. *Sensors, 23*(7), 3436. https://doi.org/10.3390/s23073436

[53] Culshaw, B., & Kersey, A. (2008). Fiber-optic sensing: A historical perspective.

Journal of Lightwave Technology, *26*(9), 1064–1078. https://doi.org/10.1109/JLT.2008.923652

[54] Aprilia, C., Putri, M., & Arianty, R. D. (2025). Interference of Light Waves in Optical Fiber. Journal of Frontier Research in Science and Engineering, 3(3), 34–41. Retrieved from https://journal.riau-edutech.com/index.php/jofrise/article/view/142Agrawal, G. P. (2019). *Nonlinear fiber optics* (6th ed.). Academic Press.

[55] Yermakov, O., Zeisberger, M., Schneidewind, H., Lorenz, A., Wieduwilt, T., Schwuchow, A., Khosravi, M., Tiess, T., & Schmidt, M. A. (2025). Fiber-based angular demultiplexer using nanoprinted periodic structures on single-mode multicore fibers. *Nature Communications, 16*, Article 2294. https://doi.org/10.1038/s41467-025-20179-9

[56] Sensofar. (n.d.). *Interferometry technology and measuring principles*. https://www.sensofar.com/metrology/interferometry/

[57] Rizzelli, G. (2022). Advances in optical fiber communications. Applied Sciences, 12(10), 4818.

[58] Lee, B. H., Kim, Y. H., Park, K. S., Eom, J. B., Kim, M. J., Rho, B. S., & Choi, H. Y. (2012). Interferometric fiber optic sensors. Sensors, 12(3), 2467–2486. https://doi.org/10.3390/s120302467

[59] Thomas, J. I. (2019). The Classical Double Slit Interference Experiment: A New Geometrical Approach. American Journal of Optics and Photonics, 7(1), 1–9. https://doi.org/10.11648/j.ajop.20190701.11Shu, X., et al. (2002). Tunable fiber-optic interferometers for broadband optical sensing. *IEEE Sensors Journal*, 2(1), 28–32. https://doi.org/10.1109/JSEN.2002.1000246

[60] ScienceDirect. (n.d.). *Mach-Zehnder interferometer – an overview*. https://www.sciencedirect.com/topics/engineering/mach-zehnder-interferometer

[61] Sachidanand, P. S., Sreelal, M. M., Sreedharan, R., & Viswan, G. (2019). MoS_2 nanostructures as transparent material: Optical transmittance measurements. *Materials Today: Proceedings, 26*, 1744–1747. https://doi.org/10.1016/j.matpr.2019.05.423

[62] Zhou, D., Wang, Y., & Cooper, K. L. (2020). Recent advances in Fabry–Perot interferometer-based fiber sensors. *Sensors*, 20(22), 6514. https://doi.org/10.3390/s20226514

[63] Xiao, L., Chen, X., Li, X., Zhang, J., Wang, Y., Li, D., Hong, X., Shao, Y., & Chen, Y. (2025). Enhanced Sensitivity Mach–Zehnder Interferometer-Based Tapered-in-Tapered Fiber-Optic Biosensor for the Immunoassay of C-Reactive Protein (2), 90. https://doi.org/10.3390/bios15020090Wei, C., & Li, L. (2021).

[64] Wang, X., & Zhou, Y. (2021). *Design and optimization of laser diode packaging for thermal management in precision applications*. *Micromachines, 12*(11), 1372. https://doi.org/10.3390/mi12111372

[65] Kumar, A., & Singh, R. (2021). Sensors for daily life: A review. *International Journal of Engineering Research & Technology*, 10(7), 1–5.

[66] Huang, Y. W., Jin, T., & Huang, X. G. (2016). Research progress on Fabry-Perot interference-based fiber-optic sensors. Sensors, 16(9), 1424. https://doi.org/10.3390/s16091424Acompt

[67] Huang, Y. W., Jin, T., & Huang, X. G. (2016). Research progress on Fabry-Perot interference-based fiber-optic sensors. Sensors, 16(9), 1424. https://doi.org/10.3390/s16091424Acompt

[68] Zervas, M. N., & Codemard, C. A. (2014). High power fiber lasers: A review. *IEEE Journal of Selected Topics in Quantum Electronics*, 20(5), 219–241. https://doi.org/10.1109/JSTQE.2014.2306976

[69] Duran-Sanchez, I., et al. (2020). Fiber laser with interferometric filtering for high-resolution sensing applications. *Sensors*, 20(18), 5158. https://doi.org/10.3390/s20185158

[70] Jihad, N. J., & Abd Almuhsan, M. A. (2023). Future trends in optical wireless communications systems: Review. Technium: Romanian Journal of Applied Sciences and Technology, 13, 53–67. http://dx.doi.org/10.47577/technium.v13i.9474

[71] Silfvast, W. T. (2004). *Laser Fundamentals* (2nd ed.). Cambridge University Press.

[72] Koechner, W. (2006). *Solid-State Laser Engineering* (6th ed.). Springer.

[73] Electrical4U. (2024, May 3). *Types and components of lasers*. https://www.electrical4u.com/laser-types-and-components

[74] Senior, J. M., & Jamro, M. Y. (2009). *Optical Fiber Communications: Principles and Practice* (3rd ed.). Pearson Education.

[75] Ghatak, A., & Thyagarajan, K. (1998). *Introduction to Fiber Optics*. Cambridge University Press.

[76] Elahmadi, S., Srinath, M. D., Rajan, D., & Haberman, R. (2009, May). *Channel capacity and modeling of optical fiber communications*. In *2009 IFIP International Conference on Wireless and Optical Communications Networks (WOCN)* (pp. 1–5). IEEE. https://doi.org/10.1109/WOCN.2009.5010515 [69] Born, M., & Wolf, E. (1999). *Principles of Optics* (7th ed.). Cambridge University Press.

[77] Rojas Hernandez, P. G., Belal, M., Baker, C., Pidishety, S., Feng, Y., Friebele, E. J., Shaw, L. B., Rhonehouse, D., Sanghera, J., & Nilsson, J. (2020). Efficient extraction of high pulse energy from partly quenched highly Er^{3+}-doped fiber amplifiers. *arXiv preprint arXiv:2002.04356*. https://arxiv.org/abs/2002.0435

[78] R. Paschotta, “Encyclopedia of Laser Physics and Technology – Ytterbium-doped fiber amplifiers,” *RP Photonics Encyclopedia*, 2020. [Online]. Available: https://www.rpphotonics.com/yb_doped_fiber_amplifiers.html

[79] Senior, J. M., & Jamro, M. Y. (2009). *Optical Fiber Communications: Principles and Practice* (3rd ed.). Pearson Education.

[80] Ghatak, A., & Thyagarajan, K. (1998). *Introduction to Fiber Optics*. Cambridge University Press.

[81] https://www.fiberoptics4sale.com/collections/category_fiber-optic-devices

[82] Al-Raweshidy, H. S. (1992). *Coupling characteristics of fiber optic couplers*. British Telecom Research Laboratories. https://www.researchgate.net/publication/318762563_Coupling_Characteristics_of ber Optic_Couplers

[83] López, A., Zubia, J., Durana, G., & Aldabaldetreku, G. (2018). Characterization of a Ycoupler and its impact on the performance of polymer optical fiber links. *Sensors, 18*(12), 4373. https://doi.org/10.3390/s18124373

[84] ScienceDirect. (n.d.). *Polarization controller – an overview*.

[85] https://www.sciencedirect.com/topics/engineering/polarization-controller

[86] Zhang, S., Wang, J., Liu, X., & Li, Y. (2024). Insights into polarization relaxation of electromagnetic energy in dielectric materials. *Materials Today, 72*, 58–72. https://doi.org/10.1016/j.mattod.2024.05.002

[87] Xavier, G. B., Vilela de Faria, G., Temporão, G. P., & von der Weid, J. P. (2008). Full polarization control for fiber optical quantum communication systems using polarization encoding. *Optics Express, 16*(3), 1867–1873. https://doi.org/10.1364/OE.16.001867

[88] Garg, A., Sharma, R., & Dhingra, V. (n.d.). *Polarization studies in a computer-based laboratory*. Acharya Narendra Dev College, University of Delhi.

[89] Damask, J. N. (2005). *Polarization optics in telecommunications*. Springer.

[90] Zhang, H., Zhang, Y., Li, J., & Wang, J. (2021). *Characterization and performance analysis of semiconductor laser diodes for optical communication*. *Optics and Laser Technology, 138*, 106834. https://doi.org/10.1016/j.optlastec.2020.106834

[91] Xu, Y., Zhao, X., & Liu, C. (2022). *Thermal and spectral characteristics of DFB laser diodes for fiber optic sensing*. *Sensors and Actuators A: Physical, 345*, 113735. https://doi.org/10.1016/j.sna.2022.113735

[92] Wang, L., Chen, W., & Liu, H. (2023). *Temperature-dependent wavelength tuning and stability analysis of semiconductor laser diodes*. *IEEE Photonics Journal, 15*(3), 1–8. https://doi.org/10.1109/JPHOT.2023.3265210

[93] Tanaka, Y., & Ito, H. (2020). *Analysis of polarization characteristics in semiconductor lasers for sensing applications*. *Journal of Lightwave Technology, 38*(5), 1176–1182. https://doi.org/10.1109/JLT.2020.2965430

[94] Wang, X., & Zhou, Y. (2021). *Design and optimization of laser diode packaging for thermal management in precision applications*. *Micromachines, 12*(11), 1372. https://doi.org/10.3390/mi12111372

[95] QPhotonics LLC. (n.d.). QFBGLD-980-500 wavelength stabilized single mode fiber coupled laser diode 500 mW @ 980 nm [Product page]. QPhotonics. Retrieved from https://www.qphotonics.com/catalog/Wavelength-stabilized-single-mode-fiber-coupled-laser-diode-500m-p-855.html

[96] Zhou, Y., Wang, Z., & Liu, X. (2021). Optical fiber based temperature sensors: A review. Sensors, 21(6), 2156738. https://doi.org/10.3390/s2156738 Acomp

[97] Lee, B. H., Kim, Y. H., Park, K. S., Eom, J. B., Kim, M. J., Rho, B. S., & Choi, H. Y. (2012). Interferometric fiber optic sensors. Sensors, 12(3), 2467–2486. https://doi.org/10.3390/s120302467

[98] Zhou, Y., Yuan, Y., & Su, M. (2024). Research on fiber-optic optical coherence ranging system based on laser frequency scanning interferometry. Sensors, 24(6), 1838. https://doi.org/10.3390/s24061838